

Report No. SRIC 68-13

KINETIC STUDIES ON THE PYROLYSIS, DESULFUR-
IZATION, & GASIFICATION OF COALS WITH EMPHA-
SIS ON THE NON - ISOTHERMAL KINETIC METHOD

Report No. SRIC 68-13

KINETIC STUDIES ON THE PYROLYSIS, DESULFUR-
IZATION, & GASIFICATION OF COALS WITH EMPHA-
SIS ON THE NON - ISOTHERMAL KINETIC METHOD

Marvin L. Vestal, Allan G. Day, III, J. S. Snyderman,
Gordon J. Fergusson, F. W. Lampe, R. H. Essenhight
and Wm. H. Johnston

With contributions from

Charles E. Waring, A. L. Warhaftig, J. H. Futrell,
Albert C. Nash, George W. Brown, Pamela P. Farkas,
Curtis A. Johnston and Arlene E. Weitzman

Final Report September 1968 Revised April 1969

Phase I Contract No. PH 86-68-65

with the

NATIONAL AIR POLLUTION CONTROL ADMINISTRATION

Paul W. Spaite, Chief, Process Control Engineering Program
E. D. Margolin, Chief, New Process Development Unit
Leon Stankus, Contract Project Officer

Scientific Research Instruments Corporation
Baltimore, Maryland

TABLE OF CONTENTS

	<u>Page</u>
<u>I. INTRODUCTION</u>	1
ABSTRACT	i
GENERAL	1
<u>II. THEORETICAL BASIS OF NON-ISOTHERMAL KINETIC MEASUREMENTS</u>	6
PYROLYSIS IN AN INERT ATMOSPHERE WITH NO BACK REACTION	7
PYROLYSIS IN A REACTIVE ATMOSPHERE WITH NO BACK REACTION	19
PYROLYSIS IN AN INERT ATMOSPHERE WITH BACK REACTION	21
PYROLYSIS IN A REACTIVE ATMOSPHERE WITH BACK REACTION	26
NON-ISOTHERMAL KINETICS OF THE BACK REACTION IN COAL PYROLYSIS	27
<u>III. EXPERIMENTAL METHODS</u>	32
TYPE OF COAL	35
<u>IV. RESULTS AND DISCUSSION</u>	37
GENERAL NATURE OF COAL PYROLYSIS	37
KINETICS OF COAL DESULFURIZATION	58
FORMS OF SULFUR	77
<u>V. CONCLUSIONS</u>	80
<u>VI. REFERENCES</u>	83
<u>VII. APPENDIX (Apparatus and Procedure)</u>	

LIST OF FIGURES

Figure		Page
1a.	Evolution of CH_3SH in a non-isothermal pyrolysis in hydrogen.	14
1b.	Graph for determining the activation energy for first order reactions from the experimental parameters.	16
2	Schematic diagram of experimental apparatus.	34
3	Sulfur removal factors for coal pyrolysis in hydrogen at one atmosphere.	41
4	Gas evolution curve for 5% sulfur coal pyrolyzed in hydrogen showing sulfur containing species and major hydrocarbons, Run N3. see Table IV for experimental details.	44
5	Gas evolution curve for 5% sulfur coal pyrolyzed in helium showing sulfur containing species and major hydrocarbons, Run N4. see Table V for experimental details.	45
6	Comparison of H_2S evolution in H_2 atmosphere, Run N3, with H_2S evolution in He atmosphere. Run N4.	48
7	Hydrogen sulfide evolution from different particle size cuts of coke by non-isothermal reaction with H_2 at one atmosphere and 100 ml/min flow rate, heating rate $5^\circ\text{C}/\text{min}$. Coke was prepared by pyrolysis of 5% S coal in He at 900°C for one hour.	57
8	Analysis of the hydrogen sulfide experimental results on the basis of separate first-order irreversible reactions.	60
9	H_2S evolution curve for different hydrogen flow rates. The parameter identifying the curve is hydrogen flow rate in ml/min.	63

LIST OF FIGURES

Figure		Page
10	Location of the high temperature peak in the H_2S evolution in hydrogen as a function of mean residence time, τ .	64
11	Comparison of the H_2S evolution curve for a fast back reaction with the calculated curve for the case of no back reaction.	65
12	Relative peak heights for hydrogen sulfide and helium sampled from the effluent of a bed of coke for Run N22. The carrier gas contained 0.103% hydrogen sulfide in helium.	67
13	Arrhenius type plot of the data from the direct measurement of the hydrogen sulfide back reaction with coke from Run N22.	69
14	Hydrogen sulfide evolution for non-isothermal pyrolysis of 250 mg pyrite in H_2 at one atmosphere, flow rate of 100 ml/min, and heating rate $5^\circ C/min$.	71a
15	H_2S evolution curve calculated by the indirect method.	73
16	Comparison of the theoretical curves for H_2S evolution in hydrogen with no back reaction with the experimental result from Run N23.	75
17	Rates for the desulfurization reactions and the H_2S back reaction as a function of temperature in hydrogen at one atmosphere.	76
18	Forms of sulfur in coke as a function of carbonization temperature, from Powell Reference 2a.	78
A1	Block diagram of experimental apparatus.	5
A2	Detailed description of coal pyrolysis gas handling system.	6
A3	Detail schematic of GLC sampling and gas handling system.	7
A4	Detail schematic of tandem GLC-Plasma Spectrograph.	8
A5	Schematic diagram of the ion optics for the scanning mass spectrometer.	9
A6	Diagram of reactor vessel used in high pressure experiments.	11

LIST OF FIGURES

Figure		Page
A7	Schematic diagram of the linear temperature programmer.	13
A8	Chromatograph calibration chart for hydrogen sulfide. (Standard 3.5 ml loop; at X1) .	18
A9	Plasmagram of 0.1 psia methyl mercaptan in 3.5 cm ³ sample loop.	20
A10	Membrane separator for mass spectrometer inlet system.	22

LIST OF TABLES

Table	Page
I Summary of Analytical Data on 5% and 1% Sulfur Coal .	36
II Summary of Data for Isothermal Hydrogen Runs .	38
III Summary of Data for Isothermal Helium Runs .	40
IV Summary of Coal Pyrolysis Experimental Data for Non-Isothermal Hydrogen Runs at One Atmosphere .	51
V Summary of Coal Pyrolysis Experimental Data for Non- Isothermal Helium Runs .	53
VI Summary of Coal Pyrolysis Experimental Data for Non- Isothermal Hydrogen Runs at Different Pressures .	54
VII Summary of Coke Pyrolysis Experimental Data for Non- Isothermal Hydrogen Runs on Cokes of Different Mesh Size .	55
VIII Apparent Kinetic Parameters for Hydrogen Sulfide Evolu- tion in the Non-Isothermal Pyrolysis of 5% Sulfur Coal in Hydrogen Atmosphere, Run N1 .	61
IX Back Reaction of Hydrogen Sulfide with Coke .	68
X Pyrite Pyrolysis Experimental Data for Non-Isothermal Hydrogen Run .	68
XI Kinetic Parameters for the Desulfurization Reactions .	72
AI Retention Times of Various Compounds in GLC for Triton 305 Column Programmed from 50 70°C and Helium Flow Rate, 50ml/min .	17
AII Mass Spectrometer Calibrations for the Gases Measured in this Work .	24

I. INTRODUCTION

ABSTRACT

The theory of the non-isothermal technique developed by Juntgen and co-workers (loc cit) for the study of the kinetics of complex heterogenous reactions has been extended to include reactive flush gases and back reactions of the products, and has been applied to experimental studies of pyrolysis, desulfurization, and gasification of coals in a series of twenty three non-isothermal experiments. In addition, facilities were constructed for isothermal experiments and a series of nineteen runs were conducted, utilizing both fast and slow heating rates to reach the isothermal operating temperature. The variables studied included coal particle size, flush-gas composition, gas flow rates, and the forms of sulfur in the coal. The experiments were performed in specially constructed facilities containing some novel features required for the successful execution of the non-isothermal technique. These included a specially constructed mass spectrometer and a plasma emission spectrometer, as well as conventional methods such as chromatography. The objectives of the work are to determine kinetics of desulfurization of coal as an aid to the design, operation, and the evaluation of new process systems for practical desulfurization.

The data and theoretical analyses developed establish the non-isothermal technique as an important method for progress toward a practical understanding of the desulfurization kinetics. A series of reaction types have been identified, and their kinetic parameters measured, during pyrolysis of coal in a hydrogen atmosphere. These are: (1) reaction of

volatile organic sulfur with hydrogen; (2) reaction of pyrite with hydrogen to form sulfide; and (3) reaction of hydrogen with the sulfide and organic sulfur associated with the fixed carbon. Sulfate in the coal was reduced to sulfide prior to its transformation to hydrogen sulfide. The kinetic parameters were measured for the back reaction of hydrogen sulfide with coke, a reaction which can be very significant under certain conditions.

Further work is in progress to apply this powerful method of non-isothermal kinetics to the study of the desulfurization of a series of ten bituminous coals. In subsequent reports the desulfurization kinetics of a variety of coals will be given and the implications of these kinetic measurements to the general mechanistic picture of coal desulfurization will be discussed.

GENERAL

The combustion of coal containing sulfur is a well-known source of air pollution. The present report is Phase I of a project concerned with the development of processes for desulfurization of coal during pyrolysis and gasification. Some potential advantages of removing the sulfur prior to combustion may be listed. In the first place, the volume of gas to be processed is ten per cent or less of that of the final flue gases and correspondingly the concentration of sulfur is high, in the two to five per cent range. Secondly, the sulfur is present largely as hydrogen sulfide for which the removal-chemistry is probably more favorable. Although utilities are naturally hesitant to enter the chemicals industry, such a development may become desirable; besides the possibility of obtaining organic chemicals from coal, treatment prior to combustion favors the recovery of sulfur as elemental sulfur which is the most readily marketable form. Finally, systems based upon removal of sulfur prior to combustion are probably more easily integrated with thermal cycles based upon gas turbines, pressurized boilers, and top heat cycles which can be more efficient.

A large number of coal gasification methods have been brought to various stages of development under the justification of various technological and economic reasons. Control of atmospheric pollution, however, was not a prime consideration in such developments. A reassessment of coal gasification technology in the light of possible contribution to desulfurization is desirable. Furthermore, recent advances in the kinetic theory of heterogenous reactions make possible new laboratory methods with greater applicability to this problem.

Phase I of this project emphasizes the study of the kinetics of coal gasification techniques on a laboratory scale with emphasis on the identification of sulfur removal reactions and on the measurements of the kinetics and the chemical balances of these reactions, both of pyritic sulfur and of organic sulfur. Furthermore, the relevant back-reactions are also studied. By measuring the kinetic parameters of all important competing reactions, including back reactions, the information thus obtained is more useful for scale-up conclusions than laboratory measurements without the basic chemical kinetic parameters. Initially the results reported in the literature were checked by a series of essentially isothermal measurements, then a more sophisticated non-isothermal technique was used to obtain the kinetic measurements required in this program.

The immense literature pertaining to the reactions and kinetics of coal gasification include several recent reviews on the chemistry of coal¹. Although these reviews cite some recent significant results such as the work of Gorin and coworkers of the Consolidation Coal Company^{27,28}, much of the work directed towards the practical kinetics of desulfurization is on the order of thirty-five years old²⁻¹⁴. This early work on the practical kinetics of coal desulfurization is summed up in three papers by Powell^{2a,b} and by Snow³. During the first four months of this project a laboratory for measurements on the heterogenous reaction kinetics of coal gasification and desulfurization was designed and constructed. The first series of experiments was carried out essentially isothermally using both fast and slow heating rates and reactive and non-reactive gaseous environments. A coal was studied with very similar composition to that used many years ago in the studies by Snow³.

Results of these experiments using modern techniques were in good agreement with those reported by Snow in 1932. This verification of Snow's results incline us to accept his data from a large range of temperatures and for several different reactive environments.

During the course of these experiments, it became clear that rapid progress toward the measurement of the kinetic data needed in this program would require the combined use of more sophisticated experimental and theoretical techniques. The recent new method established in Germany by Juntgen and co-workers¹⁵⁻²² of non-isothermal kinetic measurements was clearly the most promising new technique to apply to the measurements of desulfurization kinetics. Basically this method consists of studying the kinetics of coal pyrolysis with continually rising temperatures.

Previously reaction kinetics for coal pyrolysis were generally studied in a series of constant temperature experiments. Although tedious, the constant temperature method may give good results. Difficulties, however, are frequently encountered with irreversible reactions and with complex heterogenous systems. For example, the isothermal measurements checking Snow's data show a major dependence on heating rate. Chemical decomposition occurs erratically, making characterization of individual reactions extremely difficult. The non-isothermal method is a better-controlled and reproducible technique for carrying out such measurements. More importantly, it provides in a single experiment, data which are interpretable in terms of detailed kinetic parameters for the major reactions taking place.

The theoretical treatment, initially developed by Juntgen and coworkers and extended by us, provides a framework for discussing chemical reactions under non-isothermal conditions. It, therefore, permits us to examine more closely the influence of the simultaneous variation of temperature and

concentration on the course and velocity of the reactions. The theory is used to calculate the dependence of sulfur releasing reactions on temperature, reaction order, activation energy, frequency factor and rate of heating. The data are obtained by measurements under conditions of controlled, continuous heating of the system.

The most important result of our studies to date has been the implementation of this approach in characterizing the complex chemical processes occurring in the desulfurization of coal. In the experimental program we have constructed an apparatus that allows quasi-continuous mass spectral monitoring of the various pyrolysis products that arise during the time in which a solid coal sample (in a stream of flush gas) is being heated at a known and controlled linear rate. We have extended the theoretical treatment to include the effects of a reactive flush gas and back reactions of the gaseous products. Using this apparatus and the experimental and theoretical procedures developed and described in this report, we have established the following general conclusions.

1. As suggested by earlier work², the back reaction of hydrogen sulfide (the major desulfurization product) with coke plays an extremely significant role in the determination of the level of desulfurization achieved. We have determined kinetic parameters for this back reaction as well as for the forward reactions of desulfurization. Under conditions for which the forward desulfurization reactions achieve reasonable rates, the back reactions are extremely rapid.

2. Three separate classes of reaction have been identified which produce hydrogen sulfide during pyrolysis of coal in a hydrogen atmosphere. These reactions have been tentatively identified as: (1) reaction with the volatile organic sulfur; (2) reaction with the pyrite to form sulfide;

and (3) reaction with the sulfide and the organic sulfur associated with the fixed carbon. Kinetic parameters for each reaction have been determined. The sulfate in the coal is apparently reduced to a sulfide prior to its transformation to hydrogen sulfide.

3. The achievement of a practical process for the desulfurization of coal by reaction with hydrogen requires that the back reaction of hydrogen sulfide with coke be inhibited. This has been accomplished in the laboratory by using high flow rates of hydrogen over small samples of coal. Obviously this is not a practical industrial process, and further research will be required to develop an economically feasible method.

Before proceeding to the rational design of a practical process for desulfurization of coal along the lines suggested by the present results several additional laboratory studies will be required. First it is necessary to establish the generality of the present kinetic data before concluding that these parameters are useful for predicting the behavior of a wide variety of coals. Secondly, the use of inexpensive sulfur adsorbents as a practical method for suppressing back reactions of H_2S should be explored. Kinetic and stoichiometric measurements on potential absorbents, particularly calcined limestones and dolomites, will be required. The use of calcined limestones and dolomites as sulfur absorbents has been proposed in connection with the Consol CO_2 Acceptor Process by Gorin et al^{27,28}. The equilibrium constants for the reactions pertinent to the use of these materials in desulfurization process has been calculated by Squires²⁹; however, little kinetic data is presently available. These additional kinetic studies will be accomplished in Phase II of this project.

II. THEORETICAL BASIS OF NON-ISOTHERMAL KINETIC MEASUREMENTS

The classical, time-honored method used in a study of the reaction kinetics of a chemical system consists basically of the measurement of the extent of reaction as a function of time for a series of experiments, each at a different but constant temperature. Unfortunately, this method cannot be applied readily to the pyrolysis of a complex solid substance, such as a coal sample, because of the uncontrolled occurrence of a number of chemical reactions during the time that the sample is being heated to the desired reaction temperature. A method has been developed recently by Juntgen and co-workers¹⁵⁻²² which circumvents this difficulty by studying the reaction velocity at a constant and known heating-rate of the solid sample. From theoretical kinetic considerations these workers¹⁵⁻²² have shown how the usual kinetic parameters, activation energies and pre-exponential factors, may be derived from such experiments. Moreover, Van Heek, Jüntgen, and Peters¹⁶ have applied the method to the decomposition of basic magnesium carbonate and have shown that kinetic parameters are obtained that are in good agreement with those obtained earlier by classical, isothermal methods^{23, 24}. In addition, the observed dependence of the instantaneous reaction velocity on sample heating-rate was in agreement with the theoretical expectation²¹.

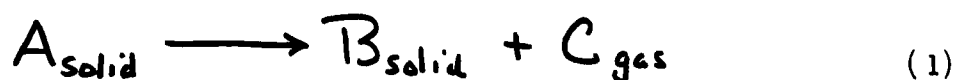
In the present work we have adapted the non-isothermal technique of Jüntgen and his colleagues to our studies of the pyrolysis of coal, both in inert and reacting atmospheres, with particular emphasis on the kinetics of formation of gaseous sulfur compounds. In the discussion of the theoretical basis which follows, we recognize four distinct pyrolytic situations, namely:

1. Pyrolysis in an inert atmosphere with no back reaction.
2. Pyrolysis in a reactive atmosphere with no back reaction.
3. Pyrolysis in an inert atmosphere with back reaction.
4. Pyrolysis in a reactive atmosphere with back reaction.

In addition to these cases that are encountered in coal pyrolysis experiments, we treat by similar methods the kinetics of the back reaction when it occurs under conditions that the forward reaction is negligible.

1. PYROLYSIS IN AN INERT ATMOSPHERE WITH NO BACK REACTION

In the pyrolysis of coal in an inert atmosphere we are concerned with the thermal decomposition of a solid to form a gaseous product. This overall reaction can be represented as



If the gaseous products are continuously removed with sufficient rapidity the back reaction may be neglected. Such a decomposition reaction (1) is often first order with respect to the solid-phase concentration of A, and if this is so, the rate equation may be written as

$$-\frac{d[A]}{dt} = k[A] \quad (2)$$

where $[A]$ is the instantaneous concentration of A in the solid phase, k is the first order rate constant and t is time. Continuous measurement of the solid phase concentration, $[A]$, is generally difficult; however, $[A]$ may be expressed in terms of the volume of evolved gas C. That is,

$$[A] = \alpha (V_0 - V) \quad (3)$$

where V is the volume of gas C evolved up to time t , V_0 is the total volume of gas C evolved as reaction (1) goes to completion, and α is the proportionality factor. In terms of the volume of evolved gas the rate equation for the decomposition reaction becomes

$$\frac{dV}{dt} = k(V_0 - V) \quad (4)$$

where $\frac{dV}{dt}$ is the instantaneous rate of production of product gas C in terms of its volume per unit time.

The first order rate constant k depends upon the temperature in a manner that is most simply described by the Arrhenius equation

$$k = k_0 e^{-\frac{E}{RT}} \quad (5)$$

where k_0 is a temperature-independent frequency factor, E is the activation energy, R is the universal gas constant and T is the absolute temperature. For an experimental situation such as considered here, in which the temperature is not constant but can be made to vary linearly with the time of reaction, we have

$$T = T_i + Mt \quad (6a)$$

and

$$\frac{dT}{dt} = M \quad (6b)$$

where M is the heating rate in units of degrees per unit time and T_i is the initial temperature of the experiment.

The rate equation, (2), may be written in its integrated form as

$$\ln \frac{[A]}{[A]_0} = - \int_0^t k dt \quad (7)$$

where $[A]_0$ is the concentration of $[A]$ at zero reaction time. Under conditions of constant temperature, ($M=0$), k is a constant independent of t and the right side of (7) integrates simply to kt . However, for non-zero values of M , k depends on the time and the integration of (7) is more involved. Since we know the relationship between temperature and time to be given by (6), we may express the integral in (7) either as a function of time or of temperature. It is more convenient to use the latter representation and so by substitution of (5) and (6) into (7) we obtain (8), viz:

$$\ln \frac{[A]}{[A]_0} = - \frac{k_0}{M} \int_{T_i}^T e^{-\frac{E}{RT}} dT \quad (8)$$

where T_i is the minimum temperature at which reaction is observed; that is, T_i is the temperature at which the concentration of A is $[A]_0$. T_i is chosen so that, by definition, no reaction occurs for $T \leq T_i$. Therefore, we may write equation (8) as

$$\ln \frac{[A]}{[A]_0} = - \frac{k_0}{M} \left[\int_0^{T_i} e^{-\frac{E}{RT}} dT + \int_{T_i}^T e^{-\frac{E}{RT}} dT \right] \quad (8a)$$

Since the first integral in the brackets is zero by definition ($T \leq T_i$) we may write (8a) for mathematical convenience as

$$\ln \frac{[A]}{[A]_0} = - \frac{k_0}{M} \int_0^T e^{-\frac{E}{RT}} dT \quad (8b)$$

The integral in (8b) is known as the exponential integral and has been extensively tabulated ²⁵. Jüntgen and co-workers ¹⁶ have used the approximation,

$$\int_0^T e^{-\frac{E}{RT}} dT \approx \frac{RT^2}{E} e^{-\frac{E}{RT}} \quad (9)$$

which is satisfactory so long as the quantity $\frac{RT}{E}$ is much less than unity. Substituting (3), (9) and the relation $[A]_0 = \alpha V_0$ into (8b) gives

$$V_0 - V = V_0 \exp \left[-\frac{k_0}{M} \frac{RT^2}{E} e^{-\frac{E}{RT}} \right] \quad (10a)$$

If we now differentiate (10a) with respect to temperature we obtain

$$-\frac{dV}{dT} = V_0 \frac{d}{dT} \left\{ \exp \left[-\frac{k_0}{M} \frac{RT^2}{E} e^{-\frac{E}{RT}} \right] \right\} \quad (10b)$$

or

$$\frac{dV}{dT} = V_0 \frac{k_0 R}{M E} \exp \left[-\frac{k_0}{M} \frac{RT^2}{E} e^{-\frac{E}{RT}} \right] \frac{d}{dT} \left(T^2 e^{-\frac{E}{RT}} \right) \quad (10c)$$

or

$$\frac{dV}{dT} = V_0 \frac{k_0 R}{M E} \left(\frac{E}{R} + 2T \right) e^{-\frac{E}{RT}} \exp \left[-\frac{k_0}{M} \frac{RT^2}{E} e^{-\frac{E}{RT}} \right] \quad (10d)$$

which upon multiplication through the bracket term by $\frac{R}{E}$ gives

$$\frac{dV}{dT} = V_0 \frac{k_0}{M} \left(1 + \frac{2RT}{E}\right) e^{-\frac{E}{RT}} \exp \left[-\frac{k_0}{M} \frac{RT^2}{E} e^{-\frac{E}{RT}} \right] \quad (10e)$$

Since the approximation (9) is valid only for $\frac{RT}{E} \ll 1$ we have finally the result

$$\frac{dV}{dT} = \frac{V_0 k_0}{M} \exp \left[-\left(\frac{k_0}{M} \frac{RT^2}{E} e^{-\frac{E}{RT}} + \frac{E}{RT} \right) \right] \quad (11)$$

for the case of first order decomposition reactions. Expressions for other reaction orders have been derived by Van Heek, Jüntgen and Peters¹⁶.

In order to relate the volume of gas evolved in a given experiment to a fixed quantity of solid, the terms V and V_0 in (11) are taken as volume of gas evolved per unit mass of solid sample. Further, the experimental quantity actually measured is the fraction of the total flowing gas that is the gas evolved by the decomposition. If we let P be the fraction of the total flowing gas (carrier gas and evolved gases) that is the evolved gas, G be the weight of the solid sample, and Q be the volume flow rate of carrier gas, then the left hand side of (11) is evaluated from the experimental variables by the relation

$$\frac{dV}{dT} = \frac{PQ}{MG} \quad (12)$$

so that an experimental value for $\frac{dV}{dT}$ in $\text{cm}^3/\text{g-deg.}$ can be obtained at each value of T and M. From experimental knowledge of T and M we can evaluate the kinetic parameters k_0 and E which are characteristic of a given solid sample.

A typical gas production curve, by which we mean a plot of $\frac{dV}{dT}$ versus T, for a given M, is shown in Figure 1a for methyl mercaptan evolution at a heating rate of $5^\circ/\text{min.}$ Actually, in the experiment, of course, the experimental gas production curve is obtained from measurement of $\frac{dV}{dT}$ as given by (12) as a function of T. At the maximum in the curve $\frac{d}{dT} \left(\frac{dV}{dT} \right) = 0$ and it can be easily shown¹⁶ that solution of this equation yields the following expressions for the kinetic parameters k_0 and E

$$E = \frac{eRT_0^2}{V_0} \left(\frac{dV}{dT} \right)_{T_0} e^{-\frac{2RT_0}{E}} \quad (13)$$

$$k_0 = \frac{ME}{RT_0} e^{\frac{E}{RT_0}} \quad (14)$$

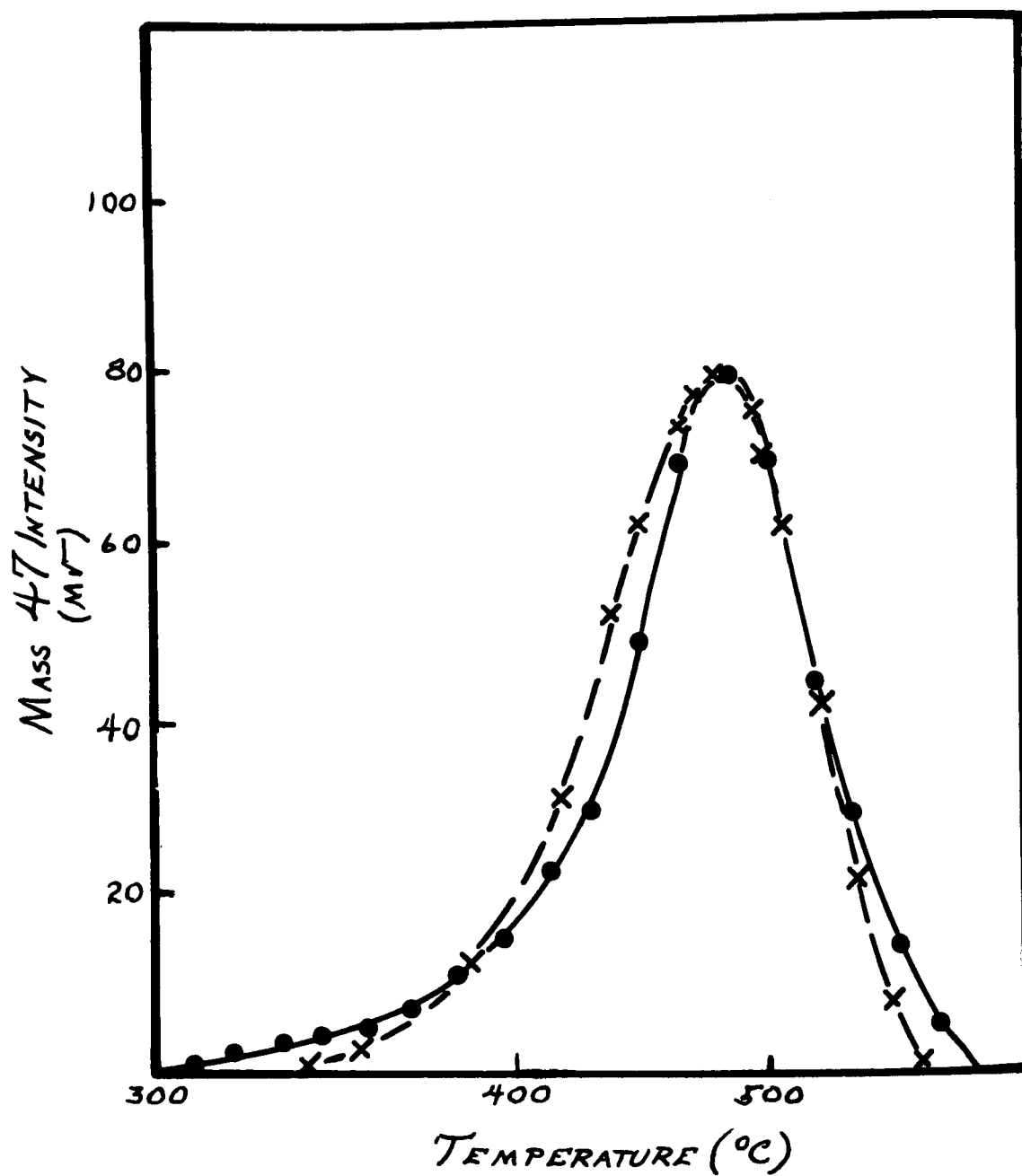


Figure 1a. Evolution of CH_3SH in a non-isothermal pyrolysis in hydrogen.
 —●— experimental data
 —x— calculated from values of E and k_0 by analysis of experimental results.

Obviously, the transcendental equation, (13), cannot be solved explicitly for E. However, we can solve it graphically to obtain from a given experimental $\frac{dV}{dT}$ vs T curve a numerical value for the activation energy E. Thus, if we define the dimensionless parameters

$$\alpha = \frac{E}{RT_0} \quad (15)$$

$$\beta = \frac{T_0}{V_0} \left(\frac{dV}{dT} \right)_{T_0} \quad (16)$$

and substitute into equation (13) we may write

$$\alpha = \beta e^{(1 - \frac{2}{\alpha})} \quad (17)$$

Taking logarithms we have

$$\frac{2}{\alpha} + \ln \alpha = 1 + \ln \beta \quad (18)$$

The quantity $\frac{2}{\alpha} + \ln \alpha$ is plotted as a function of α in Figure 1b. Thus from this figure we may obtain a unique value for α if we know the value of the function, $\frac{2}{\alpha} + \ln \alpha$.

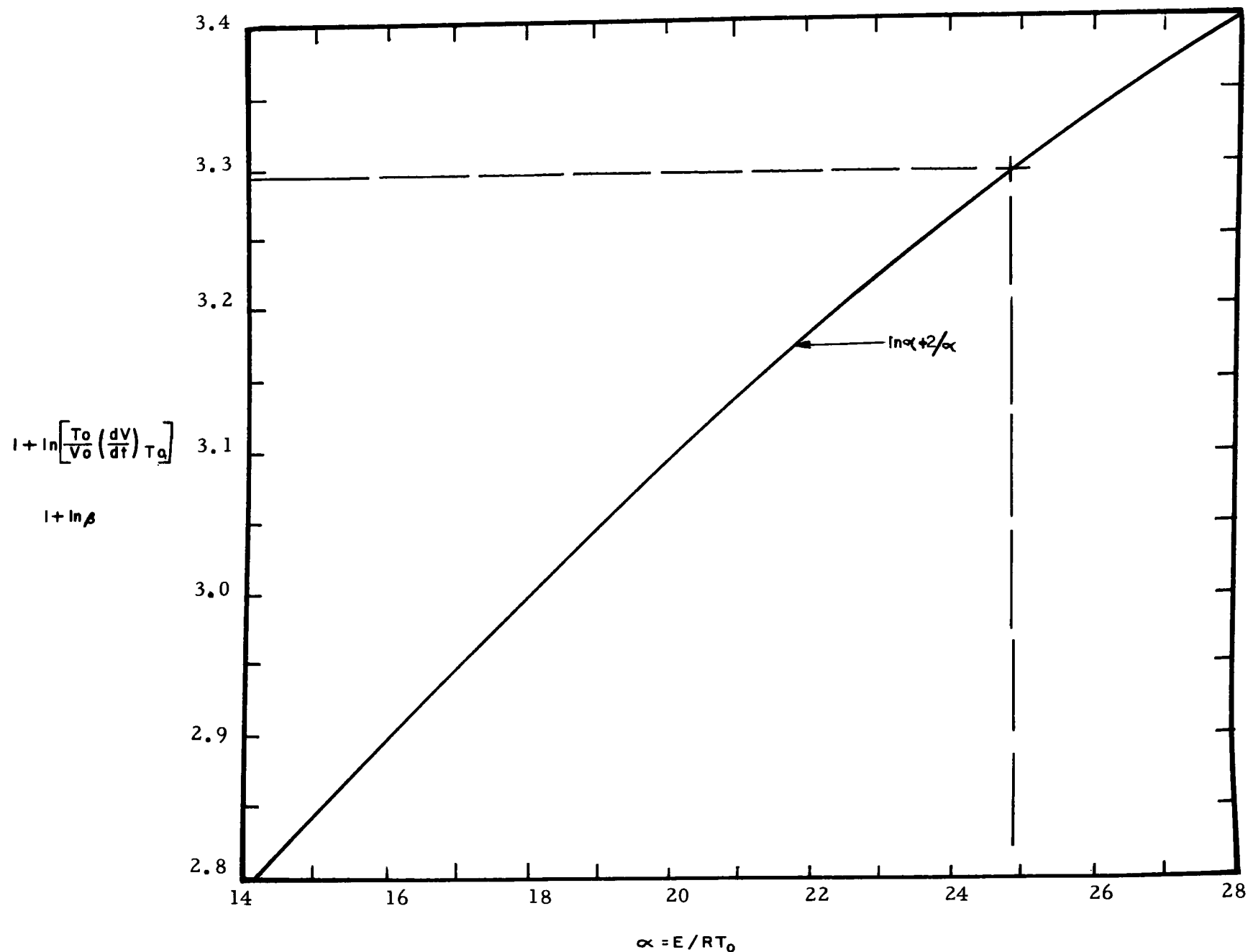


Figure 1b. Graph for determining the activation energy for first order reactions from the experimental parameters, defined in

The procedure to obtain a unique value of E from the experimental $\frac{dV}{dT}$ versus T curve is first to calculate a value of β according to equation (16), in which β is defined in terms of the experimental parameters V_0 , T_0 and $\left(\frac{dV}{dT}\right)_{T_0}$. From this value of β we may calculate $1 + \ln \beta$ and, hence, by virtue of equation (18) we have the quantity $\frac{2}{\alpha} + \ln \alpha$. From Figure 1b and the computed value of the ordinate $\frac{2}{\alpha} + \ln \alpha$, we obtain α . From this value of α , we calculate E by means of equation (15). As soon as E is thus determined, k_0 can be computed immediately from equation (14), or in terms of the dimensionless parameter α , k_0 is given by

$$k_0 = \frac{M\alpha}{T_0} e^{\alpha} \quad (19)$$

A specific example of this method of evaluation of k_0 and E is as follows: consider the evolution-rate curve for methyl mercaptan shown in Figure 1a. In this figure we have plotted the intensity of the m/e 47 ion in millivolts as a function of the temperature for a pyrolysis in hydrogen at a heating rate of 5°/min. The intensity of this ion is proportional to the concentration of methyl mercaptan in the flowing gas stream and by means of prior mass spectrometer calibration may be easily converted to concentration; however, such a conversion for the purpose of obtaining the kinetic parameters from this data is not necessary, since these parameters are obtained from the dimensionless quantities and defined by equations (15) and (16). Thus it suffices simply to use consistent units throughout, which means that the volume of methyl mercaptan evolved (area under the curve in Figure 1a) is obtained for these purposes in the units of millivolt-degrees/gram.

Thus from equation (12), we see that $\frac{dV}{dT}$ is simply proportional to the concentration of methyl mercaptan in the gas stream or to the peak height of m/e 47 in millivolts. From the curve in Figure 1a we obtain the following values:

$$V_0 = 6.0 \times 10^3 \text{ millivolt-degrees/gram}$$

$$T_0 = 740^\circ\text{K.}$$

$$\left(\frac{dV}{dT}\right)_{T_0} = 80 \text{ millivolt/gram}$$

From these experimental values we calculate β (equation 16) as

$$\beta = \frac{T_0}{V_0} \left(\frac{dV}{dT}\right)_{T_0} = 9.87$$

and hence

$$\ln \beta = 2.29$$

Then by equation 18 we have

$$1 + \ln \beta = 3.29 = \frac{2}{\alpha} + \ln \alpha$$

With this value for the quantity $2/\alpha + \ln \alpha$ we now may use Figure 1b (as shown by dotted lines on this figure) to calculate α as

$$\alpha = 24.6$$

Now by equation (15) we have

$$E = \alpha RT_0 = 36 \text{ kcal/mole}$$

and by equation (19)

$$k_0 = \frac{M_\alpha}{T_0} e^\alpha = 8.0 \times 10^9 \text{ min}^{-1}$$

The dotted line in Figure 1a is calculated from the theory using the above kinetic parameters E and k_0 and the heating rate of $5^\circ/\text{min}$. The agreement is seen to be quite satisfactory.

2. PYROLYSIS IN A REACTIVE ATMOSPHERE WITH NO BACK REACTION

In the pyrolysis of coal in a reactive atmosphere we are concerned with the reaction of a solid with the reactive gas to form a gaseous product. For the overall reaction in this case we replace (1) by (20) viz:



In a reaction such as (20) the rate is often first order with respect to both reactants and for convenience and simplicity we will consider that to be the case here. Then instead of (2), (3) and (4) we have (21), (22) and (23) viz:

$$-\frac{d[A]}{dt} = k_r [A] [D] \quad (21)$$

$$[A] = \alpha (V_0 - V) \quad (22)$$

$$\frac{dV}{dt} = k_r [D] (V_0 - V) \quad (23)$$

where k_r is the rate constant pertaining to the reactive atmosphere, $[D]$ is the concentration of reactive gas in the atmosphere, and all other quantities are as described for the case of the inert atmosphere.

For any given experiment the concentration of reactive gas in the pyrolytic atmosphere is maintained constant so that we may incorporate this constancy into the second-order rate constant k_r and write

$$k' = k_r [D] \quad (24)$$

where k' is a pseudo-first-order rate constant. Hence k' has the same units as k in equation (2), namely, seconds^{-1} , but its numerical value depends upon the concentration of reactive gas in the pyrolytic atmosphere.

In view of equation (24) we may express (21) and (23) as below:

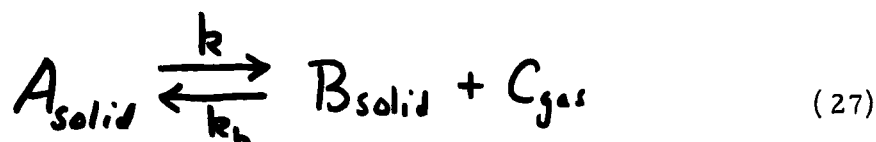
$$-\frac{d[A]}{dt} = k'[A] \quad (25)$$

$$\frac{dV}{dt} = k'(V_0 - V) \quad (26)$$

Since (25) and (26) are mathematically the same as (2) and (4), the remainder of the treatment for this case of a reactive atmosphere is identical to that of the inert atmosphere with k and k_0 of the latter treatment being replaced here by k^1 and k_0^1 . If we wish to evaluate the second order constants k_r and $k_{r,0}$ we need only divide k^1 and k_0^1 by the concentration of the reactant gas.

3. PYROLYSIS IN AN INERT ATMOSPHERE WITH BACK REACTION

For cases in which the back reaction cannot be neglected the modification of the theoretical treatment is more involved. For this situation we write the chemical reaction as



where k_b is the rate constant of the back reaction.

In the kinetic model for this complex situation it is necessary to include explicitly the geometry of the solid reactant and the velocity of flow of the inert sweep gas. For the present application we are concerned with a static bed of reactant of cross-section A and depth d , so that for a volume flow-rate of sweep gas of Q (cm^3/min) the average residence time, $\bar{\tau}$, of a volume element of gas within the bed is given by

$$\bar{\tau} = \frac{Ad}{Q} = \frac{V_B}{Q} = \frac{d}{v} \quad (28)$$

In (28), $V_B = Ad$ is the volume of the reactant bed and v is the average linear flow rate of the flush gas,

The rate of change in the concentration of the product gas C with residence time $\bar{\tau}$ in the bed is given by

$$\frac{d[C]}{d\bar{\tau}} = k[A] - k_b[C] \quad (29)$$

where the first term, $k[A]$, is the rate of formation of C and the second term, $k_b[C]$, is the rate of disappearance of C due to the back reaction, which we assume, for mathematical convenience, may be taken as first order overall. The term $[A]$ is the instantaneous concentration of solid reactant A and is assumed to be uniform over the bed.

Integration of (29) over the residence time, τ , with the boundary condition that $[C] = 0$ for $\tau = 0$, gives

$$[C]_{\tau} = \frac{k}{k_b} [A] \left\{ 1 - e^{-k_b \tau} \right\} \quad (30)$$

For a non-isothermal experiment, the rate constants k and k_b , being functions of temperature, are also time-dependent. However, for moderate heating rates and reasonably short residence times, the change in temperature ($\Delta T = M\tau$) is sufficiently small that the variation in the rate constants during the time τ may be neglected. The concentrations of solid reactant A and product gas C, namely, $[A]$ and $[C]$, are functions of real time, t , (just as k and k_b are) since the sweeping-out of the product gas C depletes the reactant. Explicitly this is given by

$$\frac{d[A]}{dt} = - \frac{Q[C]_{\tau}}{V_B} = - \frac{[C]_{\tau}}{\tau} \quad (31)$$

Combination of (30) and (31) yields (32), viz.,

$$\frac{1}{[A]} \frac{d[A]}{dt} = - \frac{1}{\tau} \frac{k(t)}{k_b(t)} \left\{ 1 - e^{-k_b(t)\tau} \right\} \quad (32)$$

where we denote explicitly that the rate constants are functions of real time t . Now for the constant rate-of-heating experiment, time and temperature are related by

$$dt = \frac{1}{M} dT \quad (33)$$

so that substitution of (33) into (32) and integration gives

$$\ln \frac{[A]_T}{[A]_0} = - \frac{1}{M\tau} \int_0^T \frac{k(\tau)}{k_b(\tau)} \left\{ 1 - e^{-k_b(\tau)\tau} \right\} d\tau, \quad (34)$$

where $[A]_0$ is the initial concentration of reactant $[A]$ in the bed. The same considerations of the lower limit to this integral as presented in the development of equations (8a) and (8b) apply here also. By using a series expansion of the exponential, this integral can be evaluated numerically using tables of the exponential integral or it may be evaluated analytically with the aid of the approximation given in equation (9). The results, however, are cumbersome and not very enlightening.

The case which is most pertinent to the present experimental study is that of a very fast back reaction, or, in other words, a very large k_b . For this situation we may assume that

$$k_b \tau \gg 1 \quad (35)$$

over the temperature range of interest. With the aid of (35), (34) reduces to (36), viz:

$$\ln \frac{[A]_T}{[A]_0} = - \frac{1}{M\tau} \int_0^T \frac{k(T)}{k_b(T)} dT \quad (36)$$

Using the Arrhenius expression for the rate constants, namely

$$k(T) = k_0 e^{-\frac{E}{RT}} \quad (37)$$

$$k_b(T) = k_{b0} e^{-\frac{E_b}{RT}} \quad (38)$$

equation (36) becomes

$$\ln \frac{[A]_T}{[A]_0} = - \frac{1}{M\tau} \frac{k_0}{k_{b0}} \int_0^T e^{-\frac{(E-E_b)}{RT}} dT. \quad (39)$$

Employing again the approximation (9) for the exponential integral we find from (39)

$$[A]_T = [A]_0 \exp \left[- \frac{1}{M\tau} \left(\frac{k_0}{k_{b0}} \right) \frac{RT^2}{(E-E_b)} e^{-\frac{(E-E_b)}{RT}} \right] \quad (40)$$

Differentiation of (40) with respect to temperature yields the gas production rate (related to $\frac{d[A]}{dT}$ by means of equation (3)) as

$$-\alpha \frac{dV}{dT} = \frac{d[A]}{dT} = -\frac{[A]_0}{M\uparrow} \frac{k_0}{k_{b0}} \exp \left[-\left\{ \frac{(E-E_b)}{RT} + \frac{1}{M\uparrow} \frac{k_0}{k_{b0}} \frac{RT^2}{(E-E_b)} e^{-\frac{(E-E_b)}{RT}} \right\} \right] \quad (41)$$

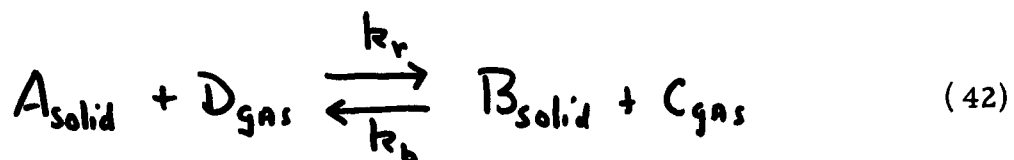
For the case of an inert sweep gas with no back reaction, we showed earlier that equation (11) applies, which with slight rearrangement in accord with (3) may be written

$$-\alpha \frac{dV}{dT} = \frac{d[A]}{dT} = -\frac{[A]_0 \uparrow}{M\uparrow} k_0 \exp \left[-\left\{ \frac{E}{RT} + \frac{\uparrow k_0 RT^2}{M\uparrow E} e^{-\frac{E}{RT}} \right\} \right] \quad (11b)$$

Comparison of (41) with (11b) shows that the dependence on temperature is identical, with $E-E_b$ in (41) replacing E in (11b). Hence the same graphical techniques described for the case of no back reaction, (equation (13) - (19)), may be applied in this case. When this is done the "activation energy" obtained is the difference $(E-E_b)$. The pre-exponential factor is obtained as $\left(\frac{k_0}{k_{b0}} \uparrow \right)$ and since \uparrow is known we obtain directly the ratio $\frac{k_0}{k_{b0}}$.

4. PYROLYSIS IN A REACTIVE ATMOSPHERE WITH BACK REACTION

In this situation we have the reaction

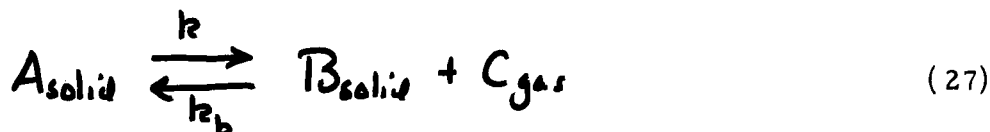


As for the case of a reactive atmosphere with no back reaction we assume the forward rate to be first-order with respect to both reactants and hence second-order overall. Thus, for this case, k_r is the second-order rate constant pertaining to the reactive atmosphere (cf (21)). Again, for a given experiment the concentration of reactive gas is maintained constant so that we may incorporate this constancy into the second-order rate constant k_r , as in (24). The treatment for this reactive atmosphere with back reaction is then identical to the treatment described in equations (28) - (41) with the exception that $k^1 = k_r [D]$ replaces k .

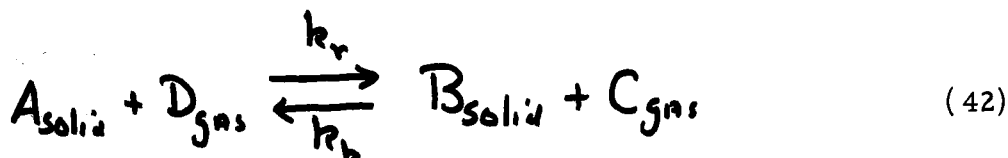
Hence from a study of the gas evolution curves, using the treatments described, we may in this case obtain $E_r - E_b$ and $\frac{k_d}{k_{b0}} = \frac{k_{r0}[D]}{k_{b0}}$. Since $[D]$ is a known quantity, we thus obtain $\frac{k_{r0}}{k_{b0}}$.

5. NON-ISOTHERMAL KINETICS OF THE BACK REACTIONS IN COAL PYROLYSIS

In our treatment of Case 3, viz.,



we showed that an analysis of the gas evolution curves of C leads to values for the activation energy difference $E - E_b$ and the frequency factor ratio $\frac{k_0}{k_{b0}}$. Similarly the same analysis applied to Case 4, viz;



permits evaluation of the activation energy difference $E_r - E_b$ and the frequency factor ratio $\frac{k_{r0}}{k_{b0}}$. In neither case can the kinetic parameters of either the forward or the reverse reactions be obtained independently as long as conditions are such that both reactions are occurring to significant extents.

Two methods that may be used to obtain the kinetic parameters of the forward and reverse reactions independently are suggested by consideration of equation (32), viz.

$$-\frac{d[A]}{dt} = \frac{d[C]}{dt} = \frac{k(t)}{k_b(t)} \frac{(1 - e^{-k_b(t)\tau})}{\tau} [A] \quad (32)$$

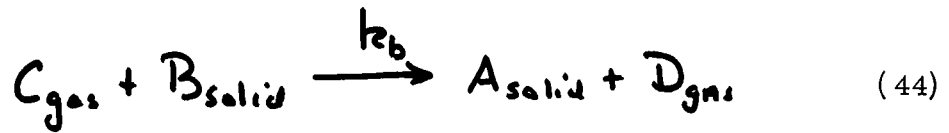
Since

$$\lim_{\tau \rightarrow 0} \left(-\frac{d[A]}{dt} \right) = \lim_{\tau \rightarrow 0} \frac{d[C]}{dt} = k(t) [A], \quad (43)$$

extrapolation of a series of gas evolution curves, conducted at increasing flow rates (decreasing τ), to $\tau=0$, should in principle yield the kinetic parameters of only the forward reaction, namely k_0 (or k_{r0}) and E (or E_r). Combination of these values with $E - E_b$ or $(E_r - E_b)$ and $\frac{k_r}{k_b}$ or $\frac{k_{r0}}{k_{b0}}$ would then yield the kinetic parameters for the reverse reaction.

The second method suggested by (32) is based on the fact that for $[A] = 0$, the forward rate is zero. Hence by studying the reaction of C with B_{solid} in the essential absence of A_{solid} we may obtain directly the kinetic parameters of the back reaction. This second method is the more convenient in practice and is developed in the following paragraphs.

Suppose a coal sample is first desulfurized to completion and all gases removed. In terms of the notation used, we have now a sample of B_{solid} (coke), the A_{solid} being completely converted. We may now introduce C_{gas} (H_2S), in either an inert sweep gas or a reactive sweep gas, D_{gas} (H_2), to the sample of B_{solid} (coke) and study either the evolution of D_{gas} or the consumption of C , via the reaction



The amount of conversion of B_{solid} to A_{solid} is kept small so that only the reaction (44) is studied. With the assumption that (44) is first order in $[C]$ ($= [\text{H}_2\text{S}]$), and that $[B]$ is so large that it may be taken as constant over the reaction, we have

$$\frac{d[C]}{dt} = -k_b[C] \quad (45)$$

where $[C]$ is the concentration of H_2S , and as before

$$k_b = k_{b0} e^{-\frac{E_b}{RT}} \quad (38)$$

For a given temperature of the bed we may integrate (45) to obtain the concentration of H_2S in the gas leaving the bed, viz:

$$[C]_f = [C]_0 e^{-k_b \tau} \quad (46)$$

where $[C]_0$ is the initial concentration of H_2S is the inlet gas and τ is the average residence time in the bed. For a non-isothermal experiment in which the heating rate is sufficiently low that the temperature change during the residence time τ is small, k_b in (46) may be considered as a constant. Assuming that this condition is met we may substitute (38) into (46) and obtain

$$\ln \frac{[C]}{[C]_0} = -k_{b_0} \tau e^{-\frac{E_b}{RT}}. \quad (47)$$

Taking logarithms of both sides of (47) and converting to base 10 gives

$$\log \left(\ln \frac{[C]_0}{[C]} \right) = \log(k_{b_0} \tau) - \frac{E_b}{2.303 R} \left(\frac{1}{T} \right). \quad (48)$$

Hence, by plotting semi-logarithmically the quantity $\ln \frac{[C]_0}{[C]}$ versus $\frac{1}{T}$, the kinetic parameters E_b and $k_{b_0} \tau$ may be determined from the slope and intercept, respectively. Since τ is known from the flow rates and bed size, k_{b_0} is determined.

Instead of measurement of the decrease in $C_s(H_2S)$, due to the back reaction (44), we may equivalently measure the formation of $D_s(H_2)$. For a 1:1 stoichiometry, which seems reasonable, we have from (44)

$$[C] = [C]_0 - [D] \quad (49)$$

so that (48) becomes

$$\log\left(\ln \frac{[C]_0}{[C]_0 - [D]}\right) = \log(k_b \tau) - \frac{E_b}{2.303 R} \left(\frac{1}{T}\right) \quad (50)$$

and the kinetic parameters are obtained from the slope and intercept of a semi-logarithmic plot of $\ln \frac{[C]_0}{[C]_0 - [D]} = \ln \frac{[H_2S]_0}{[H_2S]_0 - [H_2]}$

vs $\frac{1}{T}$.

III. EXPERIMENTAL METHODS

Two types of experiment were carried out in this examination of coal pyrolysis. The early experiments were conducted under isothermal conditions with a flush gas (either helium or hydrogen) flowing continuously over a sample of coal held at a fixed pre-determined temperature. Fast heating experiments were performed by dropping the coal sample on to a quartz wool bed in the reactor preheated to the desired reaction temperature. The volatile products of pyrolysis, swept out of the solid sample by the flush gas, were collected in cold traps and subsequently analyzed by a combination of gas chromatography and plasma spectroscopy. Tar and coke produced were analyzed for sulfur by the ASTM procedures.

The second type of experiment carried out, and the most informative, involved continuous mass spectrometric measurements of products produced under non-isothermal conditions. In this technique the coal sample is heated at a linear and known rate while the flush gas (again helium or hydrogen) continuously sweeps through the coal sample and removes volatile products. A portion of the effluent gas is fed to a mass spectrometer, which may be tuned to monitor continuously with time a pre-determined ionic mass or to scan repetitively a selected region of the mass spectrum. Most of these experiments were conducted by scanning over the range from mass 1 to mass 84 with a period of one minute. Since the heating rate was usually 5°C/min this mode of operation yields an experimental point on the gas evolution curve as a function of temperature every 5°C. For all of the sulfur compounds and for most of the other major compounds of interest, it was possible to identify a single representative ion in the spectrum which was relatively free from interference by ions produced from other substances present. With the mass spectrometer operating

at constant sensitivity the amplitude of the signal (usually expressed in millivolts) corresponding in the mass spectrum to the ion representative of a particular compound is proportional to the concentration of that compound in the effluent gas. A schematic diagram of the apparatus is shown in Figure 2, and a detailed description of the apparatus and procedures is given in the Appendix. With this arrangement the gases evolved during the pyrolysis of coal are monitored quasi-continuously as a function of time, and through the linear relationship between temperature and time also as a function of instantaneous temperature. The theoretical bases for obtaining kinetic parameters from the data obtained in these non-isothermal experiments are given in full in Chapter II.

In both types of experiments the gases condensable at liquid nitrogen temperature (including all of the sulfur compounds) were trapped from the reactor effluent and quantitatively measured using the gas chromatograph. These measurements coupled with the tar and coke sulfur analysis by the ASTM procedures were used to obtain sulfur balance determinations for each experiment. The coal sample, char residue, and tar from each experiment were weighed in the analytical balance. The total gas productions were determined by difference from these results, since many of the most abundant gases, e.g. H_2 , CH_4 , CO , are not effectively trapped at liquid nitrogen temperatures. For some of the experiments the calibrated mass spectrometer was also used for quantitative gas evolution measurements. Comparison of the GC and MS results were generally in good agreement. In the non-isothermal kinetic measurements only the relative yield of a particular gas as a function of temperature is required in the calculations; therefore, in many of the experiments the conversion to absolute units was not made.

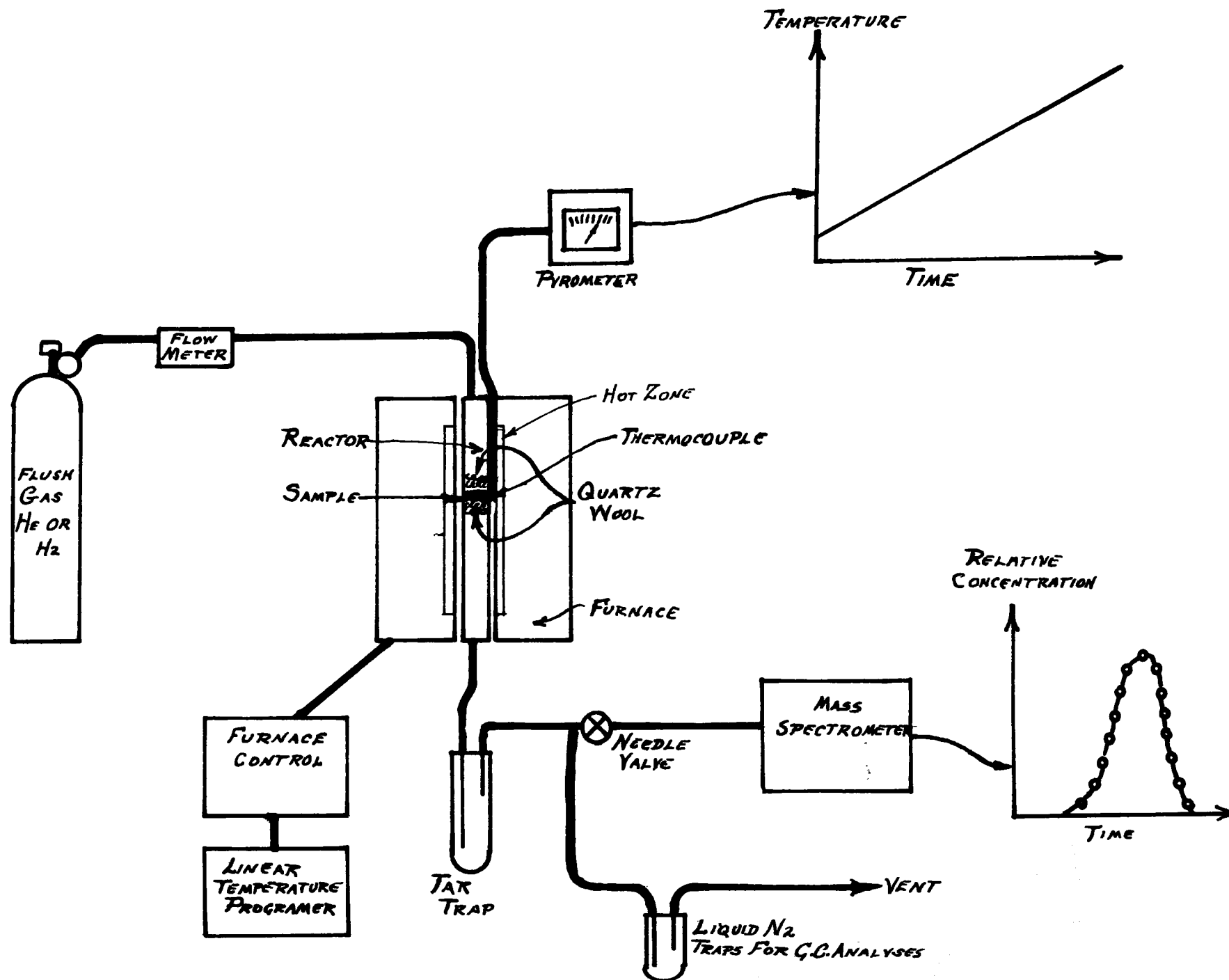


Figure 2. Schematic diagram of experimental apparatus.

The temperature measurements in these experiments were accomplished using a Chromel-Alumel thermocouple attached to the furnace block immediately adjacent to the position of the reactant bed in the reactor. The annular space between the reactor and the furnace was tightly plugged with quartz wool both top and bottom to prevent air convection through this space. The furnace used in this work gives a hot zone 12" long and the reactant bed (typically 1" long) was placed at the center of this zone. In the experiments involving high flow rates of flush gas, quartz wool was packed into the reactor on the inlet side of the reactant to provide better thermal contact with the gas. Comparison measurements between the temperature indicated by the external thermocouple and one installed in the reactant bed gave agreement within $\pm 10^{\circ}\text{C}$ over the range of experimental conditions used in these studies. Additional details of the experimental procedures are given in the Appendix.

1. TYPE OF COAL

Most of the experiments in this work were conducted on a No. 6 type, high volatile, rank C, Illinois coal containing approximately 5% sulfur. However, non-isothermal experiments were also conducted on an Illinois coal containing approximately 1% sulfur. Typical analytical data on these coals are given in Table I.

TABLE I. SUMMARY OF ANALYTICAL DATA ON 5%
AND 1% SULFUR COAL

	<u>Illinois Coal - 5%</u>	<u>Illinois Coal- 1%</u>
Forms of Sulfur (per cent of coal)		
Sulfate	0.31	0.01
Pyritic	2.50	0.26
Organic (diff)	1.95	0.60
Total	4.75	0.87
Proximate Analysis (per cent of coal)		
Moisture	9.7	8.7
Volatiles	34.0	34.8
Fixed Carbon	41.7	50.0
Ash	14.6	6.5
Sulfur in Ash (per cent of ash)	0.02	0.51
Sulfur in Fixed Carbon (per cent of coke residue from volatile matter determination)	3.75	0.60
Ultimate Analysis - dry basis		
Carbon	64.7	77.5
Hydrogen	6.0	5.7
Nitrogen	1.6	1.9
Sulfur	5.5	0.94
Ash	16.2	6.6
Oxygen (diff)	6.1	7.3

IV. RESULTS AND DISCUSSION

1. GENERAL NATURE OF COAL PYROLYSIS

Isothermal Experiments

The set of isothermal experiments in which the evolved gas composition and the extent of desulfurization of the solid reactant were studied as functions of temperature, flush gas (He or H₂), heating rate, reaction time, and coal particle size have confirmed the general picture provided years ago by the pioneering work of Powell^{2a, b} and Snow³. The results of these isothermal pyrolyses are summarized in Tables II and III.

With regard to sulfur-removal efficiency from the solid reactant by reaction with hydrogen, pertinent results of our isothermal experiments are compared in Figure 3 with the corresponding values obtained 36 years ago by Snow³. The agreement is quite good and confirms the general picture of 1932 that sulfur removal by some process begins at approximately 300°C, the amount removable by this process reaching a limit at about 500°C, and that other removal processes begin to occur above about 700°C. The results for isothermal reactions in an inert gas (helium) summarized in Table III are also in good general agreement with the earlier work by Snow using nitrogen as the inert gas.

TABLE II. SUMMARY OF DATA FOR ISOTHERMAL HYDROGEN RUNS

Run No.	Coal % S	Temp. °C	Residence Time Reaction Time	Coke Yield %	Desulfurization Factor	Sulfur Recovery, %					Total Recovery
						Coke	Tar	H ₂ S	CS ₂	SO ₂ CH ₃ SH C ₄ H ₄ S	
I3	5.4	700	3.0 sec. 10 min.	50.9	1.2	33.5	3.7	35.4	<0.1	<0.8	73
I4	4.6	1000	3.0 sec. 15 min.	53.0	0.71	39.8	0.2	25.4	2.5	<0.4	68
I5	4.6	700	3.0 sec. 15 min.	52.2	1.1	40.1	4.4	37.9	<0.1	<3.7	82
I6	4.6	700	3.0 sec. 15 min.	52.2	1.3	34.6	5.2	40.3	<0.1	<0.7	80
I7	5.0	1000	3.0 sec. 15 min.	52.4	1.5	32.0	0.1	37.4	11.6	<0.6	81
I8	4.7	1000	3.0 sec. 15 min.	50.9	1.2	45.8	2.1	43.9	9.6	<0.2	101
II2	5.0	1000	3.1 sec. 15 min.	52.4	1.4	38.9	1.8	39.5	11.7	<0.4	92
II3	5.0	1000	2.8 sec. 4-1/4 hr.	50.5	3.2	21.8	2.8	57.6	8.9	<0.4	91
II4	5.0	1000	11 sec. 4-1/4 hr.	50.5	1.1	47.6	2.5	37.6	12.4	<0.4	100 ⁽⁶⁾
II5	5.0	1000	3.5 sec. 4-1/4 hr.	53.8	3.6	24.2	7.6	55.9	0.3	1.3	89
II6	5.0	1000	2.7 sec. 4-1/4 hr.	52.2	7.1	10.7	6.5	69.6	0.9	0.7	88
II7	5.0	1100	3.0 sec. 4-1/4 hr.	50.1	3.8	16.8	0.5	55.6	9.7	<0.2	83

Notes For Table II

- (1) all 3 gram samples except I14 which was 11 grams.
- (2) all samples 20/40 mesh coal except I15 which was 100/200 mesh.
- (3) quartz reactor for all runs except I3, I4, and I5 which were in stainless steel reactor.
- (4) all coal injections into the furnace were gravity feed at the indicated temperature except I15 and I16 in which the coal was in place prior to heating.
- (5) purge gas at 1 atmosphere pressure.
- (6) assumed efficiency because a portion of the gas sample was lost during analysis - other sulfur recovery values are based on this assumption.
- (7) In I15 and I16 the rate of heating was approximately 33°/min.

TABLE III. SUMMARY OF DATA FOR ISOTHERMAL HELIUM RUNS

Run No.	Coal % S	Temp. °C	Residence Time Reaction Time	Coke Yield %	Desulfurization Factor	Sulfur Recovery, %					Total Recovery
						Coke	Tar	H ₂ S	CS ₂	SO ₂ CH ₃ SH C ₄ H ₄ S	
I1	3.8	700	1.0 sec. 10 min.	55.8	0.74	54.2	4.4	36.1	<0.1	<0.1	95
I2	4.0	1000	3.0 sec. 10 min.	59.2	0.75	52.4	4.2	27.4	7.5	<0.3	92
I9	4.8	1000	3.0 sec. 15 min.	53.9	0.93	46.2	1.3	30.9	10.3	<0.5	89
I10	5.0	700	3.0 sec. 15 min.	56.5	0.94	46.2	5.0	38.6	<0.1	<0.6	90
I11	5.0	700	3.1 sec. 15 min.	55.0	0.85	48.3	5.4	36.3	<0.1	1.4	91
I18	5.0	1100	3.1 sec. 4-1/4 hr.	54.8	1.8	34.8	0.4	55.2	6.3	<0.1	97
I19	5.0	900	23 sec. 1.7 hr.	58.3	0.91	49.5	6.3	37.5	<0.2	1.4	95

Notes

- (1) all 3 gram samples except I19 which was 23 grams and I1 which was a combined total of three 1 gram pyrolyses.
- (2) all samples 20/40 mesh coal.
- (3) quartz reactor for all runs.
- (4) all coal injections into the furnace were gravity feed at the indicated temperature except I19 in which the coal was in place prior to heating.
- (5) purge gas at 1 atmosphere pressure.
- (6) in I19 the rate of heating was approximately 33°/min.

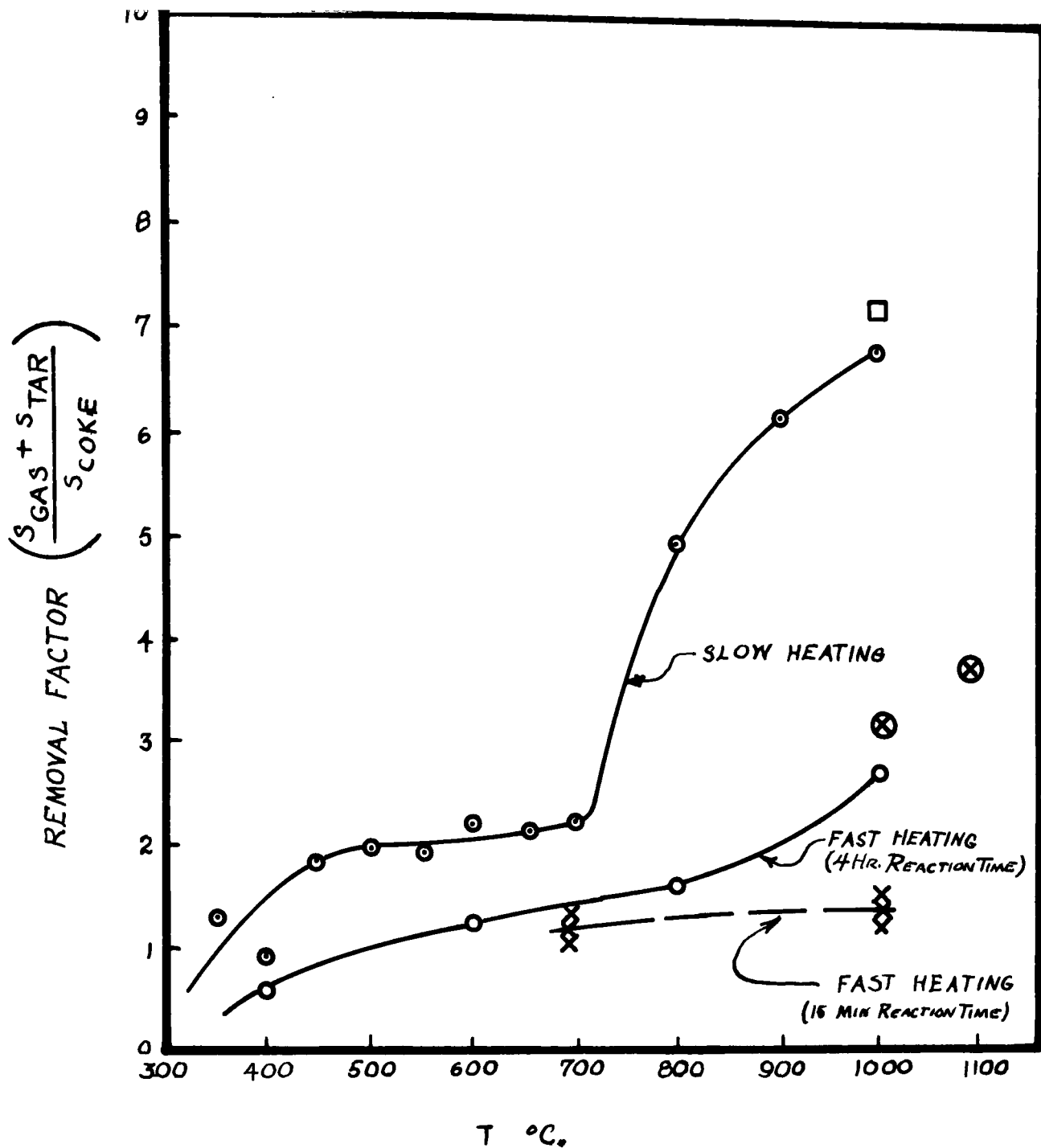


Figure 3. Sulfur removal factors for coal pyrolysis in hydrogen at one atmosphere.

⊙, ○ R.D. Snow, Ind. Eng. Chem. 24, 903 (1932).

X this work, fast heating; 15 minute reaction time

⊗ this work, fast heating; 4 hour reaction time

□ this work, slow heating (33°/min)

While useful in filling a confirmatory role of this old general picture of coal pyrolysis, the isothermal type of coal pyrolysis experiment is not well-suited toward making further mechanistic advances in our understanding of this complex chemical conversion and hence warrants little further discussion.

However, a few results from the isothermal experiments should be noted. In the fast heating experiments to 1000°C in both hydrogen and helium, Runs I2, I4, I7, I8, I9, I12, I13, I14, I17 and I18, a substantial amount of the total gaseous sulfur evolved is in the form of carbon disulfide, while in the experiments employing the slower heating rates, Runs I15, I16, I19, the CS₂ evolution is quite small. Also the slower heating rate produces a substantial increase in the desulfurization efficiency as previously observed by Snow³. All of these isothermal experiments were conducted using coal in the 20/40 mesh range of particle size except for run I15 which used a 100/200 mesh cut. This run, which was otherwise similar to run I16, gave, contrary to expectations, a lower desulfurization factor than obtained for the larger particle size. However, upon examination of the solid residue from run I15 after completion of the experiment, it was found that the fine coal had agglomerated into a dense solid mass. Therefore, it appears that the effective particle size for this experiment, at least during the high temperature part of the experiment, was in fact larger rather than smaller.

Non-isothermal Experiments

In the non-isothermal pyrolysis studies, the theoretical basis of which was developed in Chapter II, the primary data obtained are the rates of evolution of the various gases

$$\frac{dV_i}{dt} = M \frac{dV_i}{dT} \quad (51)$$

as functions of the temperature, where M is the heating rate of the solid coal sample. Such data which provide immediately a very informative picture of the overall pyrolysis in hydrogen and helium are shown in Figures 4 and 5, respectively.

The composition of the gas evolved is quite complex with H₂, CH₄, H₂S, C₂H₆, C₃H₈, C₆H₆, CO, CO₂, CH₃SH, CS₂, and SO₂ having been firmly identified in relative abundances that are very sensitive to the reaction temperature. This variation of gaseous product composition with temperature is not unexpected since such a wide variety of products are undoubtedly formed by a set of parallel and consecutive chemical reactions, each proceeding at a temperature-dependent rate in accord with its frequency factor and activation energy.

It is seen that with both flush gases the maximum rate of total gas evolution occurs at 425°C, coincident with the maximum evolution-rate of ethane and propane (and other hydrocarbons at lower concentrations, not shown in the figures). Below 500°C the evolution rate of

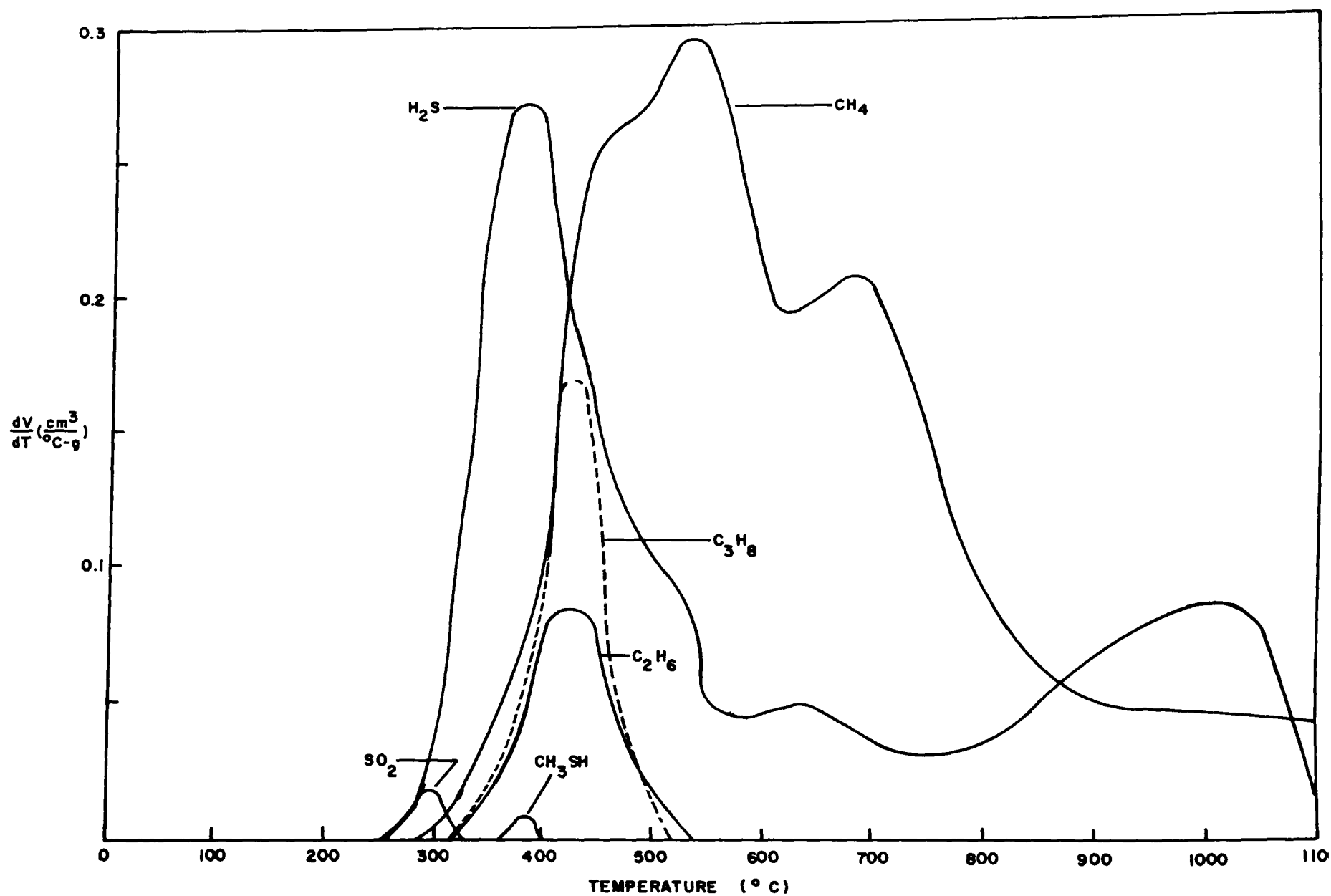


Figure 4. Gas evolution curve for 5% sulfur coal pyrolyzed in hydrogen showing sulfur containing species and major hydrocarbons, Run N3, see Table IV for experimental details.

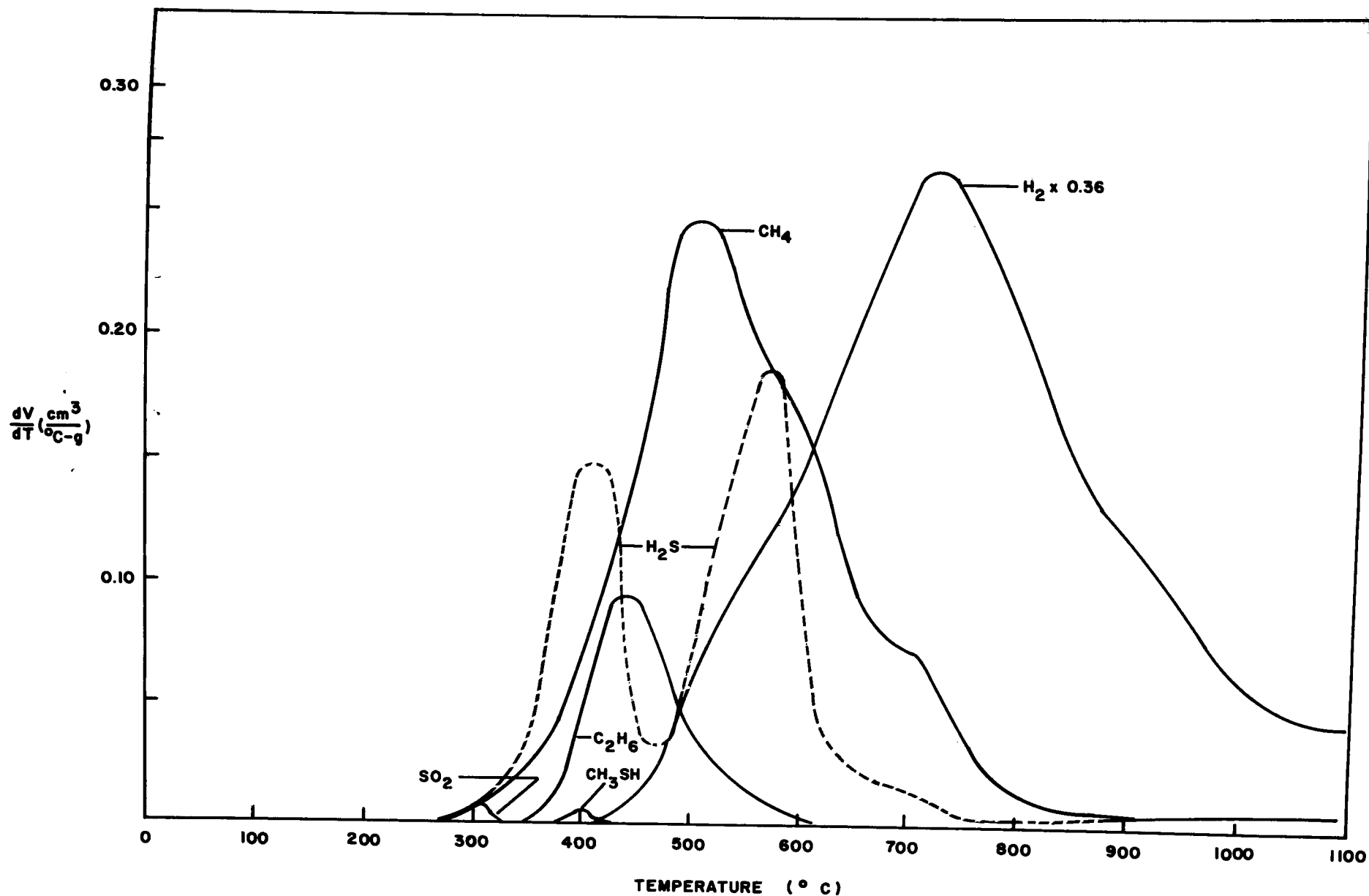
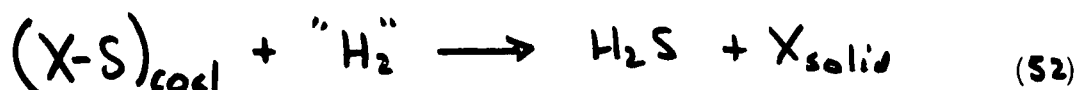


Figure 5. Gas evolution curve for 5% sulfur coal pyrolyzed in helium showing sulfur containing species and major hydrocarbons, Run N4, see Table V for experimental details.

methane is comparable with both flush gases but above 500°C the rate of methane formation is significantly greater in the hydrogen atmosphere. Hydrogen evolution from the coal was not measurable in the hydrogen-atmosphere experiments but in the case of a helium atmosphere, for temperatures above 550°C, it proceeds at a higher rate than that of any other gaseous product. Moreover, the area under the evolution-rate curve shows hydrogen to be the most abundant product of a complete coal-pyrolysis. While interesting and complex problems in their own right, the evolution-rates and evolution-mechanisms of the hydrogen and hydrocarbons are not of prime interest in this research and, except where they bear directly upon the desulfurization kinetics, will not be discussed further.

All of the sulfur-containing species show maxima in their evolution rates below the maximum rate of total gas evolution, namely, 425°C. The maximum rate of evolution of sulfur dioxide is at 300°C with both hydrogen and helium flush gases. The maximum evolution-rate of methyl mercaptan and the first maximum (with increasing temperature) in the evolution rate of hydrogen sulfide occur at 375°C in a hydrogen atmosphere but are shifted to 400°C when helium is used as a flush gas. The second maximum in the hydrogen sulfide evolution-rate that is observed in the helium atmosphere does not correspond to any peak found in the hydrogen atmosphere, but interestingly does appear to coincide with the onset of hydrogen production in the helium atmosphere. This coincidence suggests that the second maximum found in helium may be due to a reaction of sulfur in the coal with hydrogen produced

from the coal; this second maximum would not, of course, be observed in the hydrogen atmosphere because of the constant presence throughout the experiment of large amounts of hydrogen. For convenience, the hydrogen sulfide evolution curves for the two flush gases are shown together in Figure 6. Here we see that the low-temperature maximum in helium is lower in amplitude and lies at a temperature 25° higher than the corresponding maximum in hydrogen. Such a shift would be expected if a rate process similar to that described in Section II-2 viz;



was involved in both atmospheres. The term " H_2 " denotes hydrogen in close proximity to sulfur in the coal and (since it is supplied externally) would be greater in the case of the hydrogen atmosphere than is the case of the helium atmosphere. To show that the shift is in the direction predicted theoretically, consider equation (11) as modified for the case of a reactive atmosphere with no back reaction as described in Chapter II-2. Thus for H_2S evolution we have

$$\frac{dV_{H_2S}}{dT} = \frac{V_0 k_0'}{M} \exp \left[- \left(\frac{E'}{RT} + \frac{h_0'}{M} \frac{RT}{E'} e^{-\frac{E'}{RT}} \right) \right] \quad (53)$$

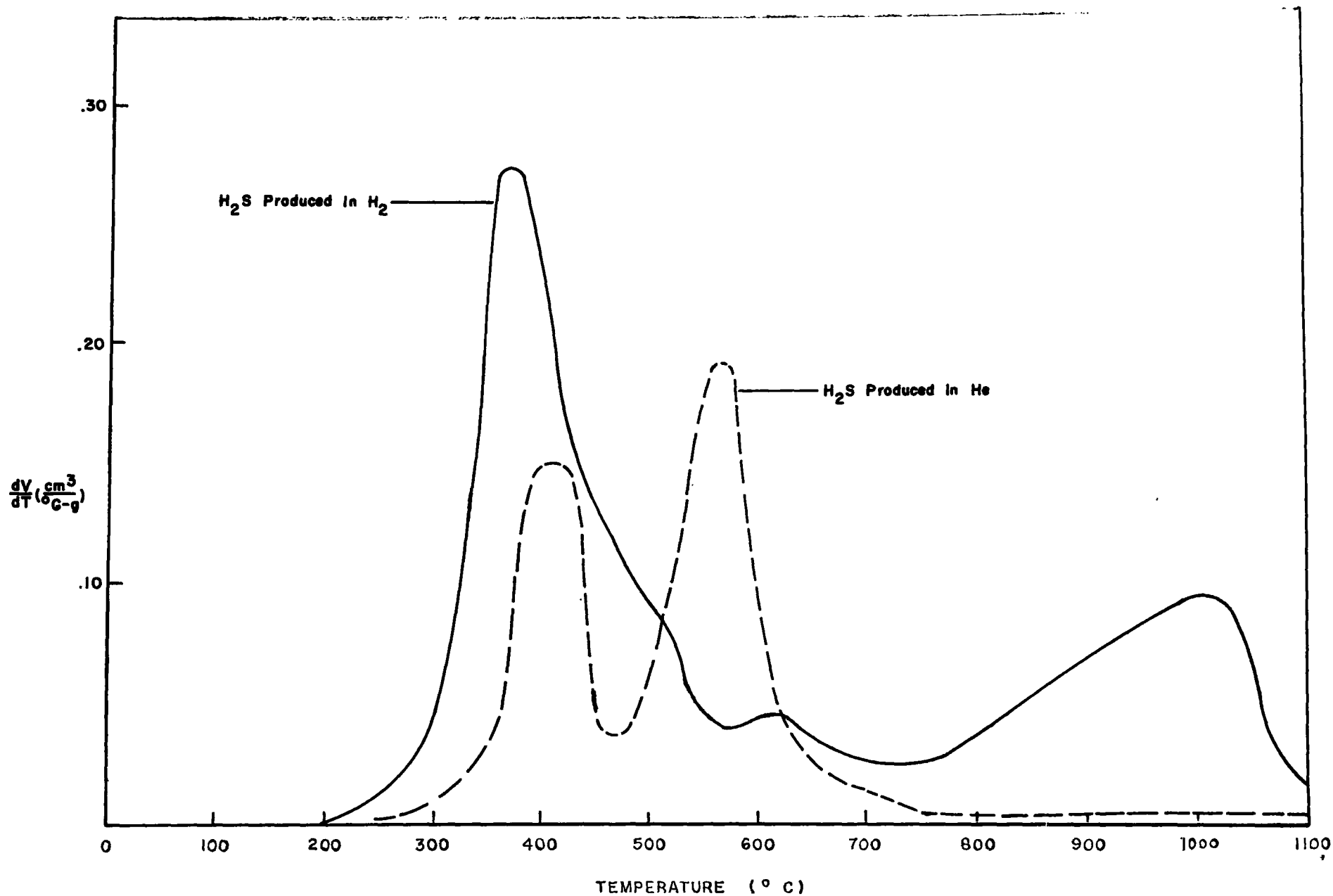


Figure 6. Comparison of H₂S evolution in H₂ atmosphere, Run N3, with H₂S evolution in He atmosphere, Run N4.

where $k_0^1 = k_r [H_2]$. The variation of this rate with $[H_2]$ can be expressed as the variation with the pseudo first-order rate constant k_0^1 . For a maximum in $\frac{dV_{H_2S}}{dT}$ we have then

$$\frac{\partial}{\partial k_0^1} \left(\frac{dV_{H_2S}}{dT} \right) = 0 \quad (54)$$

or

$$1 - \frac{k_0^1}{M} \frac{RT_{max}^2}{E'} e^{-\frac{E'}{RT_{max}}} = 0 \quad (55)$$

This transcendental equation cannot be solved explicitly for the dependence of T_{max} on k_0^1 (and hence on $[H_2]$). However, for a very small temperature shift from some reference temperature, T_0 , it is easily shown that

$$T_{max} \approx \frac{E'}{R \ln \left(\frac{RT_0^2}{ME'} k_0' \right)} = \frac{E'}{R \ln \left(\frac{RT_0^2}{ME'} k_r [H_2] \right)} \quad (56)$$

showing that T_{max} decreases as $[H_2]$ increases. Such a result would be predicted also for the case of a reactive gas with back reaction (Section II-4). We may conclude, then, that the low-temperature maximum in the hydrogen sulfide evolution-rate arises from a reaction whose rate depends upon the concentration of hydrogen in the vicinity of sulfur as well as on the sulfur concentration. The reaction involved cannot be the intramolecular elimination of H_2S from compounds originally contained in the coal, unless such compounds were first hydrogenated in the rate determining step.

Above $750^\circ C$, practically no additional hydrogen sulfide is evolved in a helium atmosphere while in a hydrogen atmosphere a process (or processes) occurs whose rate attains a broad maximum at 1000° .

The overall temperature-(or time) integrated results of the non-isothermal pyrolysis experiments, which are in a form to be compared with the results of the isothermal pyrolyses, are summarized in Tables IV-VII.

The effect of hydrogen flow rate, or gas residence time, was investigated in non-isothermal runs N1, N10, N11, N12, and N23. The effect of helium flow rate was checked in runs N2 and N13. The effect of particle size on the desulfurization kinetics was studied in runs N5, N6, N7, N8 on samples of coke to avoid difficulties due to agglomeration. Most of these experiments were conducted on a 5% sulfur Illinois coal, but some

TABLE IV. SUMMARY OF COAL PYROLYSIS EXPERIMENTAL DATA FOR NON-ISOTHERMAL HYDROGEN RUNS AT ONE ATMOSPHERE.

Run No.	Coal % S	Temp. °C Heating Rate	Residence Time Reaction Time	Coke Yield %	Desulfurization Factor	Coke	Tar	H ₂ S	CS ₂ SO ₂ , CH ₃ SH C ₄ H ₄ S	Total Recover
N1	5.0	25-1100 5°/min.	3.0 sec 4.0 hr	51.6	6.7	10.9	4.5	67.1	0.3 < 0.7	83
N3	5.0	125-1100 6°/min.	3.0 sec 2.7 hr	50.8	4.8	16.1	4.6	73.0	<0.2 1.7	95
N10	5.0	25-1100 5°/min	0.72 sec 4 hr	51.2	9.6	8.5	5.6	67.0	<0.1 9.3	90
N11	5.0	25-1100 5°/min	0.39 sec 3.9 hr	49.9	10.2	7.9	5.0	66.6	<0.1 8.0	88
N12	5.0	25-1100 5°/min	1.7 sec 3.9 hr	52.4	9.1	10.0	5.1	81.3	<0.1 3.4	100
N14	0.87	25-1100 5°/min	0.40 sec 4.0 hr	57.7	3.6	41.6	7.9	123	<0.1 20.4	193
N16	4.2	25-1100 5°/min	3.2 sec 3.9 hr	53.4	3.0	33.4	4.7	89.1	<0.1 6.1	133
N 17	0.87	25-1100 5°/min	3.1 sec 3.9 hr	57.5	3.5	21.2	6.3	40.0	<0.1 27.4	95
N23	4.2	25-900 5°/min	0.031 sec 3.0 hr	56.8	(5)	<0.1	0.7	22.8	<0.1 9.8	33 ⁽⁶⁾

Notes for Table IV

- (1) all 3 gram samples except N23 which was 0.308 gram
- (2) all samples 20/40 mesh coal
- (3) quartz reactor for all runs except N16 in which the stainless steel reactor was used and N17 in which the stainless steel with quartz liner reactor was used.
- (4) in runs where the reaction time exceeds that required for the temperature rise at the given rate, the temperature was held constant at the maximum temp. for approx. 20 minutes.
- (5) since sulfur in the coke was not detected above the limits of sensitivity of 0.01 mg S, a desulfurization factor cannot be calculated.
- (6) sulfur recovery was low because gas trapping at the high flow rate used (1 l/min) was inefficient.

TABLE V. SUMMARY OF COAL PYROLYSIS EXPERIMENTAL DATA
FOR NON-ISOTHERMAL HELIUM RUNS.

Run No.	Coal % S	Temp °C Heating Rate	Residence Time Reaction Time	Coke %	Desulfurization Factor	Sulfur Recovery, %					Total Recovery
						Coke	Tar	H ₂ S	CS ₂	SO ₂ CH ₃ SH C ₄ H ₄ S	
N2	5.0	25-1100 5°/min.	3.1 sec. 4.0 hr. (6)	56.7	0.96	44.7	2.3	34.6	0.9	4.4	87
N4	5.0	150-1100 5°/min.	3.0 sec. 3.2 hr.	53.3	← (5) →						
N13	5.0	25-1100 5°/min.	0.36 sec. 4.0 hr.	57.3	1.8	41.8	5.7	63.4	<0.1	4.3	115
N15	0.87	25-1100 5°/min.	0.39 sec. 3.6 hr.	61.3	1.9	49.5	6.6	69.5	<0.1	17.9	143

Notes

- (1) all 3 gram samples.
- (2) all samples 20/40 mesh coal.
- (3) quartz reactor for all runs.
- (4) purge gas at 1 atmosphere pressure.
- (5) coke sample lost during analysis, so these figures unavailable.
- (6) in cases where the reaction time exceeds that required for the temperature rise at the given rate, the temperature was held constant at the maximum temperature for approximately 20 minutes.

TABLE VI. SUMMARY OF COAL PYROLYSIS EXPERIMENTAL DATA FOR NON-
ISOTHERMAL HYDROGEN RUNS AT DIFFERENT PRESSURES

Run No.	Pressure atm.	Temp. °C Heating Rate	Residence Time Reaction Time	Coke %	Desulfuri- zation Factor	Sulfur Recovery, %				SO ₂ CH ₃ SH C ₄ H ₄ S	Total Recovery
						Coke	Tar	H ₂ S	CS ₂		
N18	5	25-1100 5°/min.	15.5 sec. 3.8 hr.	47.3	1.2	24.3	2.7	21.9	1.4	3.4	54
N19	5	25-1100 5°/min.	2.0 sec. 3.4 hr.	35.7	7.8	13.5	3.0	95.4	<0.1	6.1	118
N20	5	25-1100 33°/min.	3.7 sec. 1.8 hr.	40.1	5.1	18.0	4.5	82.5	<0.1	4.4	109
N21	1/8 ⁽⁵⁾	25-1100 5°/min.	0.37 3.4 hr.	56.0	1.9	26.6	3.8	46.4	<0.1	2.0	79

Notes

- (1) all 3.0 gram samples except N20 which is 6.0 gram.
- (2) all samples 20/40 mesh coal with 4.2% sulfur.
- (3) stainless steel reactor with quartz liner used for all runs except N21 in which quartz reactor was used.
- (4) in runs where the reaction time exceeds that required for the temperature rise at the given rate, the temperature was held constant at the maximum temperature for that time.
- (5) purge gas was a hydrogen-helium mixture of 1/8 atmosphere hydrogen and 7/8 atmosphere helium.

TABLE VII. SUMMARY OF COKE PYROLYSIS EXPERIMENTAL DATA FOR NON-ISOTHERMAL HYDROGEN RUNS ON COKES OF DIFFERENT MESH SIZE.

Run No.	Coke, % S Mesh	Temp. °C Heating Rate	Residence Time Reaction Time ⁽⁴⁾	Coke %	Desulfurization Factor ⁽⁵⁾	Sulfur Recovery, %		
						Coke	H ₂ S	Total Recovery
N5	4.91 20/40	25-1100 4°/min.	1.5 sec. 4.4 hr.	89.2	4.9	27.9	53.7	82
N6	4.65 40/100	25-1100 5°/min.	1.5 sec. 4.1 hr.	87.0	9.6	17.5	64.3	82
N7	3.76 100/200	25-1100 5°/min.	1.4 sec. 4.3 hr.	82.5	9.1	22.6	76.1	99
N8	3.72 minus 200	25-1100 5°/min.	1.5 sec. 4 hr.	73.1	10.4	20.3	78.6	99

Notes

- (1) all 1.5 gram samples.
- (2) quartz reactor for all runs.
- (3) purge gas at 1 atmosphere pressure.
- (4) reaction time includes approximately 20 minute period at end of run when the sample was held constant at the maximum temperature.
- (5) desulfurization factor was calculated based on the original coal sample from which the coke was prepared, see Run 119.
- (6) the CS₂, SO₂, CH₃SH and C₄H₄S % S recovery was < 0.1% in all runs.

comparison measurements were conducted on a 1% sulfur Illinois coal in Runs N14, N15, and N17. Analytical data for these coals are summarized in Table I of Chapter III. The effect of hydrogen pressure was studied in runs N18, N19, N20, and N21 and the results are summarized in Table VI.

These results indicate that increasing the hydrogen pressure from 1 atmosphere to 5 atmospheres, at constant gas residence time, does not significantly increase the desulfurization factor under the experimental conditions employed. Additional work on the effect of hydrogen pressure on the reaction kinetics is required. The results on the 1% sulfur coal indicate that the desulfurization behavior of this coal is qualitatively similar to that for the 5% sulfur coal. Further work is required to establish quantitative differences and to correlate these differences with differences in amounts and forms of sulfur in the coals.

Investigations of the effect of particle size were carried out on samples of coke, because of the tendency of the coal sample towards agglomeration on heating. The coke samples were prepared from the original coal samples by heating to 900° in helium at 1 atmosphere pressure and holding for 1 hour at this temperature. The coke sample so formed was ground and sieved into four approximately equal portions of 20-40 mesh, 40-100 mesh, 100-200 mesh and minus 200 mesh. Half of each sample was analyzed for total sulfur while the other half was desulfurized in a non-isothermal experiment in a hydrogen atmosphere. The results, summarized in Table VII and Figure 7 indicate that below about 100 mesh there is little or no effect of particle size, under the experimental conditions used in these experiments.

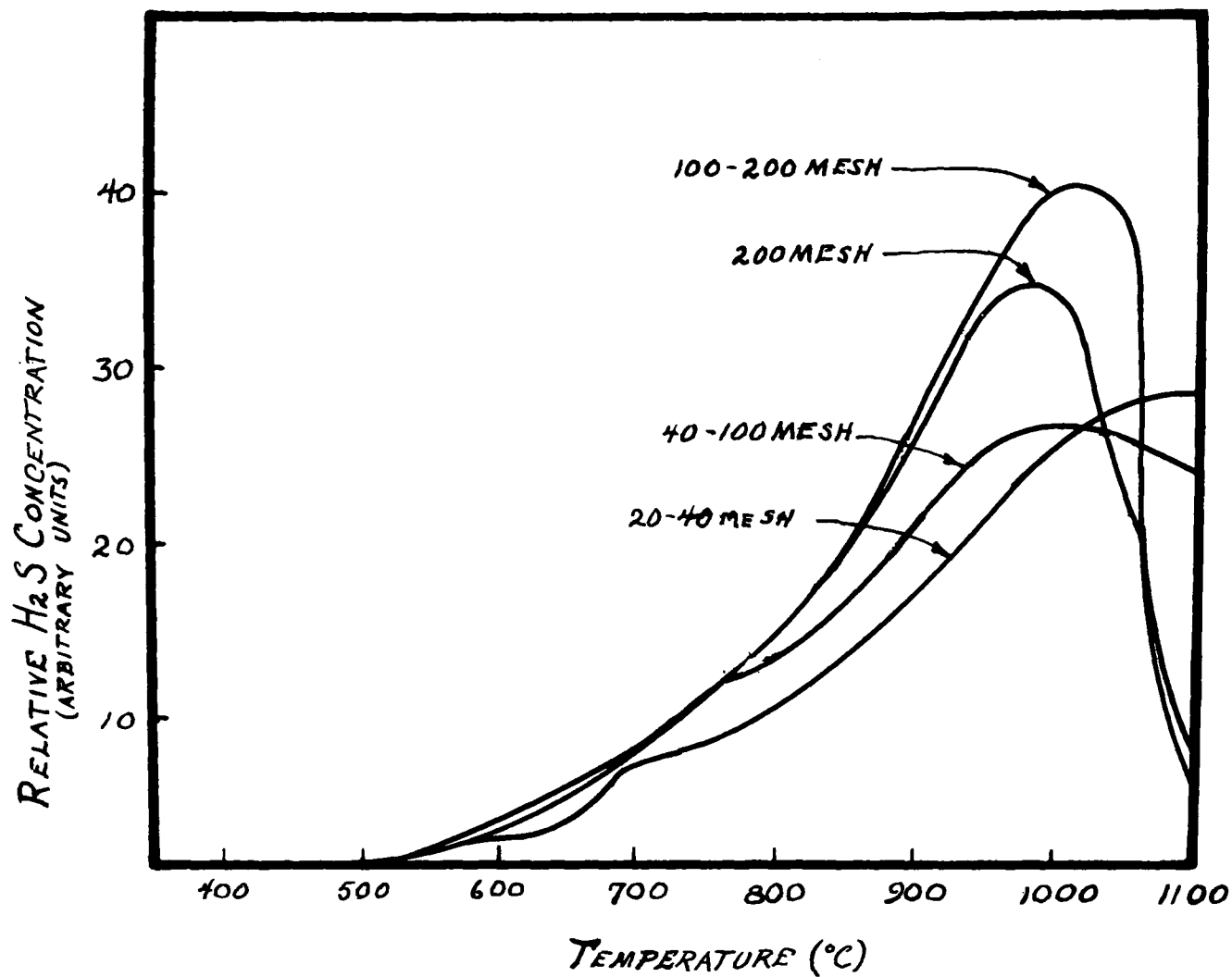
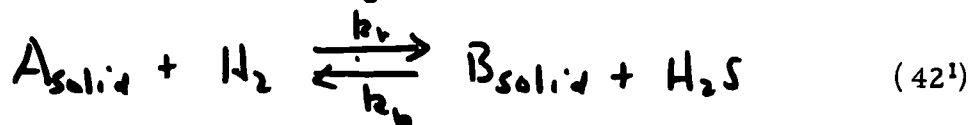


Figure 7. Hydrogen sulfide evolution from different particle size cuts of coke by non-isothermal reaction with H_2 at one atmosphere and 100 ml/min flow rate; heating rate $5^{\circ}C/min$. Coke was prepared by pyrolysis of 5% S coal in He at $900^{\circ}C$ for one hour.

2. KINETICS OF COAL DESULFURIZATION

A complete kinetic treatment, in terms of a set of elementary heterogenous and homogenous reactions and the evaluation of the frequency factors and activation energies of each reaction, is precluded by the immense complexity of the system. Nonetheless, a practical kinetic picture of this complex system that provides a useful framework within which to consider design of a large scale desulfurization process may be obtained. To develop this picture we consider the evolution rates of hydrogen sulfide (since it is by far the most abundant sulfur-containing gas) in terms of the four types of process discussed in the theoretical section, specifically



Analysis of the hydrogen sulfide evolution curves in hydrogen (a typical run being shown in Figure 8) on the basis of the irreversible processes (1¹) and (20¹) and by means of the theoretical treatment described in Section II lead to the conclusion that six separate processes are required to give a reasonable theoretical fit to the data, each process being characterized by a value of k_0 and E . The k_0 value for these studies may be only pseudo first-order but because of the large $[H_2]$ is indistinguishable from true first-order. Certainly in the case of the lowest-temperature process to produce hydrogen sulfide the rate constant determined does depend on $[H_2]$, since, as explained, a measurable shift occurs when helium is substituted for hydrogen. The results obtained from this simplest case of irreversible reaction are shown as apparent frequency factors and apparent activation energies in Table VIII.

Since the apparent kinetic parameters were obtained on the basis of reactions (1¹) and (20¹), one may attribute validity to them only if the reverse reactions of the hydrogen sulfide with the coke are negligible. That such back-reaction complications are probably important has been suggested in earlier studies of coal desulfurization,²⁶ in which it was observed that some of the forward reactions (desulfurization) are accelerated by an increase in flow rate of the flush gas. Moreover, investigations of the inhibiting effect of hydrogen sulfide on desulfurization of low-temperature chars^{27,28} have shown quite conclusively that the reverse reactions of hydrogen sulfide with coke are important.

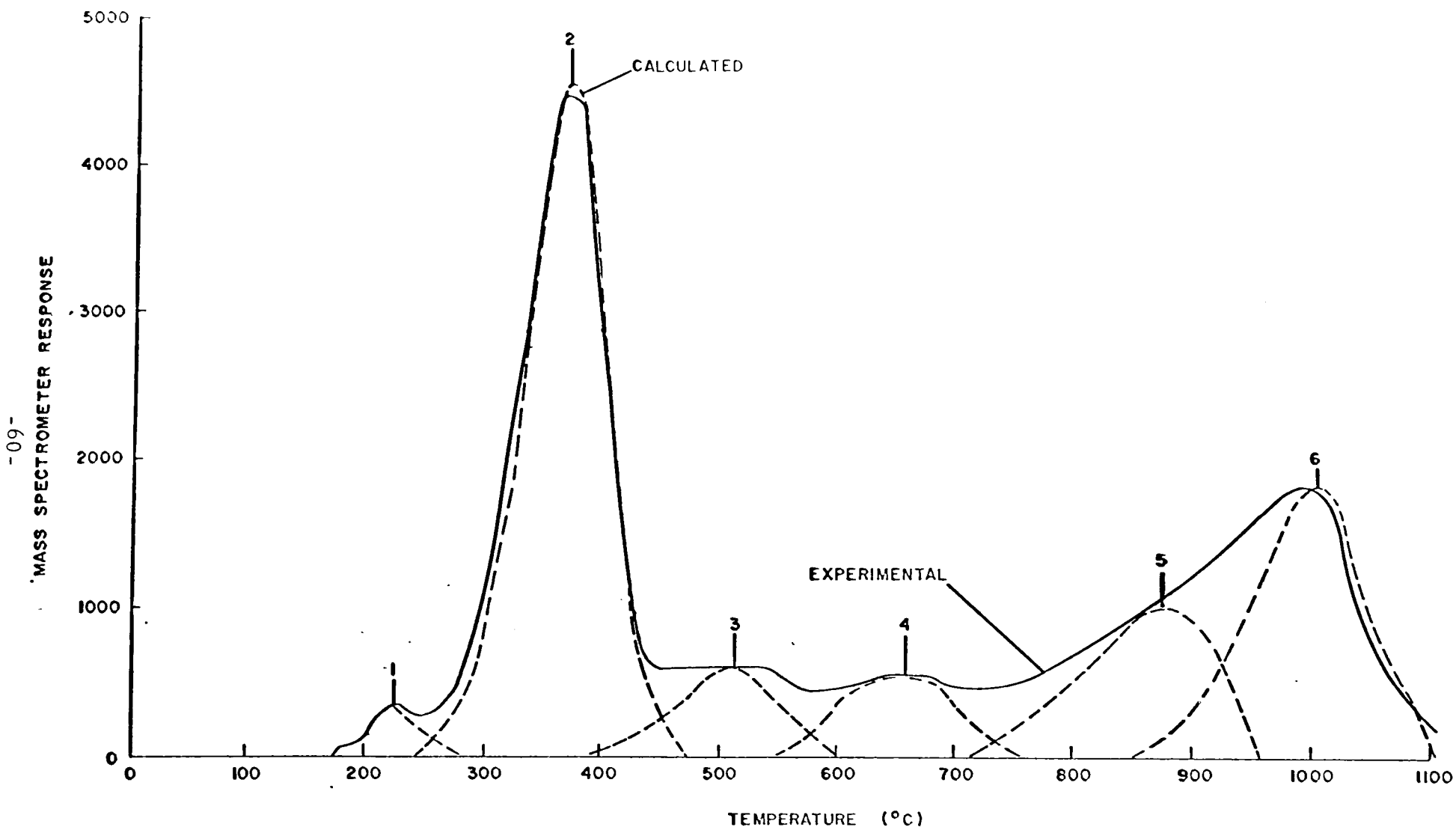


Figure 8.

Analysis of the hydrogen sulfide experimental results on the basis of separate first-order irreversible reactions.

TABLE VIII: APPARENT KINETIC PARAMETERS FOR HYDROGEN SULFIDE EVOLUTION IN THE NON-ISOTHERMAL PYROLYSIS OF 5% SULFUR COAL IN HYDROGEN ATMOSPHERE, RUN N1

<u>Reaction No.</u>	<u>T₀ (°C)</u>	<u>E(kcal/mole)</u>	<u>k₀(min⁻¹)</u>	<u>% of Total</u>
1	225	26	5 x 10 ¹⁰	2
2	380	25	3 x 10 ⁷	43.5
3	510	27	3 x 10 ⁶	7.5
4	650	33	5 x 10 ⁶	8
5	875	43	1 x 10 ⁷	15
6	1000	69	5 x 10 ¹⁰	24

To assess further the possibility of this complication, a series of non-isothermal experiments in hydrogen were conducted at different flow rates of hydrogen, ranging from 100 ml/min to 800 ml/min (Runs N1, 10, 11, 12). The hydrogen sulfide evolution curves obtained in these experiments are shown in Figure 9. The effect of flow rate of flush gas on the prominent high-temperature peak is quite dramatic showing a shift to lower temperatures as the flow rate is increased. The effect on the prominent low-temperature peak is not nearly so pronounced (if indeed it is real) and is opposite in direction. Such shifts with flow rate are in accord with the occurrence of significant back reactions. Furthermore, the direction of the shift is predicted by equation (41) to depend upon whether $E-E_b$ is equal to or greater than zero.

The temperature of the high-temperature maximum is plotted as a function of the mean residence time τ in Figure 10. The extrapolation to $\tau=0$ (infinite flow rate) shows that the position of the high-temperature evolution-rate maximum would be in the range of 600-650°C if no back reaction were occurring. In Figure 11 are shown according to Sections II-2 and II-4 two actual extreme cases, one for no back reaction and one for a fast back reaction. The change of shape, as well as position of the maximum, with flow rate shows that neglect of back reaction of hydrogen sulfide with some components of the solid coke can yield completely misleading results.

To confirm directly the occurrence of a back reaction of hydrogen sulfide with the coke, we prepared a sample of coke from the original coal by pyrolysis in hydrogen at five atmospheres pressure for 1.8 hours, using a hydrogen flow rate of 800 std ml/min. We then passed

RELATIVE PROBABILITY (ARB. UNITS)

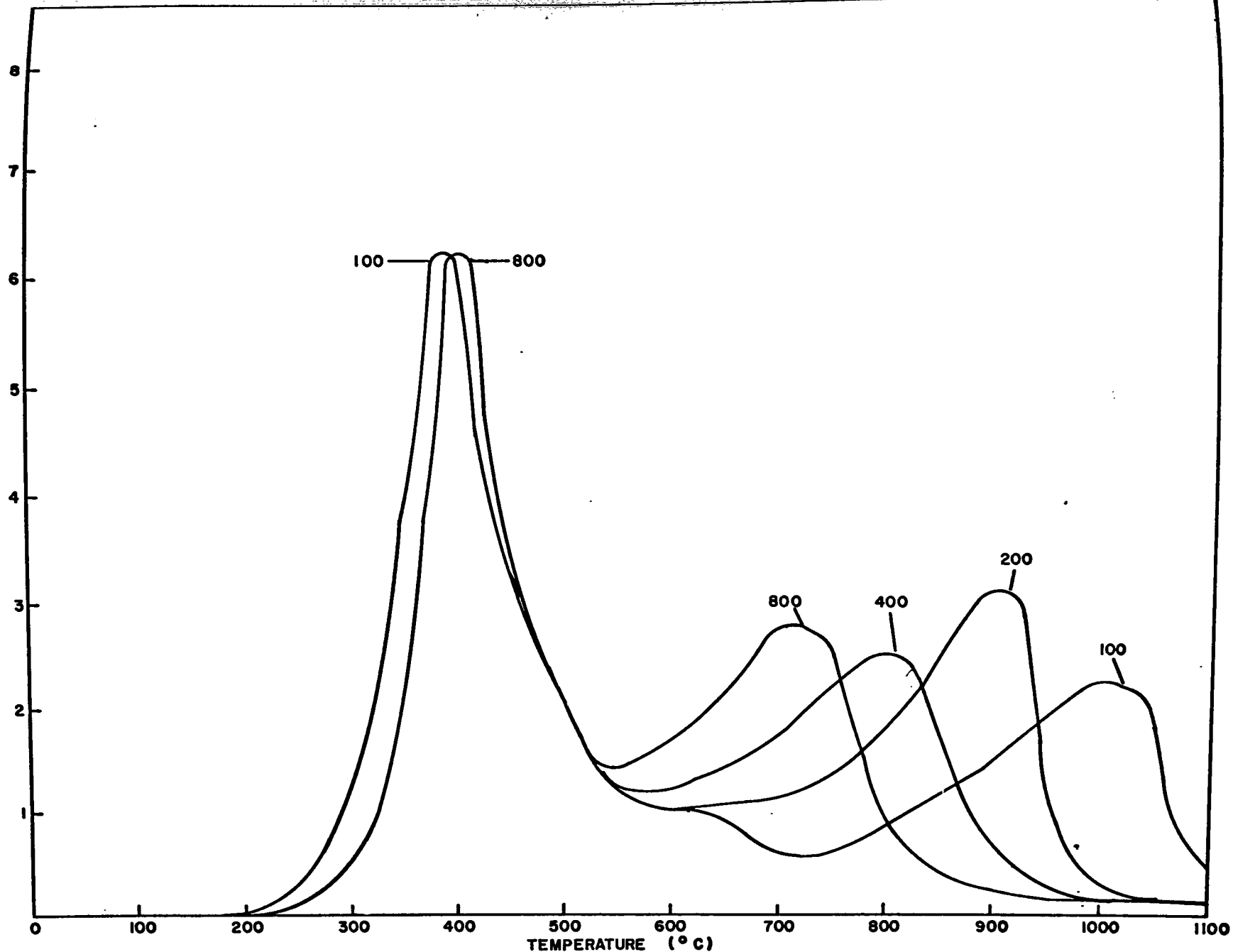


Figure 9. H₂S evolution curve for different hydrogen flow rates. The parameter identifying the curve is hydrogen flow rate in ml/min.

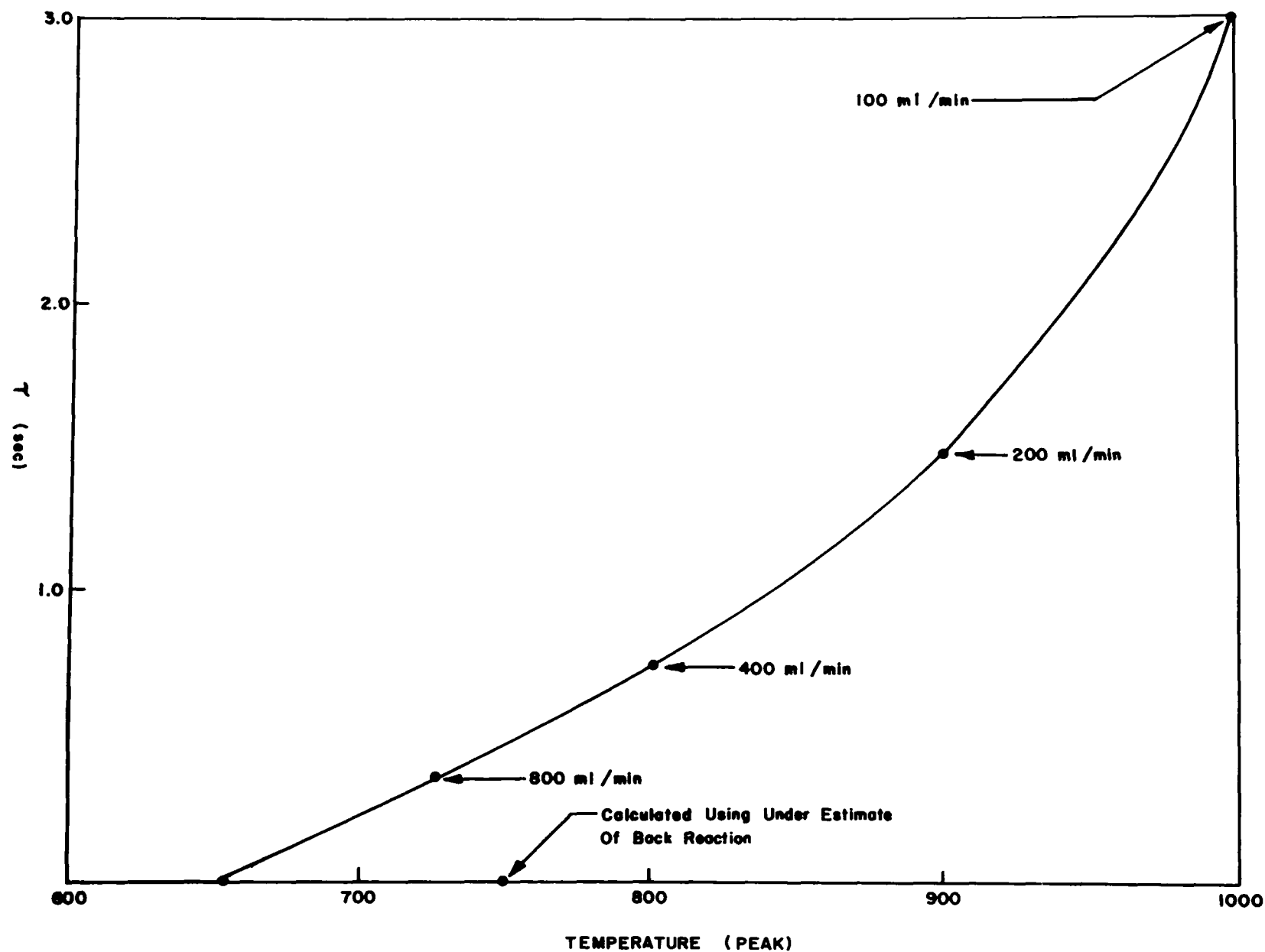


Figure 10. Location of the high temperature peak in the H_2S evolution in hydrogen as a function of mean residence time, τ .

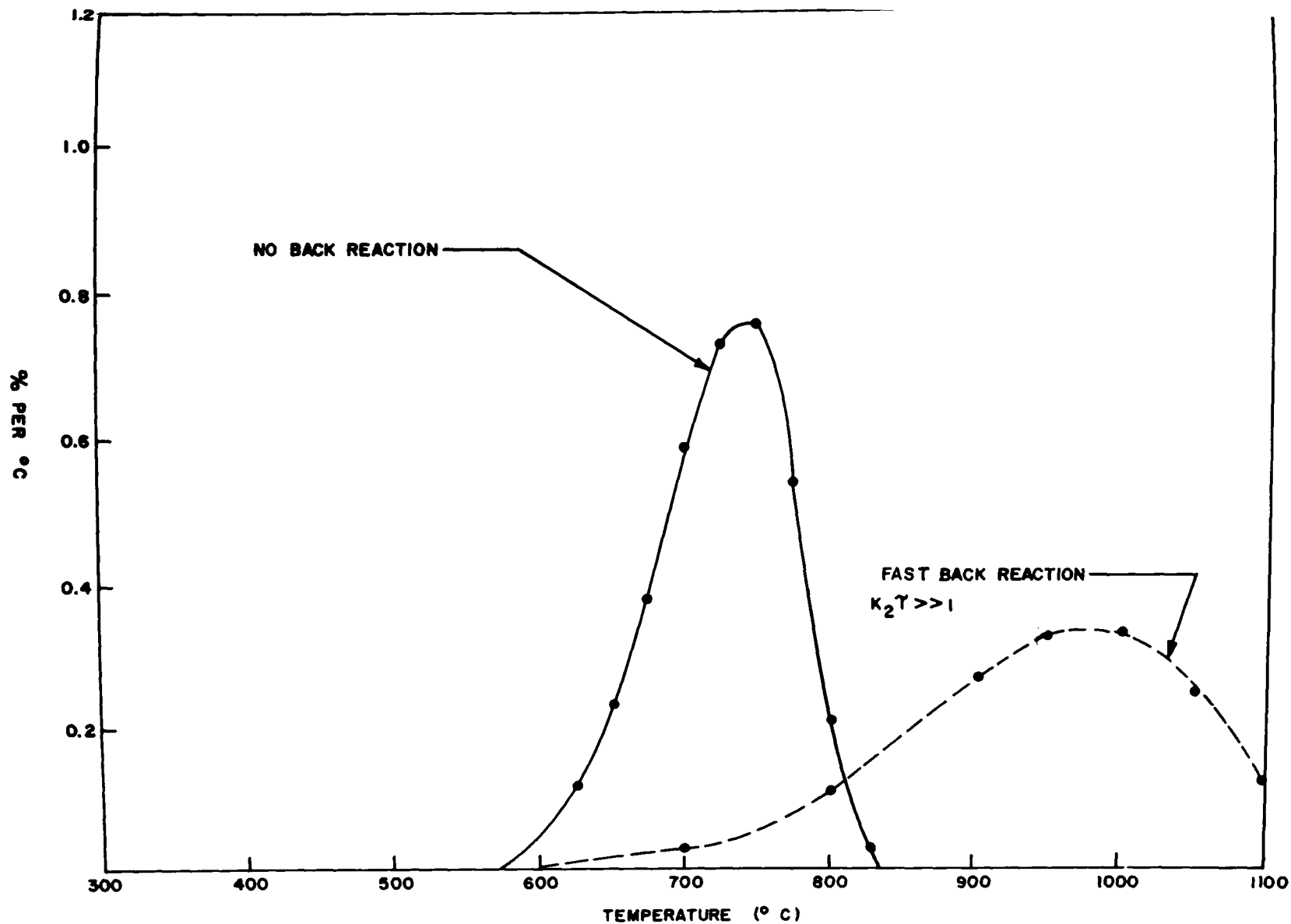


Figure 11. Comparison of the H₂S evolution curve for a fast back reaction with the calculated curve for the case of no back reaction.

a flush gas, comprised of 1000 ppm of hydrogen sulfide in helium, over the coke in a non-isothermal experiment. Monitoring the concentration of hydrogen sulfide in the flush gas as a function of temperature showed conclusively that hydrogen sulfide reacts very rapidly with the coke produced and does so over the temperature range of interest in desulfurization kinetics. In Figure 12 is shown a plot of the outlet concentrations of hydrogen sulfide as a function of temperature. The difference between inlet and outlet hydrogen sulfide concentrations is proportional to the probability of absorption of hydrogen sulfide in the bed and we shall assume that the disappearance is due to back reaction with coke. As can be seen from Figure 12 the hydrogen sulfide consumption begins at about 300°C, rises to a peak at 425°, declines slightly, and then rises continuously until at 775° all of the hydrogen sulfide in the feed gas is consumed by the bed. The integrated results of this experiment are depicted in Table IX.

In the discussion of the theoretical basis of our experimental methods we showed in equation (48) that for such a situation we may write

$$\log \left(\ln \frac{[H_2S]_0}{[H_2S]} \right) = \log(k_{b0}T) - \frac{E_b}{2.303R} \left(\frac{1}{T} \right) \quad (48)$$

Therefore, a log-ln plot of the ratio of the inlet and outlet hydrogen sulfide concentrations versus $\frac{1}{T}$ in accord with equation (48¹) (Figure 13) yields a straight line whose slope is $-\frac{E_b}{2,303R}$ and whose intercept at $\frac{1}{T} = 0$ is $\log k_{b0}T$. From this plot we obtain the following kinetic parameters for the back reaction of hydrogen sulfide with coke:

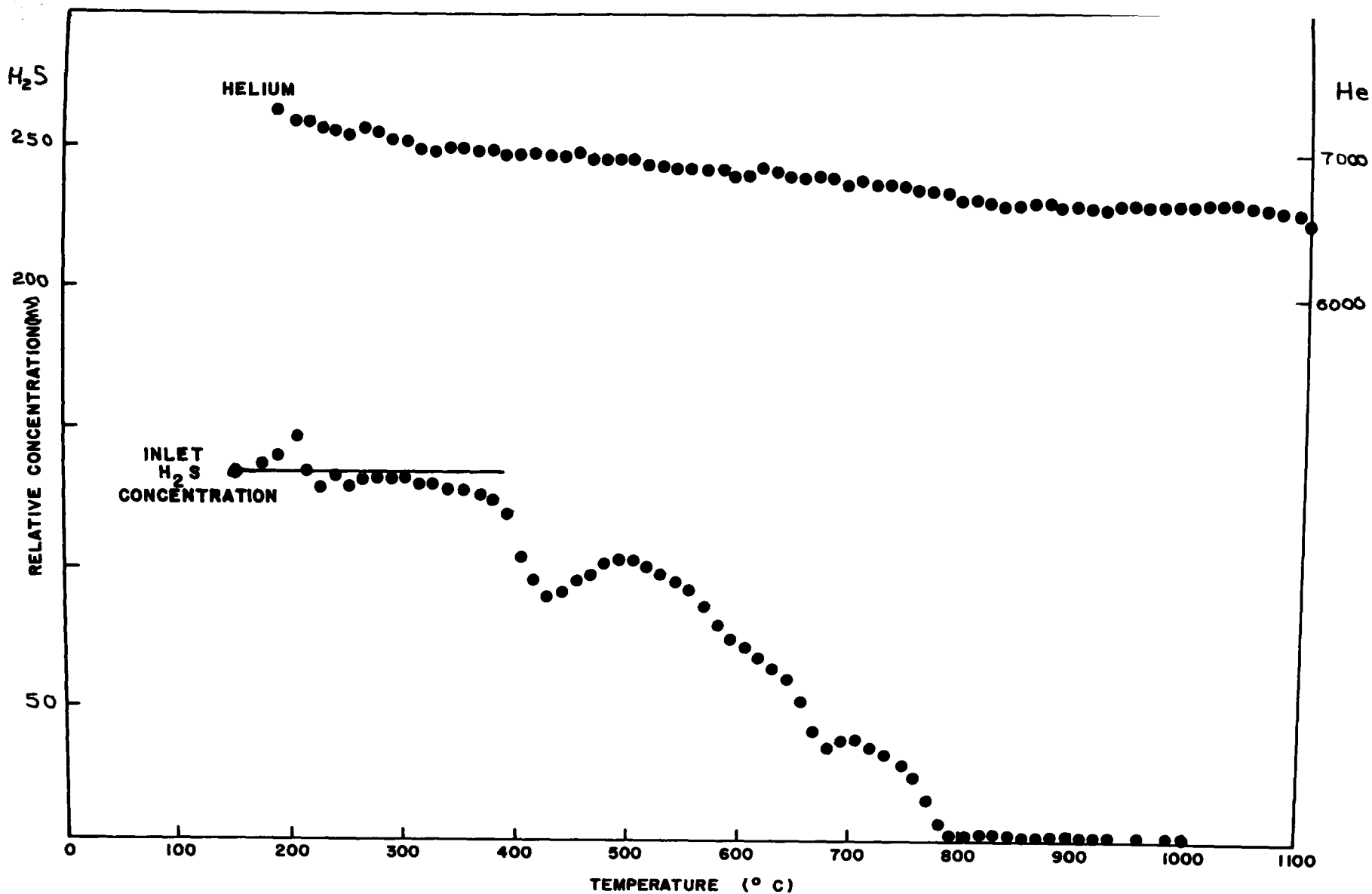


Figure 12. Relative peak heights for hydrogen sulfide and helium sampled from the effluent of a bed of coke for Run N22. The carrier gas contained 0.103% hydrogen sulfide in helium.

TABLE IX BACK REACTION OF HYDROGEN SULFIDE WITH COKE

Run No.	Sample	Wt, g	H ₂ S Concentration	Temp. °C Heating Rate	Residence Time Reaction Time	Solid Residence, %	Sulfur %			
							Coal ⁽⁴⁾	Coke ⁽⁵⁾	Coke	H ₂ S ⁽⁶⁾
N22	coke from Run N20	1.130	0.1% in helium	25-1100 33°/min to 200 7°/min to 1100	0.14 sec. 2.4 hr.	95.1	4.2	1.9	4.2	

Notes

- (1) 20/40 mesh coke.
 (2) quartz reactor.
 (3) purge gas at 1 atmosphere pressure
 (4) in coal sample from which coke was prepared.
 (5) in coke sample before reaction with H₂S.
 (6) in coke sample after reaction with H₂S.

TABLE X PYRITE PYROLYSIS EXPERIMENTAL DATA FOR NON-ISOTHERMAL HYDROGEN RUN

Run No.	Sample	Wt. g % S	Purge Gas	Temp. °C Heating Rate	Residence Time Reaction Time	Solid Residence, %	Sulfur Recovery, %				Total Recovery
							Solid Residue	H ₂ S	CS ₂	SO ₂ CH ₃ SH C ₄ H ₄ S	
N9	pyrite	0.252 52.5	hydrogen	25-1100 5°/min	0.25 sec. 3.8 hr.	41.6	<0.1	102	<0.1	<0.1	102

Notes

- (1) 100/200 mesh pyrite.
 (2) quartz reactor
 (3) purge gas at 1 atmosphere pressure.

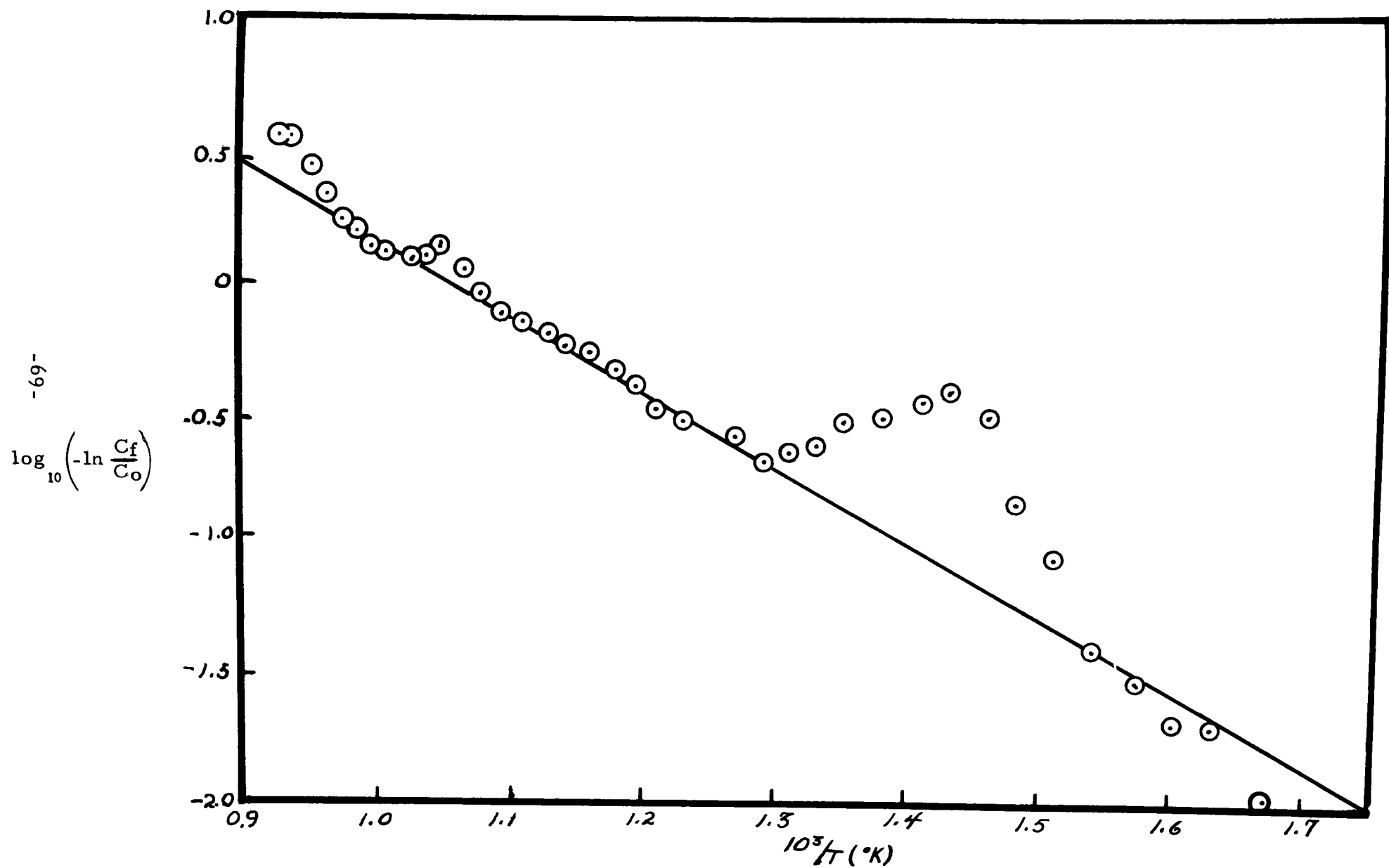


Figure 13. Arrhenius type plot of the data from the direct measurement of the hydrogen sulfide back reaction with coke from Run N22.

$$E_b = 13.1 \text{ kcal/mole}$$

$$k_{b0} = 6 \times 10^5 \text{ min}^{-1} \text{ gram}^{-1}$$

With the kinetic parameters, determined as above, for the back reaction of hydrogen sulfide with coke, we may use the theoretical treatments of Sections II-3 and II-4 to obtain the kinetic parameters of the desulfurization (forward reaction) using non-reactive and reactive flush gases, respectively.

For example, application of the treatment of Section II-4 to the actual high-temperature hydrogen sulfide evolution peak obtained in the experiment with a flow rate of 100 ml/min depicted in Figure 9 yields directly the values

$$E - E_b = 29.8 \text{ kcal/mole}$$

$$\frac{k_o}{\tau k_{b0}} = 6.2 \times 10^3 \text{ min}^{-1} \text{ g}^{-1}$$

In this particular experiment $\tau = 3$ seconds. From τ and the kinetic parameters of the back reaction, namely, k_{b0} and E_b , we obtain from these data the kinetic parameters of this desulfurization reaction as

$$k_o = 1.9 \times 10^8 \text{ min}^{-1} \text{ g}^{-1}$$

$$E = 43 \text{ kcal/mole}$$

When a sample of pure pyrite was desulfurized in a non-isothermal experiment using hydrogen as flush gas, we obtain a sharp evolution peak of hydrogen sulfide at about 500° and a broad lower peak at a higher temperature. The experimental results are shown in Figure 14 and Table X. We conclude that the peak at 500° corresponds to reduction of pyrite to sulfide and that the higher temperature peak corresponds to reaction of the sulfide with hydrogen to form hydrogen sulfide. Since non-isothermal experiments on coal samples show consistently a sharp peak at 380°, we conclude that this lowest-temperature peak in coal desulfurization is due to attack of hydrogen on organic sulfur. Thus, we have identified three separate type-reactions that produce hydrogen sulfide from coal in a hydrogen atmosphere. The kinetic parameters determined for these processes, as just described for the hydrogen sulfide formation from sulfide, are shown as "Indirectly Determined" values in Table XI. Using these kinetic parameters the "expected" three peaks in a coal desulfurization non-isothermal experiment are calculated and shown in Figure 15.

In Section II-5 we pointed out that an alternative way to obtain the kinetic parameters of the desulfurization reaction (forward reaction) would be to measure the apparent values (such as given in Table XI) for various flow rates and extrapolate the apparent values to infinite flow rate

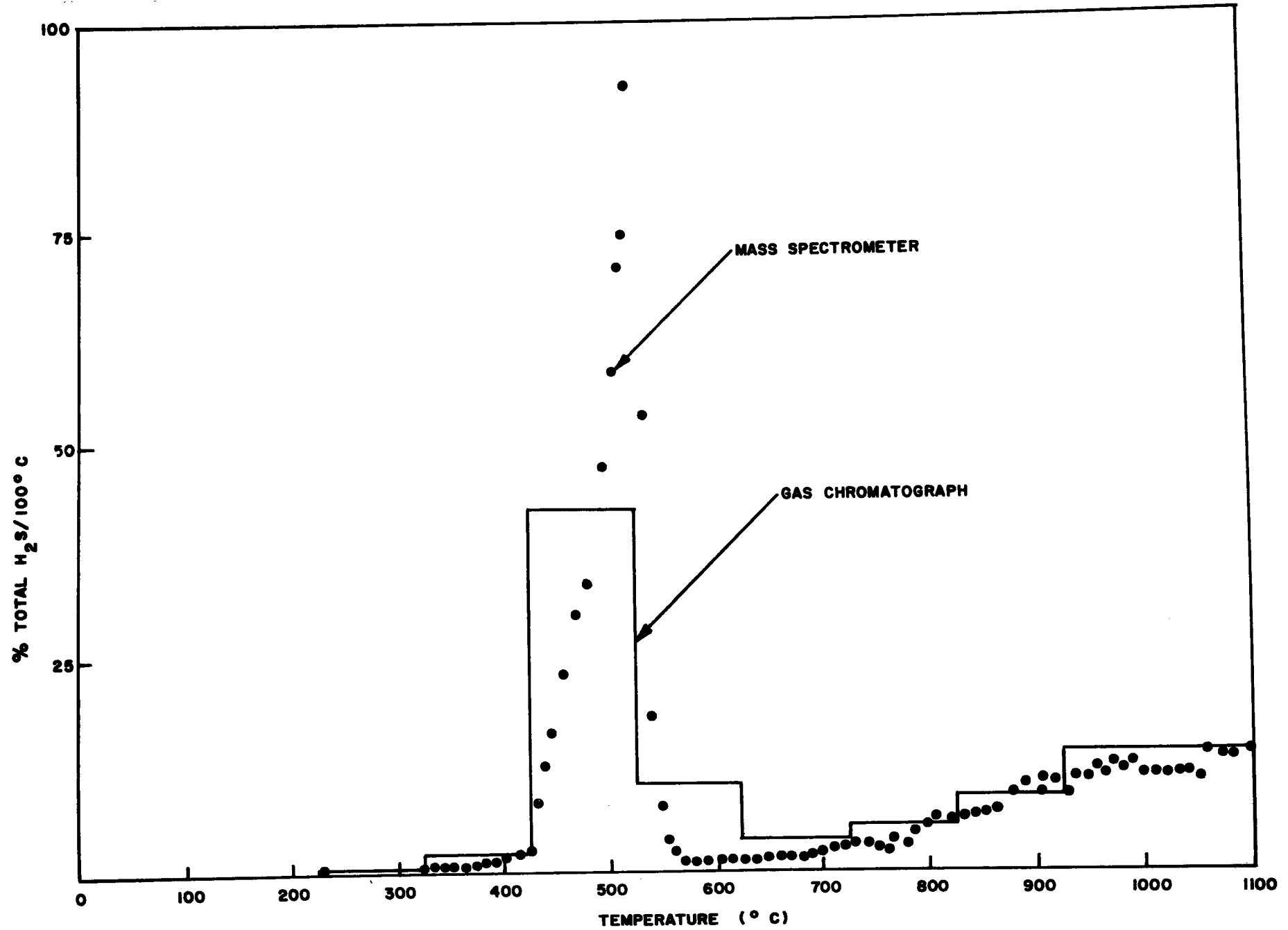


TABLE XI. KINETIC PARAMETERS FOR THE DESULFURIZATION REACTIONS

REACTION NUMBER	1	2	3
IDENTIFICATION (Tentative)	Organic-S + $\begin{cases} \text{H}_2 \\ \text{volatiles} \end{cases}$ $\longrightarrow \text{H}_2\text{S}$	$\text{FeS}_2 + \text{H}_2$ $\longrightarrow \text{H}_2\text{S}$	$\text{FeS} + \text{H}_2$ $\longrightarrow \text{H}_2\text{S}$
INDIRECT DETERMINATION			
E (kcal/mole)		36.5	43
k ₀ (min ⁻¹)		1.9 x 10 ⁹	1.9 x 10 ⁸
DIRECT MEASUREMENT			
E (kcal/mole)	32	38	44
k ₀ (min ⁻¹)	4.2 x 10 ⁹	9.4 x 10 ⁹	2.7 x 10 ¹⁰

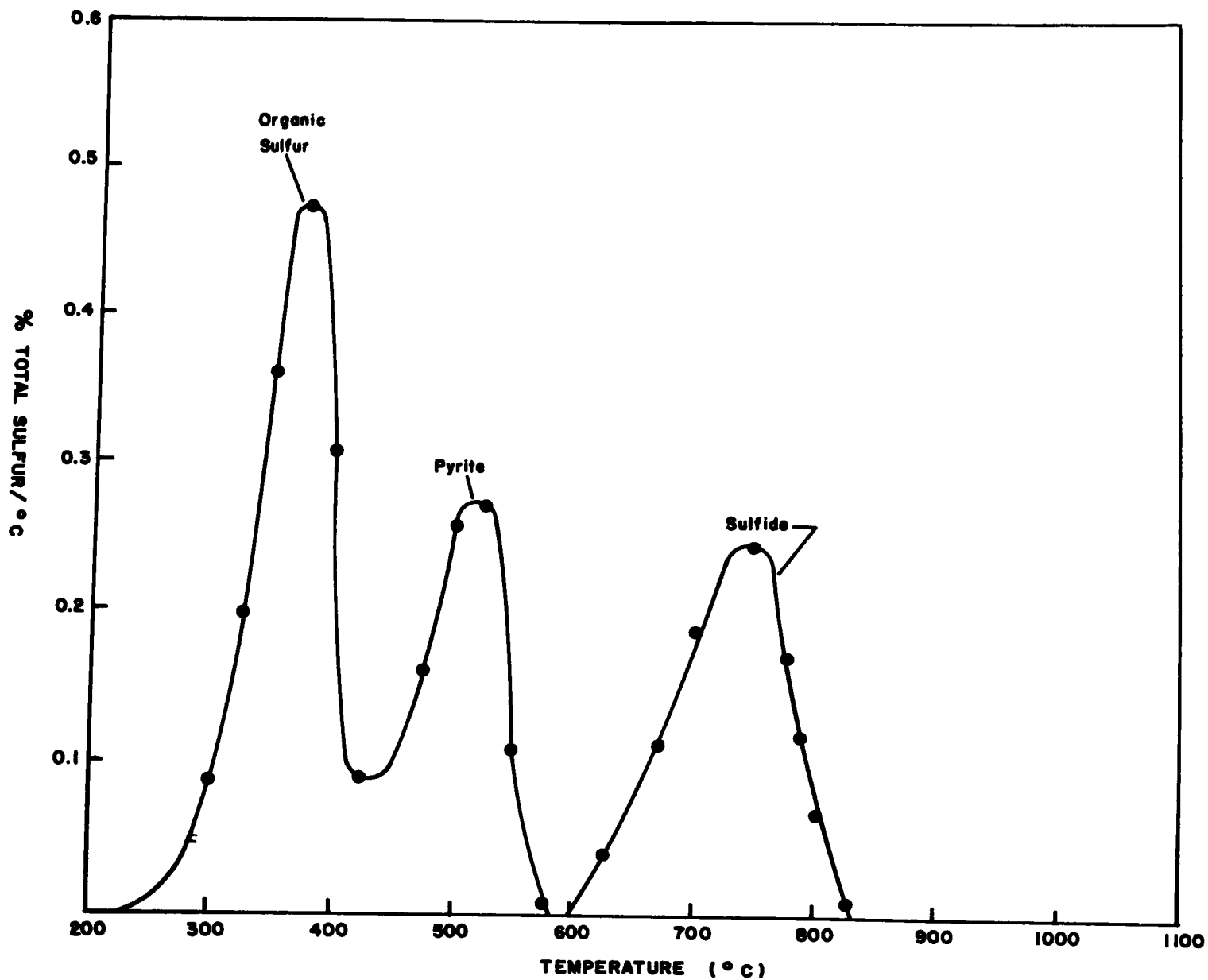


Figure 15. H_2S evolution curve calculated by the indirect method.

or zero residence time. In order to attempt this extrapolation we have studied in Run N23 the evolution curves of hydrogen sulfide in non-isothermal experiments for a residence of 0.03 seconds. This residence time is 100 times smaller than that used in the desulfurization experiment, described above, that permitted calculations of the kinetic parameters of the formation of hydrogen sulfide from sulfide. In this short residence time experiment, the results of which are shown in Figure 16, we find the three peaks expected, in accord with the three kinetic reaction-types identified and shown in Table XI. The locations of these peaks are at 400°C, 500°C and 590°C in reasonable agreement with the expectations shown in Figure 15. Above 650°C there is a tail on the hydrogen sulfide evolution curve extending to 800°C, which is apparently due to some back reaction occurring even at this short residence time. Analysis of these three peaks by the theory described in Section II-2, using the assumption that $\tau = 0.03$ seconds corresponds to an extrapolation to $\tau = 0$, leads to the kinetic parameters shown as "Directly Determined" in Table XI. Considering the extreme rapidity of the back reaction and the assumptions involved in both methods of treatment we consider the agreement as satisfactory. In Figure 17 the rates of the three desulfurization reactions and the hydrogen sulfide back reaction are shown as functions of the temperature, using the "direct" determination.

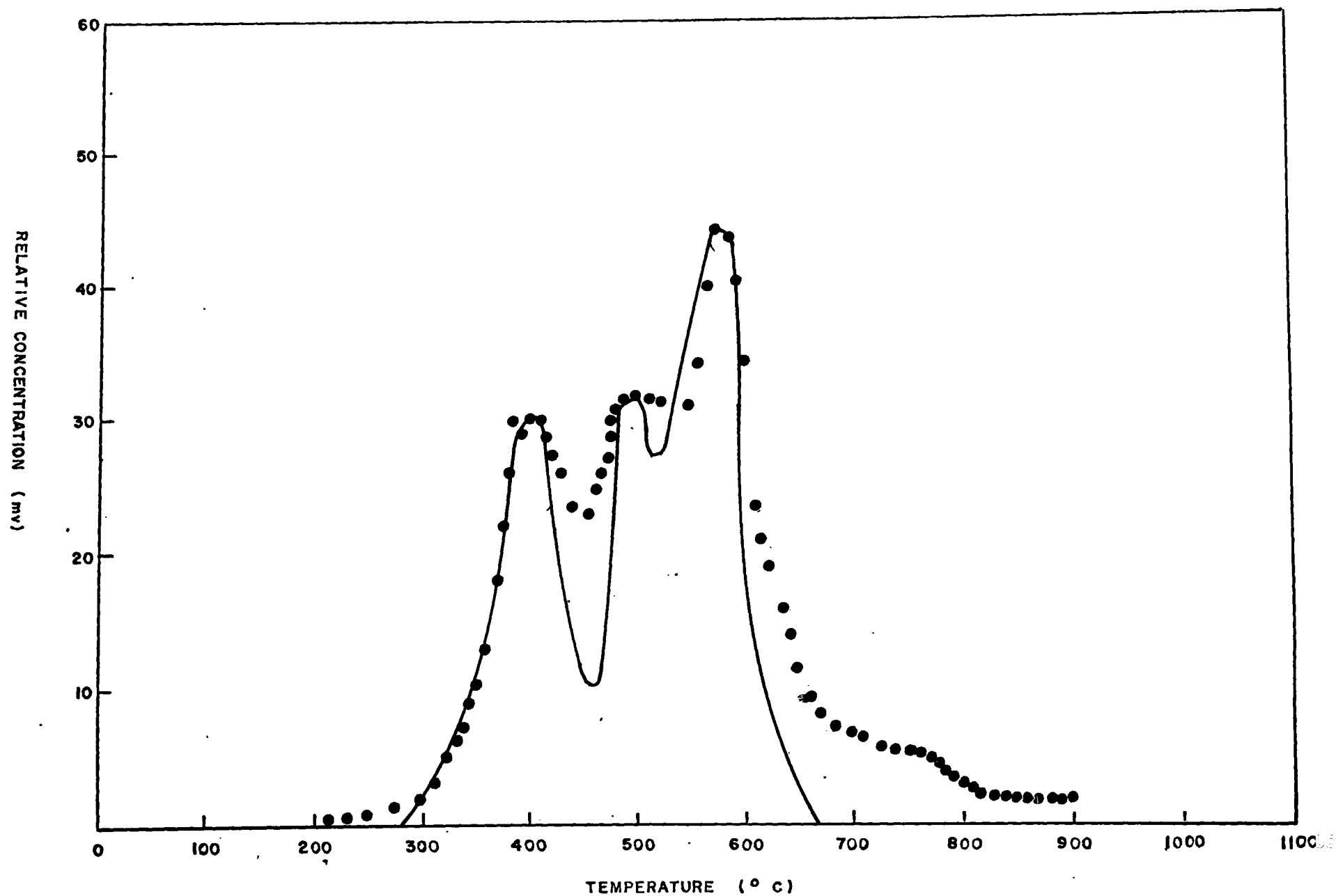


Figure 16. Comparison of the theoretical curves for H_2S evolution in hydrogen with no back reaction with the experimental result from Run N23.

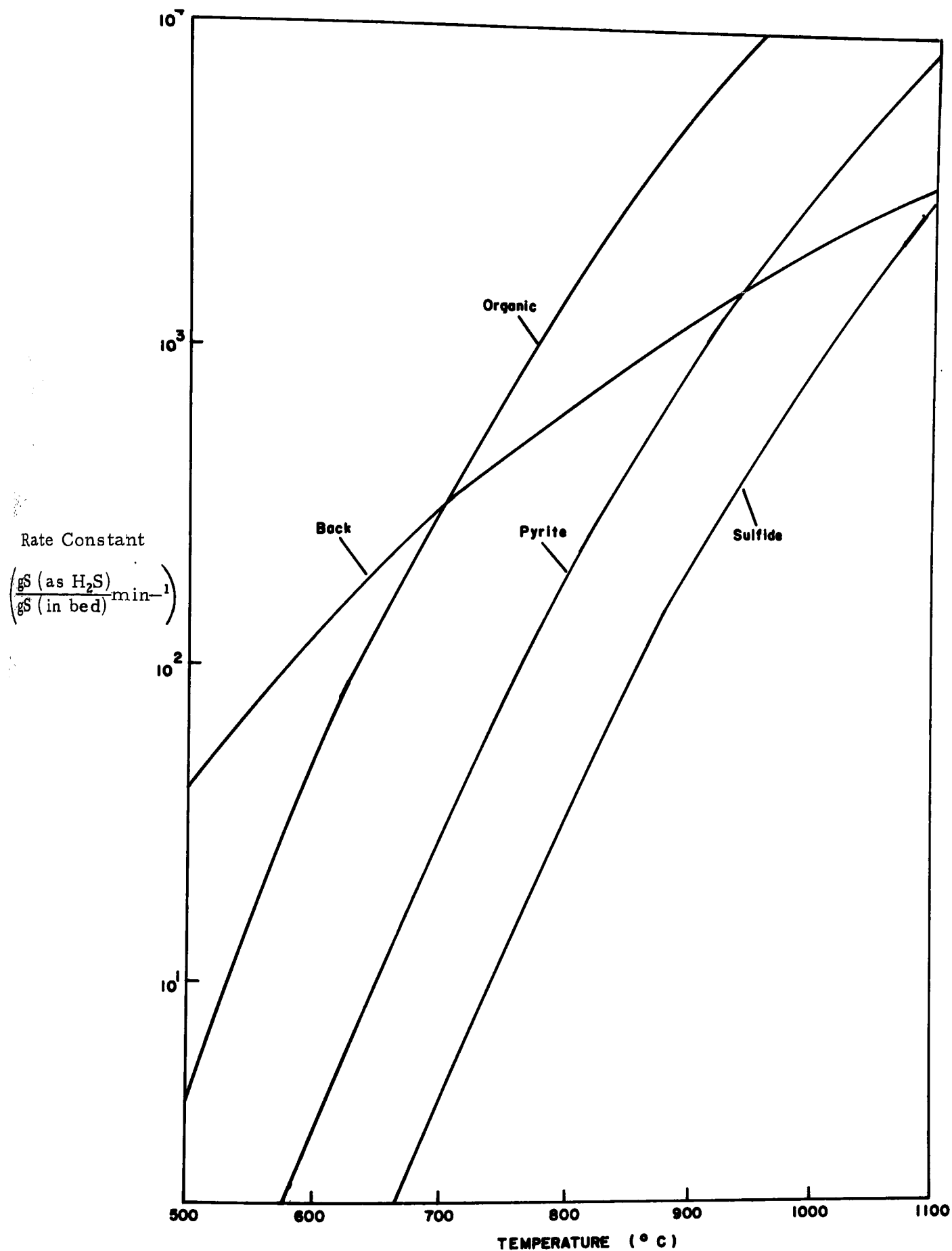


Figure 17. Rates for the desulfurization reactions and the H₂S back reaction as a function of temperature in hydrogen at one atmosphere.

In the short residence time experiment just described, the coke produced was analyzed for combustible sulfur by combustion in oxygen at 1100°C. The condensable gases were trapped at liquid nitrogen temperature and analyzed for sulfur dioxide using the gas chromatograph. No sulfur dioxide was detected when the sensitivity limit corresponded to 0.01 milligrams of sulfur as sulfur dioxide. This result indicates that at least 99.9% of the combustible sulfur was removed by the reaction with hydrogen.

3. FORMS OF SULFUR

The results obtained under conditions of minimal back reaction, or correction for it, indicate that the original assumptions concerning which forms of sulfur are involved in the three desulfurization reactions were somewhat in error. The total organic sulfur cannot be accounted for by the gas evolution peak occurring at 400°C; rather it appears that this peak corresponds to the organic sulfur associated with the volatiles and that the remainder of the organic sulfur is removed along with the inorganic sulfide by the reaction peaking at 590°C. Powell^{2a} has studied the variation of forms of sulfur in the coke as a function of carbonization temperature for several different coals. His results for a high-volatile bituminous Tennessee coal containing approximately 4% sulfur are given in Figure 18 and show the complete reduction of the sulfate below 500°C and the reduction of the pyrite below 525°C. There

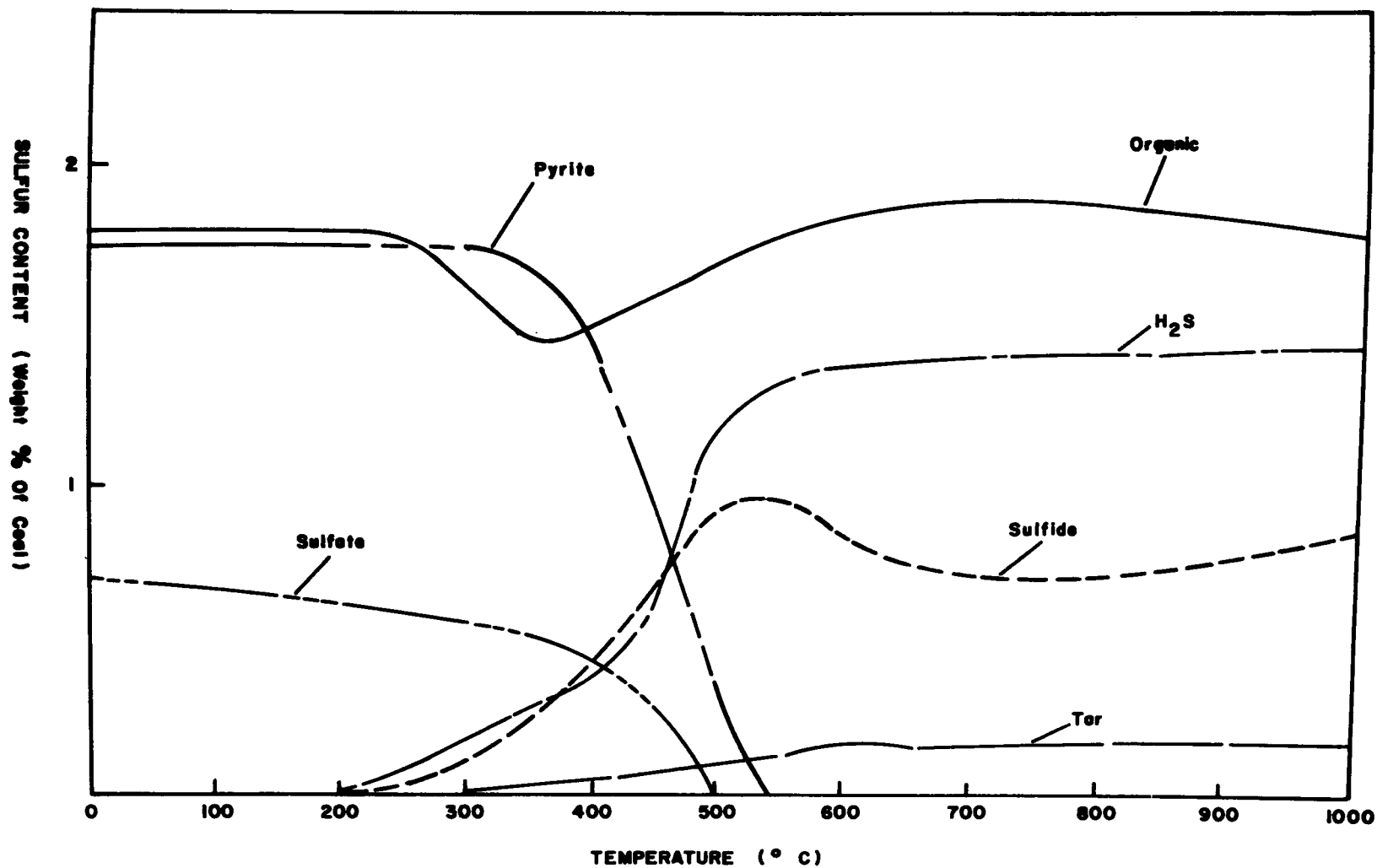


Figure 18. Forms of sulfur in coke as a function of carbonization temperature, from Powell, Reference 2a.

is a minimum in the organic sulfur content at about 370°C. Above 600°C his results show essentially no variation in the forms of sulfur with increasing temperature. From his results and ours it appears to be possible to assign forms of sulfur to each of our three observed reactions. The lower temperature reaction, peaking at 400°C, corresponds to reduction of sulfur associated with the volatile organic material. The second peak at 500°C, as shown by our measurements on pyrite, corresponds to the reduction of pyrite to sulfide. Also, at a temperature below 500°C the sulfate is reduced to sulfide, possibly accompanied by the evolution of a very small part of the sulfur as sulfur dioxide. The process peaking at 590°C corresponds to the reduction of the sulfide and the organic sulfur associated with the fixed carbon. At present it is not clear why these two dissimilar reactions apparently occur as a single process. The reasons for the persistence of organic sulfur and inorganic sulfide in the coke even at high reaction temperatures are clear from our measurements on the kinetics of the back reaction. Under the conditions at which Powell's experiments^{2a} were performed, and under the conditions of most of our experiments, the back reaction of hydrogen sulfide with the coke is so fast at high temperatures that the probability of hydrogen sulfide escaping from the bed is extremely small. The products of these back reactions are apparently both organic sulfur species and inorganic sulfide.

V. CONCLUSIONS

As a direct result of the studies described in this report we have reached the following conclusions pertinent to development of a practical coal desulfurization process.

1. The non-isothermal method is an extremely powerful technique for obtaining the kinetic data necessary for the rational development of coal desulfurization processes.
2. The back reaction of hydrogen sulfide with coke is the most important factor limiting the rate and efficiency of desulfurization.
3. Practical desulfurization can possibly be accomplished during pyrolysis and without complete gasification by intimately mixing a suitable sulfur absorbent with the coal in the pyrolyzing reactor, provided a sulfur absorbent can be found possessing the following properties:
 - (a) The reaction of H_2S with the absorbent must be competitive with the reactions of H_2S with coke under the conditions for which the primary desulfurization reactions proceed at practical rates.
 - (b) Reactions of hydrogen and other gases present in the reactor with the sulfur-laden absorbent to desorb sulfur compounds must be slow compared to the absorption reactions.
 - (c) The absorbent must be such that the sulfur-free coke can be physically separated from the absorbent or such that the coke can be gasified without causing the release of the sulfur housed by the absorbent.

4. The rate of the slowest desulfurization reaction is sufficiently fast at 750°C and one atmosphere of hydrogen that at least 99% desulfurization can be accomplished with a reaction time of 0.5 minutes, provided the sulfur absorbent competes effectively with the coke for the hydrogen sulfide under these conditions. The desulfurization reaction rates are increased at higher hydrogen pressures and the frequency factors for the reactions are probably proportional to hydrogen pressure in the range near one atmosphere. However, precise measurements of the kinetic effect of hydrogen pressure is obscured in the present results by the effect of the back reaction. When high-volatile bituminous coals are used, the hydrogen produced from the coal may be an adequate source.

5. Below about 0.1 mm the effect of particle size on the reaction kinetics appears to be small. The small effect of particle size observed in this work is possibly due to variation in the actual residence time used in the studies on particle size effects. Since the effect of the back reaction was not understood at the time these experiments were conducted, adequate control over the appropriate reaction variables was not exercised.

6. Heating rate effects are probably due to the fast back reaction. At fast heating rates the velocity of the back reaction becomes very large before any substantial amount of hydrogen sulfide can escape from the bed, thus slowing the overall rate of the desulfurization reactions. In pyrolysis of coal mixed with a suitable sulfur absorbent the effect of heating rate should be much smaller.

These conclusions indicate that desulfurization during coal gasifications prior to combustion for power may be feasible and possibly economically practical, provided a suitable sulfur absorbent can be found.

The recent work of Squires²⁹ suggests that calcined dolomites possess many of the required properties. Substantial additional work is required to elucidate further the kinetics of the reactions involved in the desulfurization of coal; to establish the generality with which the present results apply to a variety of coals; to identify suitable high-temperature sulfur absorbents; and to determine the kinetics of the pertinent absorption and regeneration reactions. Also additional data on the kinetics of coal gasification reactions will probably be required to complete the laboratory evaluation and development of a practical process.

VI. REFERENCES

1. (a) H.H. Lowry, editor, "Chemistry of Coal Utilization", Vols. I and II, John Wiley and Sons, Inc., New York 1945.
(b) H.H. Lowry, editor, "Chemistry of Coal Utilization", Supplement, John Wiley and Sons, Inc., New York 1963.
(c) D.W. Van Krevelen, "Coal", Elsevier Publishing Company, New York, 1961.
2. (a) Powell, Ind. and Eng. Chem. 12, 1069 (1920).
(b) Powell, Ind. and Eng. Chem. 12, 1077 (1920).
3. Snow, Ind. and Eng. Chem. 24, 903 (1932).
4. Foerster and Geissler, Z. Angew Chem. 35, 193 (1922).
5. Sperr, Proc. 2nd Inter. Conf. Bituminous Coal I, 560 (1928).
6. Ditz and Wildner, Brennstoff - Chem. 5, 149 (1924).
7. Campbell, Bull. Am. Inst. Mining Eng. 1916, 177.
8. Wibaut and Stoffel, Rec. Trav. Chīm. 38, 132 (1919).
9. Monkhouse and Cobb, Gas J. 156, 234 (1921).
10. Wibaut, Rec. Trav. Chīm. 38, 159 (1919).
11. Wibaut, Brennstoff-Chem. 3, 273 (1922).
12. Parr and Layng, Mining and Met. 1920, No. 158, Sec. 4.
13. McCallum, Chem. Eng. 11, No. 1, 27 (1910).
14. Wibaut and LaBastide, Rec. Trav. Chīm. 43, 731 (1924).
15. Jüntgen, Erdöl and Kohle 17, 180 (1964).
16. Van Heek, Jüntgen, and Peters, Brennstoff-Chem. 48, No. 6, 35 (1967)
Translation by Scientific Research Instruments, Inc., Baltimore, 1968.
17. Peters and Jüntgen, Brennstoff - Chemie 46, 175 (1965).
18. Van Heek, Jüntgen, and Peters, Ber. Bunsen. Phys. 71, 113 (1967).
19. Van Heek, Jüntgen, and Peters, "Theoretische und experimentelle Vorstudien zur Kinetik der Kohlenwissenschaftliche Tagung, Munster 1. bis 3, June 1965.
20. Jüntgen and Traenckner, Brennstoff-Chem. 45, 105 (1964).
21. Jüntgen and van Heek, Fuel 47, 103 (1968).

22. Hanbaba, Jüntgen, and Peters, Ber. Bunsenges. phys. Chem. 1968, 72 (to be published).
23. Button, Greg, and Winsor, Trans. Faraday Soc. 48, 63 (1952).
24. Pechkovski and Zvedin, C.A. 56, 5460 (1962).
25. Pagurova, "Tables of the Exponential Integral," Pergamon Press, New York, 1961.
26. Mason, Ind. Eng. Chem. 51, 1027 (1959).
27. Zielke, Curran, Gorin, and Goring, Ind. Eng. Chem. 46, 53 (1954).
28. Batchelor, Gorin and Zielke, Ind. Eng. Chem. 52, 161 (1960).
29. Squires, A.M., "Fuel Gasification", Advances in Chemistry, Series 69, Robert F. Gould, editor (American Chemical Society, Washington, D.C., 1967)Chapter 14.

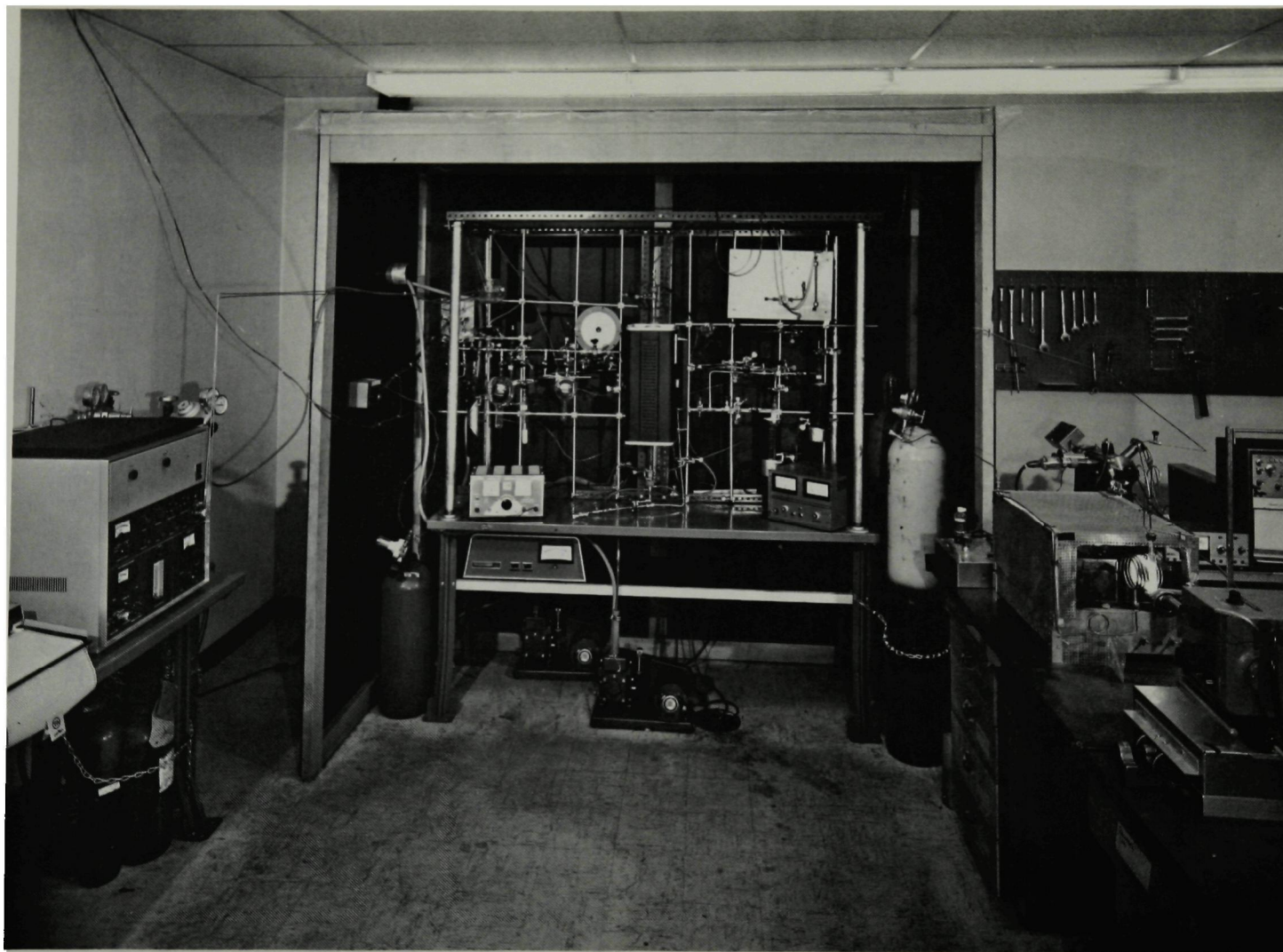
APPENDIX

During the first four months of this project a laboratory for measurements on the heterogenous reaction kinetics of coal gasification and desulfurization was constructed. Photographs of this laboratory are presented in Plates I, II, and III.

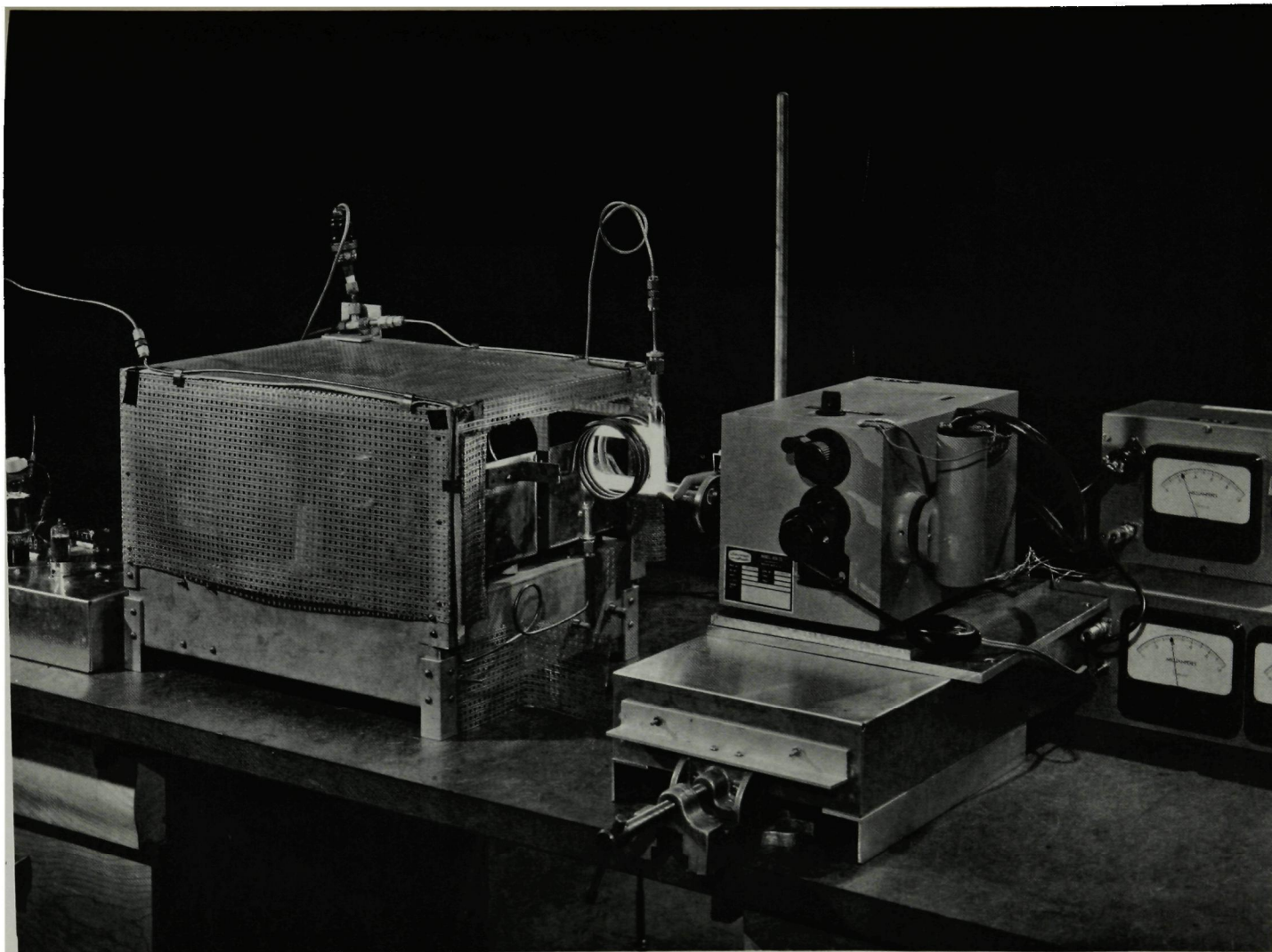
APPARATUS

The experimental apparatus consisted of three main sections; the combustor-gasification furnace and gas collection traps, the GLC sampling and gas handling system, and the analytical section which included the gas chromatograph, plasma spectrograph, and the mass spectrometer. A block diagram of this apparatus is shown in Figure A1. Detailed descriptions of each section are shown in Figures A2-A5.

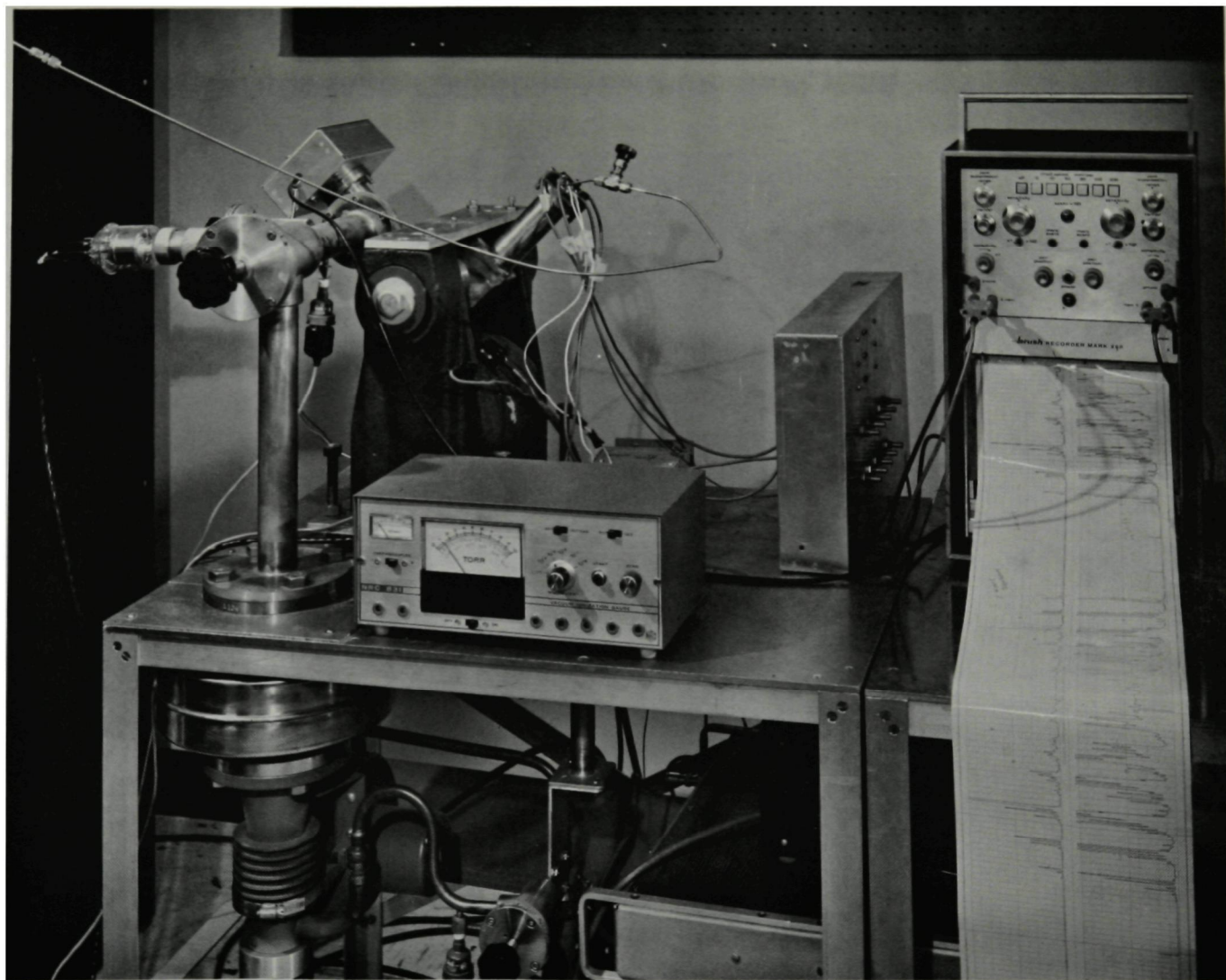
The reactor used in most of these measurements was constructed from a 75 cm length of 20 mm I.D. quartz tubing with 1.5 mm walls as supplied by the Thermal American Fused Quartz Company. This tubing was sealed at both ends with stainless steel O-ring connectors which were adapted for this purpose from NRC-Norton Company connectors. These fittings were epoxied to the quartz tube and connected the reactor vessel to the flow system. Stainless steel water cooled jackets, which also served as plugs to the reactor tube were used in the early runs. They consisted of a double sleeve encapsulation around 1/4" O.D. tubing formed by 1/2" O.D. and 3/4" O.D. tubing in a concentric arrangement. Overall length of the water cooled jackets was 4.5". This cooling effect at the inlet of the reactor



**LABORATORY FOR THE STUDY OF COAL GASIFICATION AND
DESULFURIZATION**



PLASMA SPECTROGRAPH FOR COAL-SULFUR ANALYSES



**MASS SPECTROMETER FOR NON-ISOTHERMAL KINETICS OF COAL -
SULFUR CHEMISTRY**

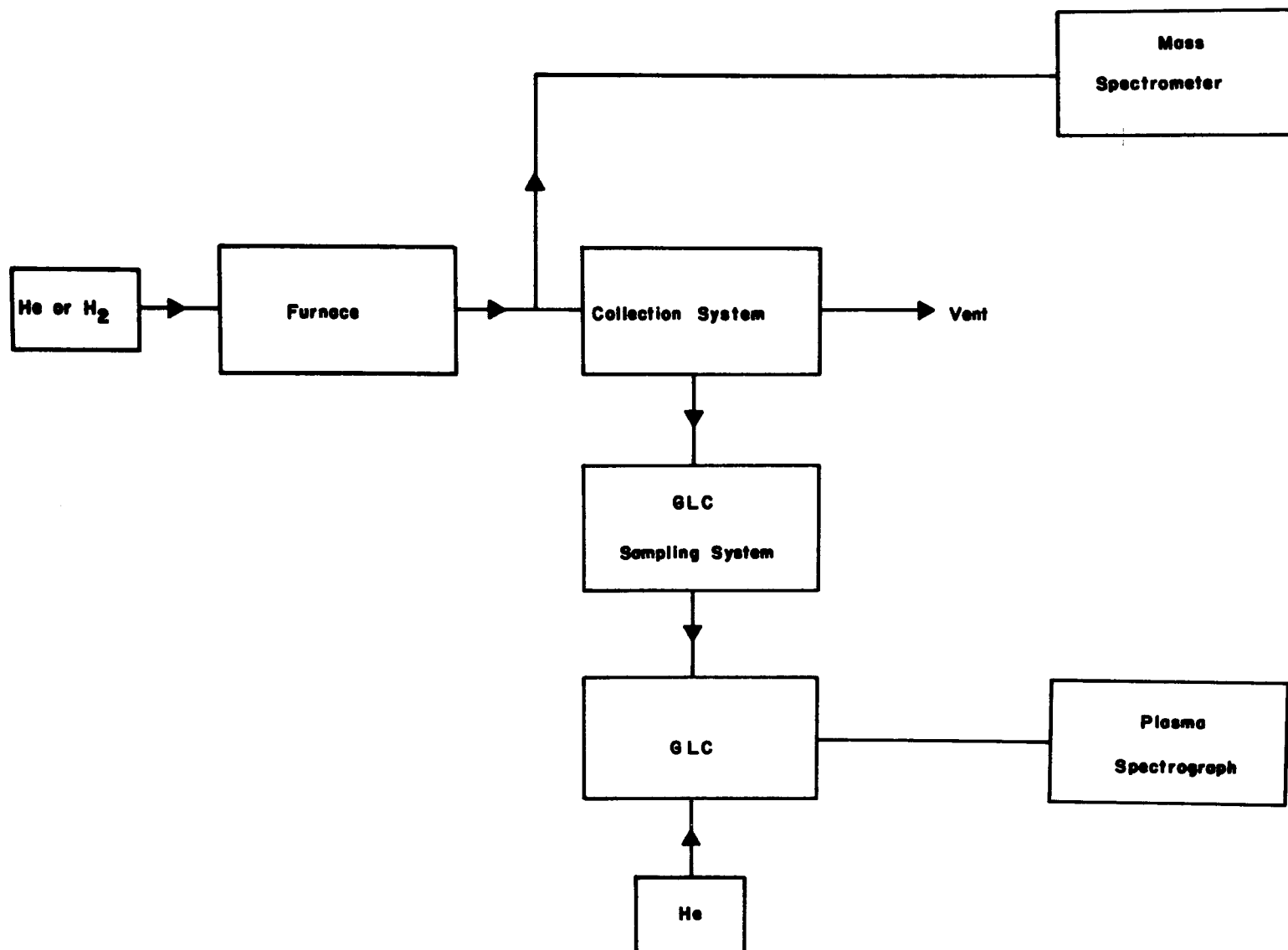


Figure A1. Block diagram of experimental apparatus.

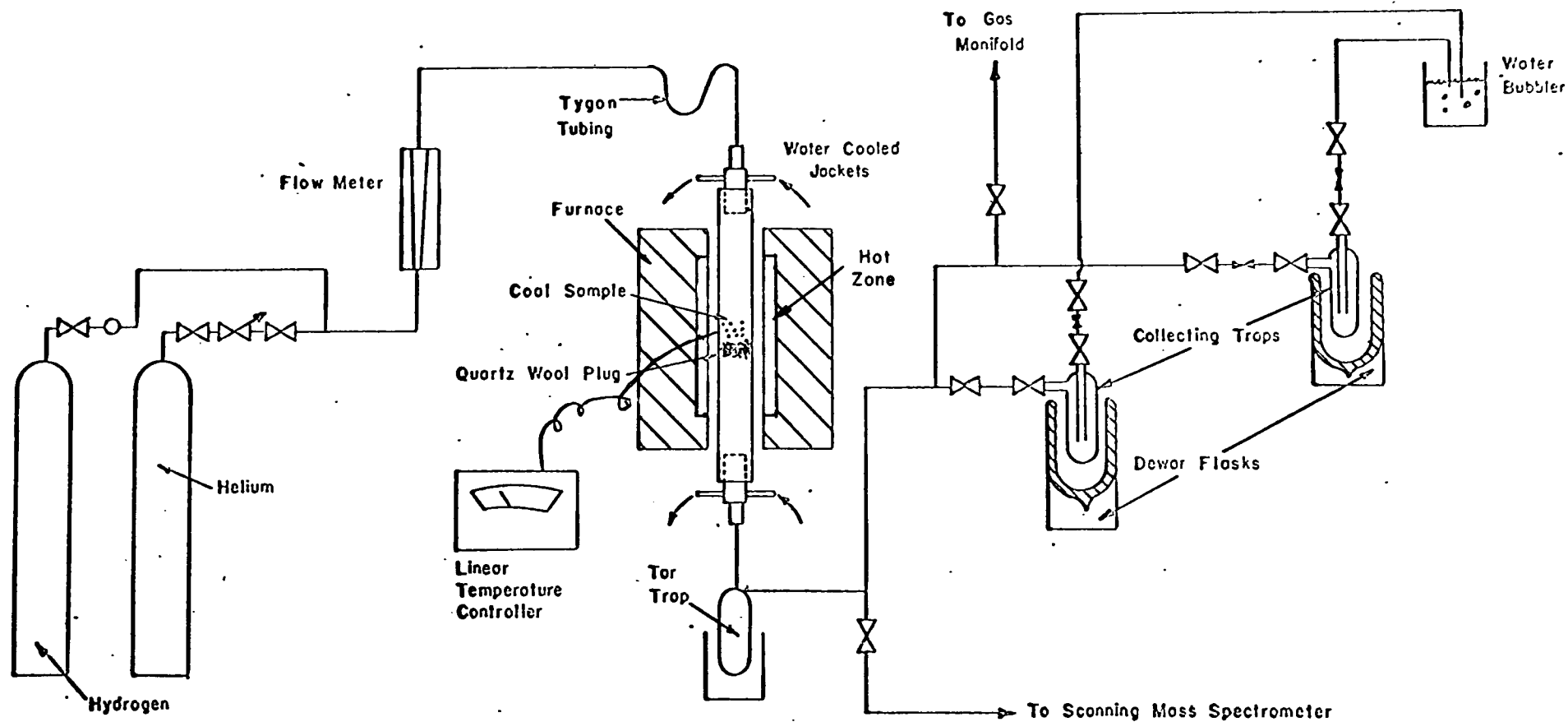


Figure A2. Detailed description of coal pyrolysis gas handling system.

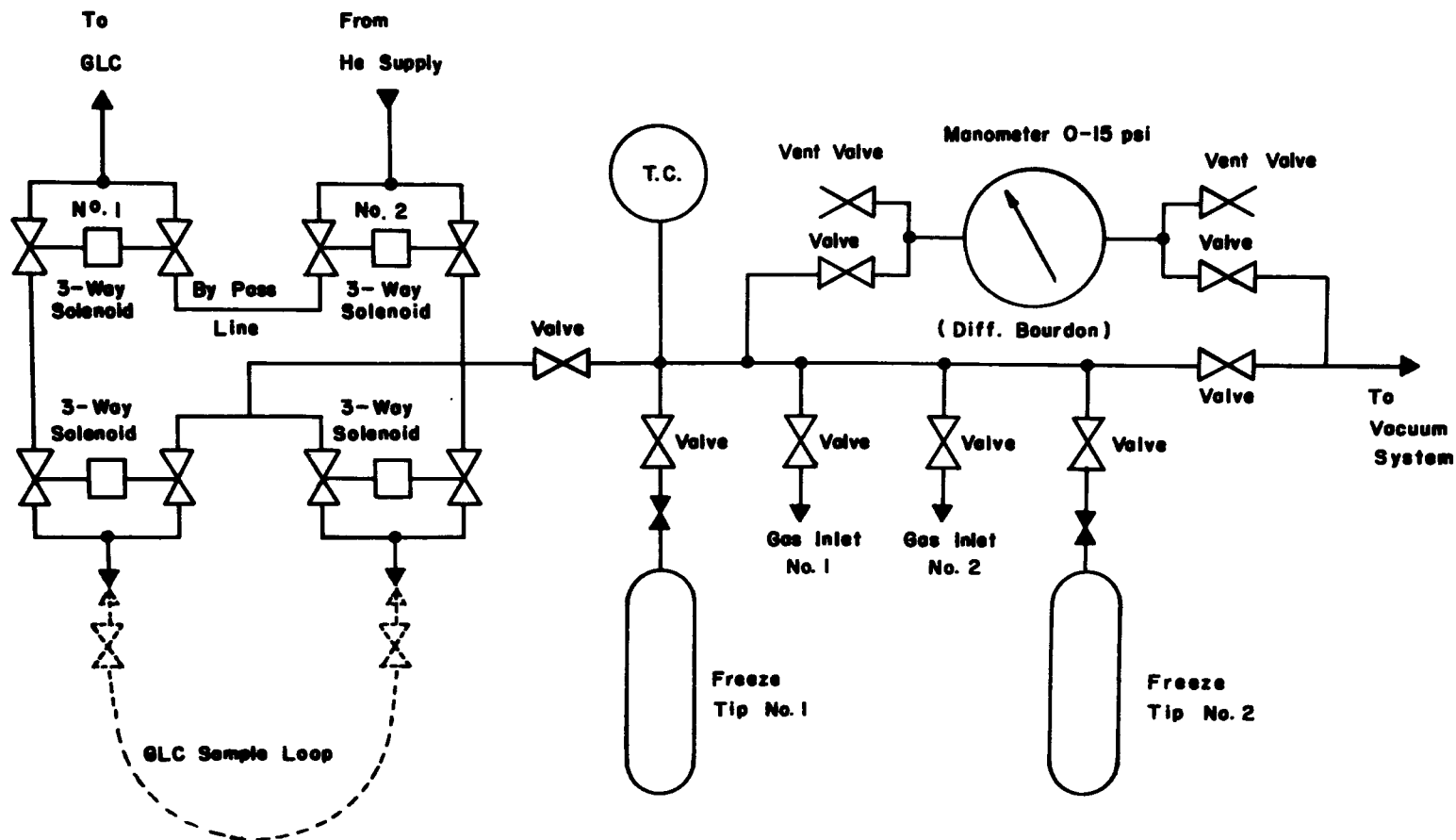


Figure A3. Detail schematic of GLC sampling and gas handling system.

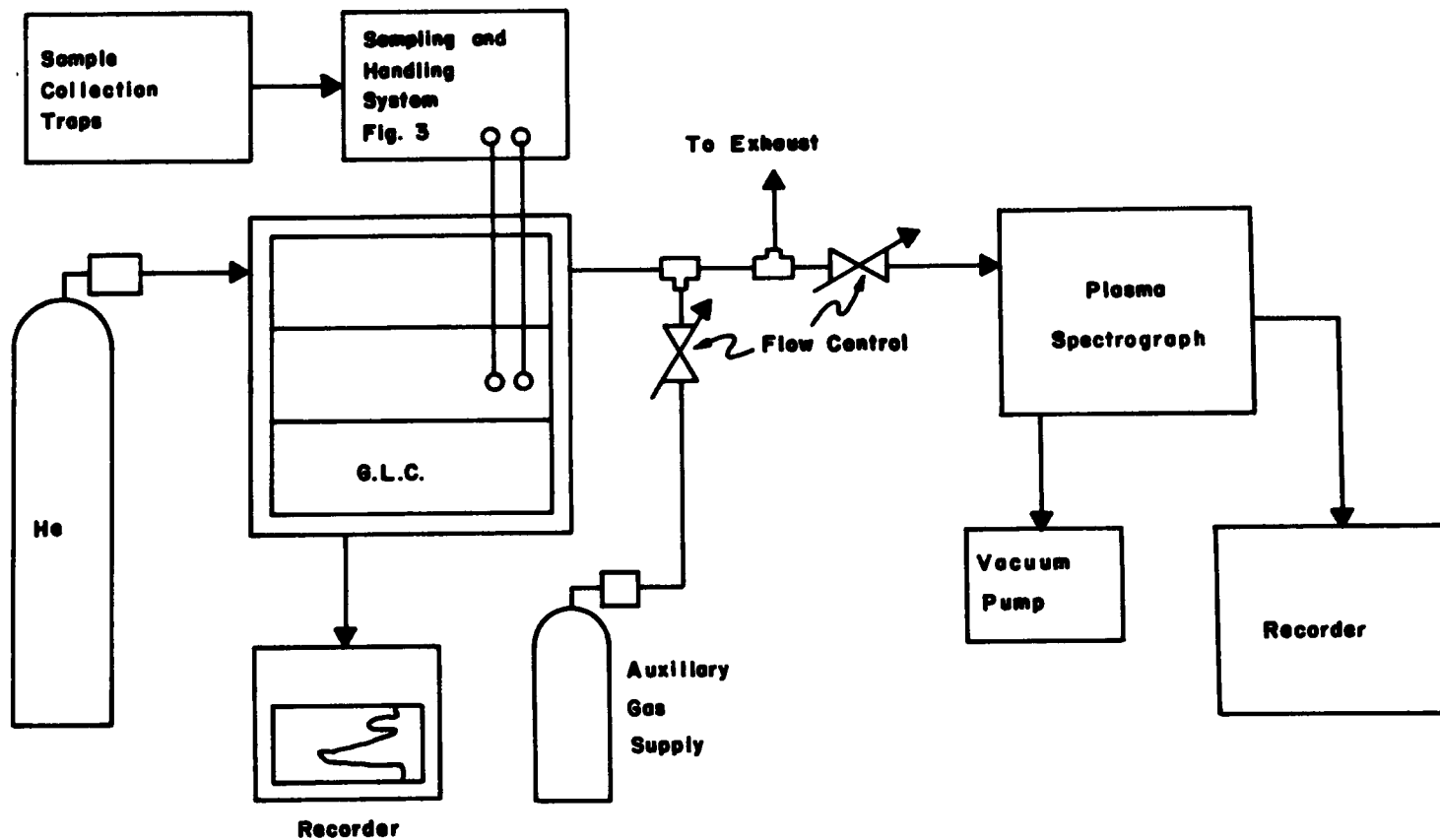


Figure A4. Detail schematic of tandem GLC-Plasma Spectrograph.

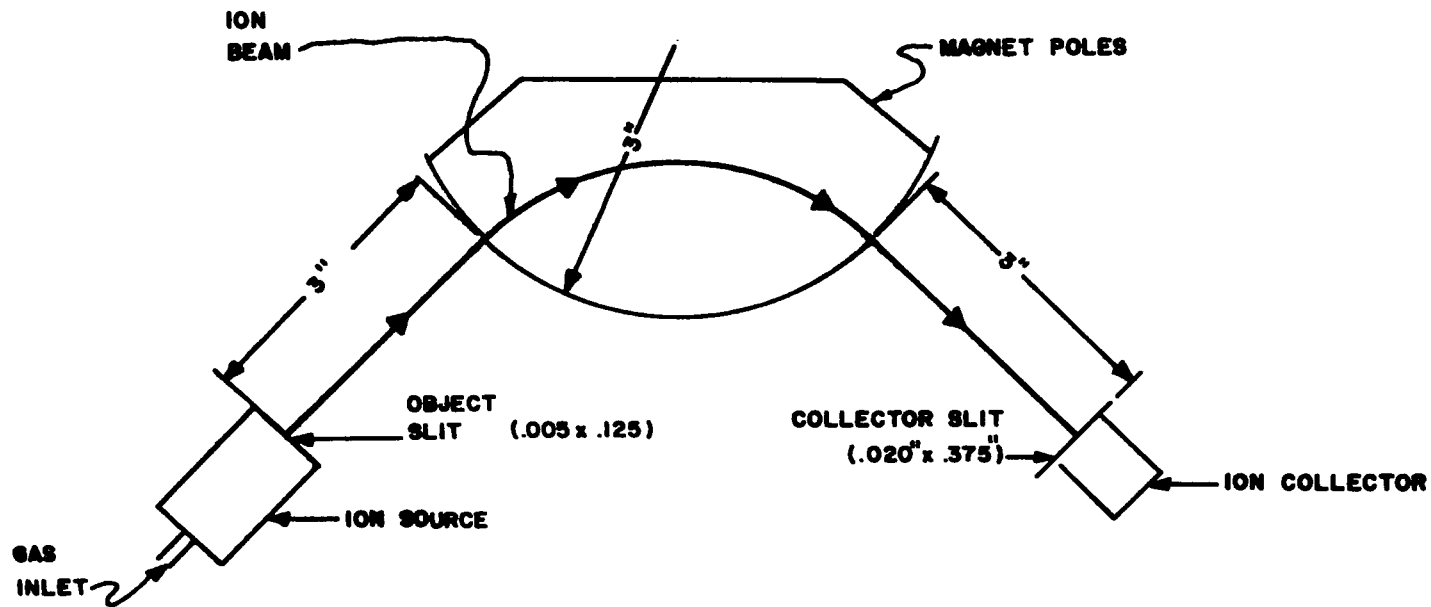


Figure A5. Schematic diagram of the ion optics for the scanning mass spectrometer.

tube occasionally caused the coal particles to agglomerate in the inner tube of the water cooled jacket during a gravity feed, and both jackets were found to be unnecessary and were eliminated during the later runs. They were replaced by a 3/4" O.D. to 1/4" O.D. stainless steel reducing fitting which was compatible with the O-ring connectors.

Two other reactor vessels were also used. A stainless steel reactor, 3/4" O.D. and .065" wall-thickness, but similar in all other respects to the quartz reactor described above, was used in Runs I3, I4, and I5. This tube was discarded because of the possibility of a reaction with the H_2S at high temperatures. The reactor shown in Fig. A6 was used for the high-pressure series, Runs N17 to N20. The inside liner was a 76 cm length of 17.8 mm O.D. quartz tubing with 1.5 mm thick walls from Thermal American Fused Quartz Company. The outside jacket was 1" O.D. stainless steel tubing with .083" walls. The end plug and elbow connector were standard 1" Swagelok stainless steel fittings.

The quartz wool used to support the coal in the reactor was approximately 1 gram of Thermal American Fused Quartz Company quartz mat No. 550 cut and rolled to form a plug. Matheson Company, pre-purified hydrogen, 99.95% minimum purity, or high purity helium, 99.995% minimum purity, were used as the carrier gas. Flow rates were monitored with a Brooks Instrument Division flowmeter Sho-Rate "150" Model 1355 with tubes in the R-2-15 series.

The furnace was a Lindberg/Hevi-Duty Model No. 54032 with Control Console Model 59344. It has a maximum temperature range of 1200°C and is capable of control to $\pm 1^\circ C$. This furnace is designed for heat applications requiring close temperature control, uniformity and fast heat-up and uses silicon carbide rods as heating elements. The inner

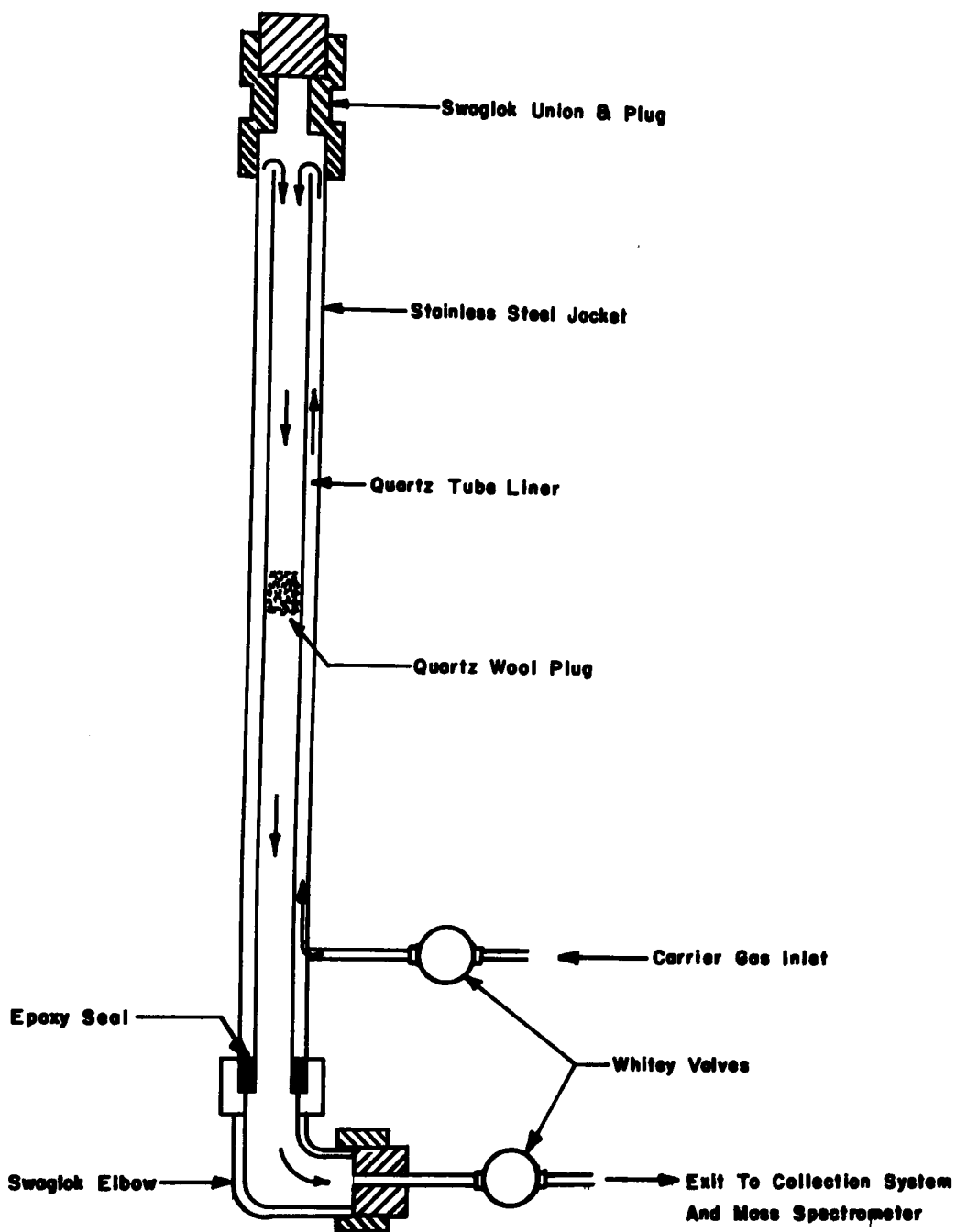


Figure A6. Diagram of reactor vessel used in high pressure experiments.

unit which contains the two semicylindrical heating units is enclosed in an insulating brick and steel case, and air convection between this unit and an outer steel shell reduce the surface temperature of the furnace to below 100°C at the maximum temperature. The heating elements are 12" long and, because of this long heating path, gas flowing through the reactor is sufficiently heated before it reaches the coal sample in the center of the heating zone. In the later runs a quartz wool plug was placed on top of the coal to furnish additional hot contact with the carrier gas. This furnace incorporates an API contactless controlling pyrometer placed at the mid-point of the heating elements as shown in Figure A2. The position of the pointer of the meter reading the furnace thermocouple voltage is sensed optically, providing a sensitive yet very reliable design.

For the non-isothermal constant-heating-rate experiments the apparatus was modified by adding a linear temperature programmer to the furnace control. This was a laboratory model designed and built at Scientific Research Instruments Corporation to be compatible with the Lindberg furnace described previously. In designing the programmer to operate with the furnace and its controller it was desirable that no changes be made to the Lindberg unit. The linear programmer shown in Figure A7 was therefore constructed and has proven very satisfactory in actual use.

The unit generates a linearly increasing voltage of opposite polarity to the thermocouple output voltage. The generated voltage is in series with the thermocouple output so that furnace temperature then rises linearly to maintain zero input voltage to the API controller. Actual furnace temperature can be read any time desired either by connecting a recorder directly across the thermocouple output or by depressing the READ TEMPERATURE switch and reading temperature on the meter in the controller.

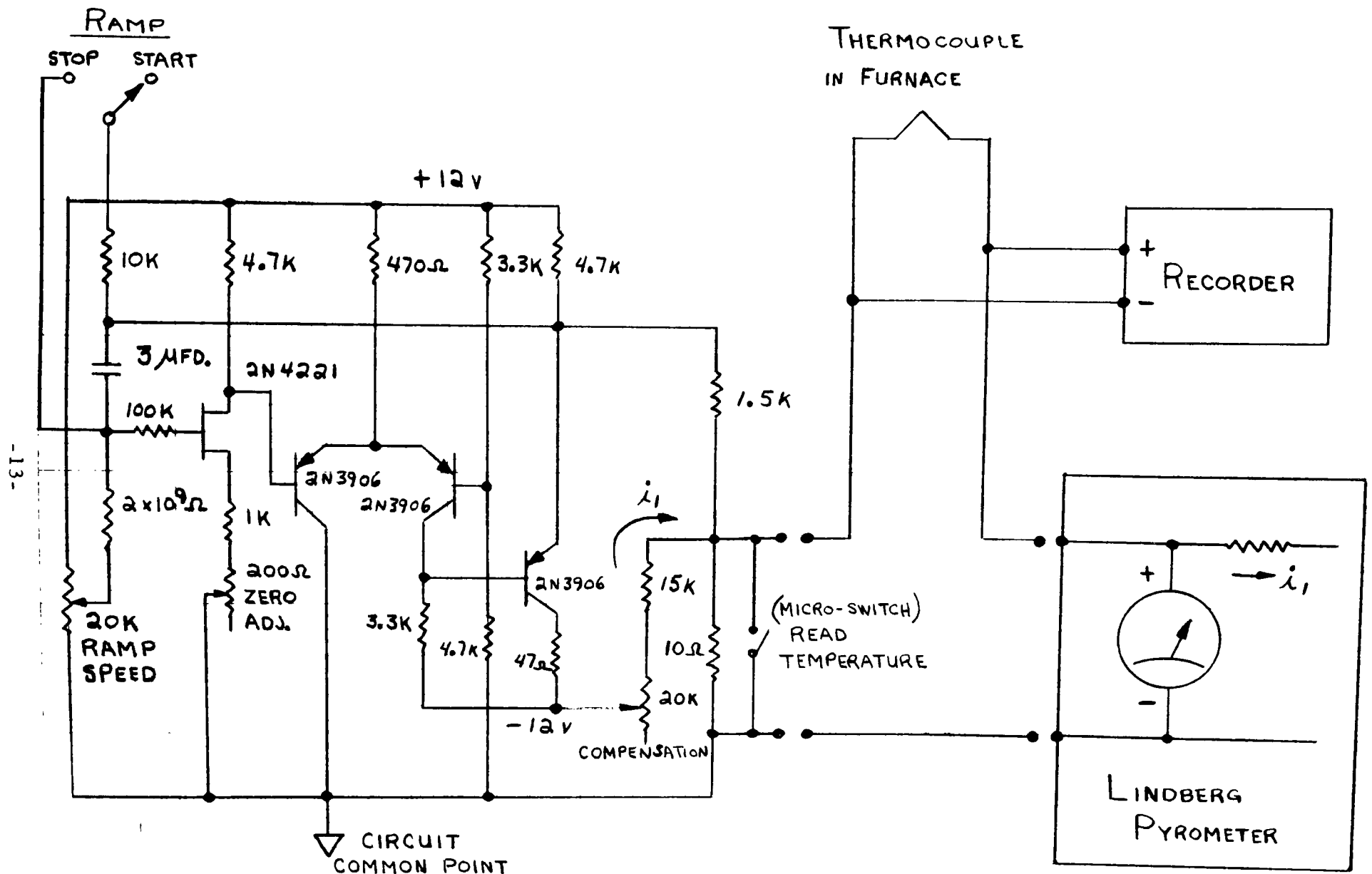


Figure A7. Schematic diagram of the linear temperature programmer.

The ramp generator is basically conventional and begins with an RC time constant composed of a $3\mu\text{f}$ low-leakage capacitor and a 2×10^9 ohm resistor. Voltage across the capacitor is sensed by a 2N4221 FET transistor, to provide the necessary high input impedance. The following three transistors comprise a differential pair and an emitter follower. Feedback to the capacitor linearizes the ramp over the 10 volt output range. Ramp speed is adjustable with the RAMP SPEED control and may be changed during a run if different linear temperature rise rates are needed. Maximum ramp voltage is 10 volts -- a resistance divider (1.5K and 10 ohms) injects a portion of this voltage in series with the thermocouple.

The controller in the Lindberg furnace incorporates thermocouple burn-out protection by passing a small current, i_1 , through the thermocouple. In order to prevent the accuracy of the readings on the Lindberg controller being affected by the added 10 ohms in the thermocouple circuit, it is necessary to compensate by passing an equal and opposite current, $-i_1$, through the 10 ohm resistor. This current can be adjusted by the COMPENSATION control which is set, with the furnace at room temperature and ramp control in STOP position, so that no change of meter deflection occurs upon operating the READ TEMPERATURE switch.

In most runs, a Hoke Inc., 75 ml stainless steel sampling cylinder, No. 4HS75, was adapted for use as a tar trap. Either Hoke 75 or 150 ml high pressure stainless steel sampling cylinders, No. 4HS75 and 6HS150, respectively, or standard Pyrex glass vapor traps were used as gas collection traps. The traps were immersed in liquid nitrogen so that gases which were condensable in liquid nitrogen were collected, while light

gases such as methane and carbon monoxide and the carrier gas were not collected and were vented to the atmosphere. In coal runs No. 113 and 115-118 the traps were arranged in parallel; in all other runs, the traps were connected in series. After Run No. 110, the traps were 1/2 filled with 3 mm diameter Pyrex beads to increase the collection efficiency.

All components of both the coal gasification and collection system, shown in detail in Figure A2 and the GLC sampling and gas handling system shown in Figure A3 were stainless steel. Unless otherwise specified, connecting lines were 1/4" O.D. with .020" wall: the valves used were Whitey Research Tool Co., IVS4-316. Background pressure in the gas handling system was maintained at approximately 25 μ by a Welch 1400B two-stage vacuum pump. This sampling system was also used for the purification and injection into the GLC of calibration standards as well as the volatile pyrolysis products.

A carrier flow loop accessory on the chromatograph unit was used with 1/8" O.D., .020" wall stainless steel tubing to extend the carrier flow lines prior to injection in the column so that they could be connected to the GLC Sample System. This provides a means for gas injections of samples whose pressures ranged from a few torr to several atmospheres. Injection into the GLC was made by switching the 3-way solenoids, see Figure A3 so that the helium carrier gas was diverted from the bypass line to the sample loop sweeping out the gas sample and carrying it to the columns. The solenoids used were Allied Control Co., Inc. Model RSV-30384 stainless steel with Viton seats.

Detailed descriptions of the analytical apparatus are shown in Figures A4 and A5. The chromatograph used was a Varian Aerograph Model 202-1C dual column unit with thermal conductivity detectors and

a linear temperature programmer. Two 10 ft., 1/4" O.D. stainless steel columns with 20% Triton 305 on acid washed, DMCS, chromosorb G were used with the chromatograph. Operating conditions were: initial GLC column temperature 50°C, programmed after 5 minutes at a rate of 4°/min to 70°C; detector temperature, 100°C; injector temperature, 85°C; detector current 200 ma; and helium flow rate, 50 ml/min. Matheson Co. high purity helium was used as the carrier gas. Retention times for various compounds under these operating conditions are given in Table A1.

The sulfur-containing products of the coal gasifications were calibrated under these GLC conditions by injecting into the GLC from a known volume, gas standards at different known pressures. The volume used was the 3.5 ml GLC sample loop, see Figure A3; pressures were read on a Wallace and Tiernan pressure gage Model FA-141. An example of a calibration curve for H₂S, obtained in this manner, is shown in Figure A8. This calibration was done using Matheson Co. CP grade H₂S. Other gas calibrations were made with Matheson Co. sulfur dioxide, commercial grade, and methyl mercaptan, 99.5% minimum purity. J.T. Baker Chemical Co. reagent grade carbon disulfide was used in the CS₂ calibration; Aldrich Chemical Co. technical grade thiophene was used in the C₄H₄S calibration. Chromatograms were recorded on a 10" Varian Aerograph Model 20 recorder and peak areas were measured using a K and E Planimeter Model 62-005. Using 1.0 cm² as the smallest measurable peak and 115.5 cc as the expansion volume, the GLC sensitivity was 0.013 mgS. Details of this calculation are shown in the following section. Although 115.5 cc was the expansion volume used when the gas was expanded directly from the gas trap into the GLC sample loop and larger expansion volumes were often used when large quantities of gaseous product were present, the smaller expansion volume represents a lower limit on the sensitivity.

TABLE AI. RETENTION TIMES OF VARIOUS COMPOUNDS IN
GLC FOR TRITON 305 COLUMN PROGRAMMED
FROM 50 -70°C AND HELIUM FLOW RATE, 50 ML /MIN.

<u>Compound</u>	<u>Retention Time (min)</u>
Air	2.1
H ₂ S	3.1
CH ₄	2.1
CO	2.1
CO ₂	2.1
COS	2.5
SO ₂	14.7
CH ₃ SH	6.0
CS ₂	8.8
C ₆ H ₆	23.0
(C ₂ H ₅) ₂ S	26.5
C ₄ H ₄ S	40.5

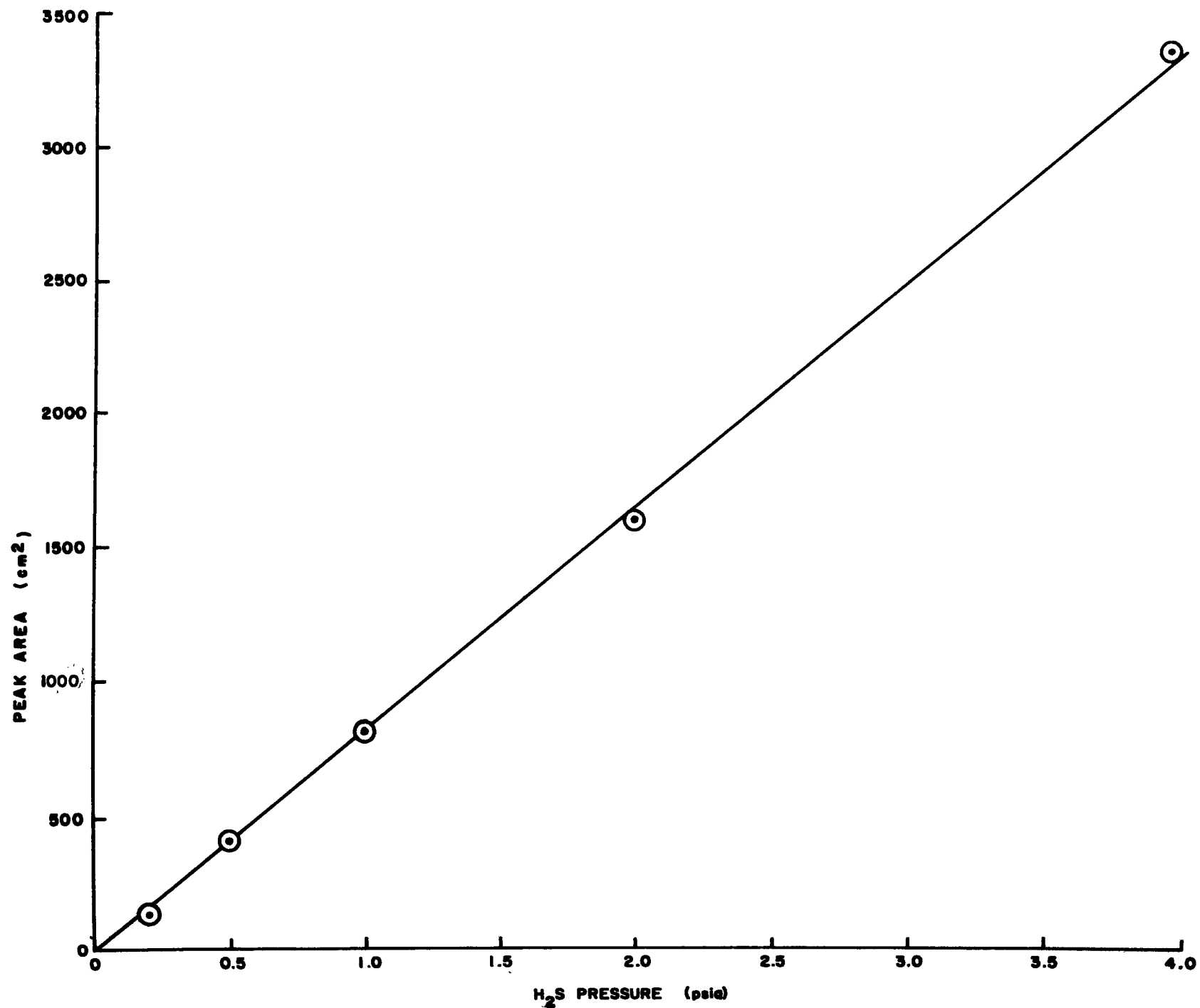


Figure A8. Chromatograph calibration chart for hydrogen sulfide.

Since 0.013 mg was in all cases equal to or less than 1/10% of the total sulfur, this GLC sensitivity was more than sufficient for measuring the sulfur balance. The SO_2 , MeSH , CS_2 , and $\text{C}_4\text{H}_4\text{S}$ chromatographic sensitivities were similar to that for H_2S .

For Runs 11 to 113 a plasma spectrograph was connected, in tandem, to the exit of the chromatograph as shown in Figure A4 and a small portion of the effluent was carried into the plasma detector. The detection system for monitoring the spectral emission for the helium plasma included a Jarrell Ash Monochrometer Model 82-410 with a Cs-Sb photomultiplier, an electrometer and a Bausch and Lomb one channel strip chart recorder. A Wratten No. 15 filter with a light transmission cut-off at 5200 Å was installed ahead of the monochrometer to reduce scattered light and increase sensitivity. Qualitative analysis of sulfurous gases exiting from the GLC was made by monitoring the 5454 Å sulfur atomic line. Since spectral studies indicated that this particular sulfur line was superimposed on a carbon molecular band, a relative indication of sulfur to carbon atom ratio was made by alternately recording the 5454 Å sulfur line and the part of the carbon molecular band at 5448 Å. This method gave two simultaneous peaks corresponding to sulfur and carbon concentrations. An example of this type of plasmagraph is shown in Figure A9.

Various compounds were run under the conditions described above to check peak shape sensitivity and retention time. The retention time for H_2S is approximately 3.5 minutes in the GLC and delayed by 15 seconds in the corresponding plasma spectrogram. This delay between the chromatogram and the spectrogram is the mean gas flow time between the thermal conductivity detector and the take-off needle valve of the plasma spectrograph. Since this delay is constant, it did not cause any ambiguity.

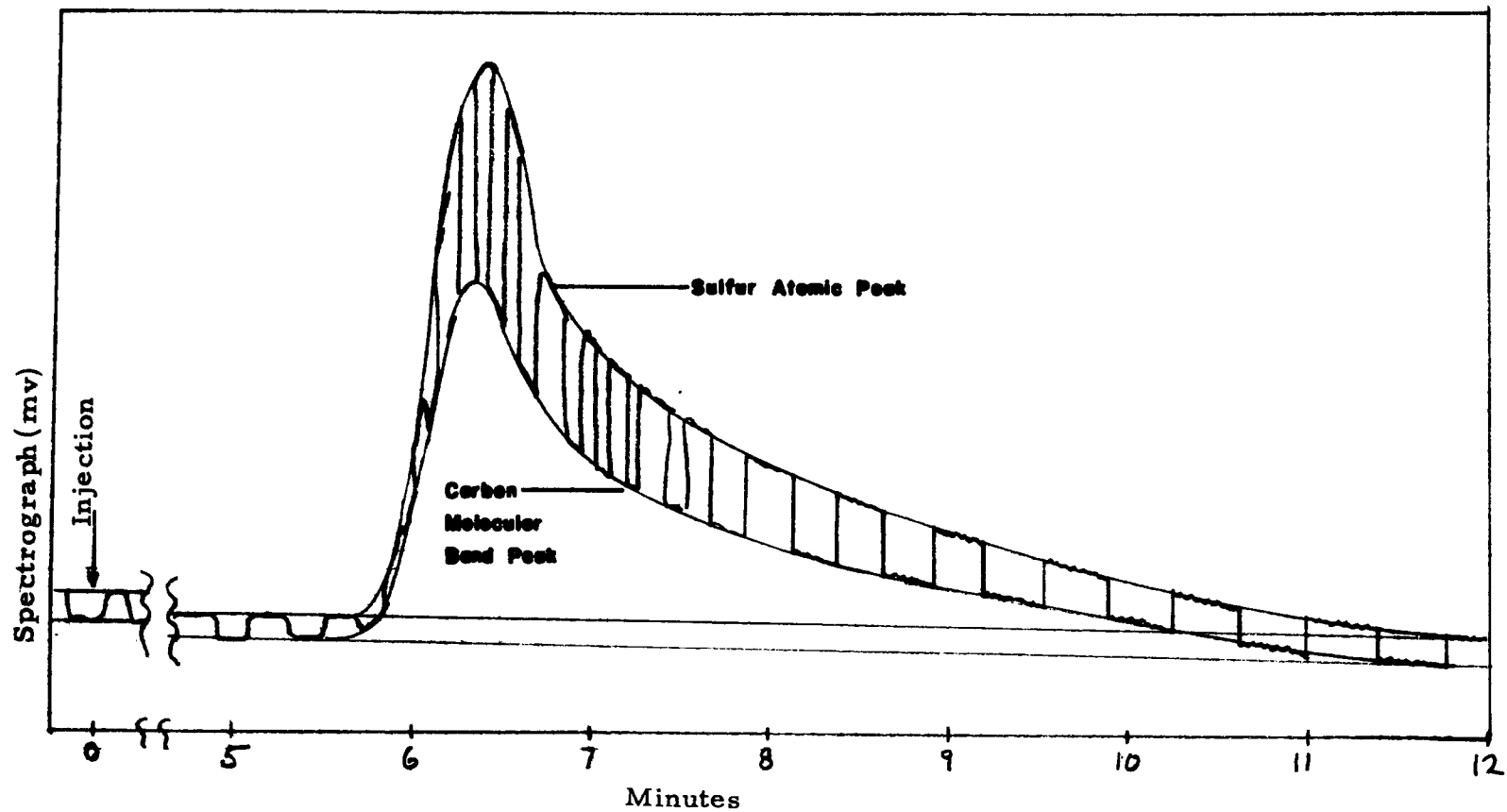


Figure A9. Plasmagram of 0.1 psia methyl mercaptan in 3.5 cm³ sample loop.

The scanning mass spectrometer used in the non-isothermal constant heating rate experiments was designed and built at Scientific Research Instruments Corporation for this project. For the first two non-isothermal measurements the mass spectrometer was connected to the reactor flow system using a membrane separator as shown in Figure A10. This separator increased the sensitivity of the measurement substantially for those components to which the membrane was highly permeable, such as H_2S and benzene. It was found, however, that this enhancement in sensitivity was not necessary and for all of the later experiments the membrane separator was replaced by a stainless steel needle valve.

A schematic diagram of the ion optics of this instrument is given in Figure A5. The ion trajectories follow a 3" radius of curvature through 90° of magnetic deflection. This instrument uses a fixed ion accelerating voltage and is magnetically scanned by linearly varying the current to the magnet using a motor driven potentiometer. For all of the experiments conducted the mass range from mass 1 to mass 84 was scanned every 50 seconds.

The electrometer connected to the ion collector uses a 10^{11} ohm resistor and gives a full scale output of 10 volts for 10^{-10} ampere ion current. The time constant for the electrometer is approximately 1 millisecond. In scanning the spectra the output of the electrometer was connected to a Brush Mark 280 two channel recorder. The sensitivities of the individual channels of the recorder could be selected according to the ion currents being monitored to cover any range from 10 volts full scale, down to 100 millivolts. Peaks corresponding to 2 millivolts were clearly recognizable above noise.

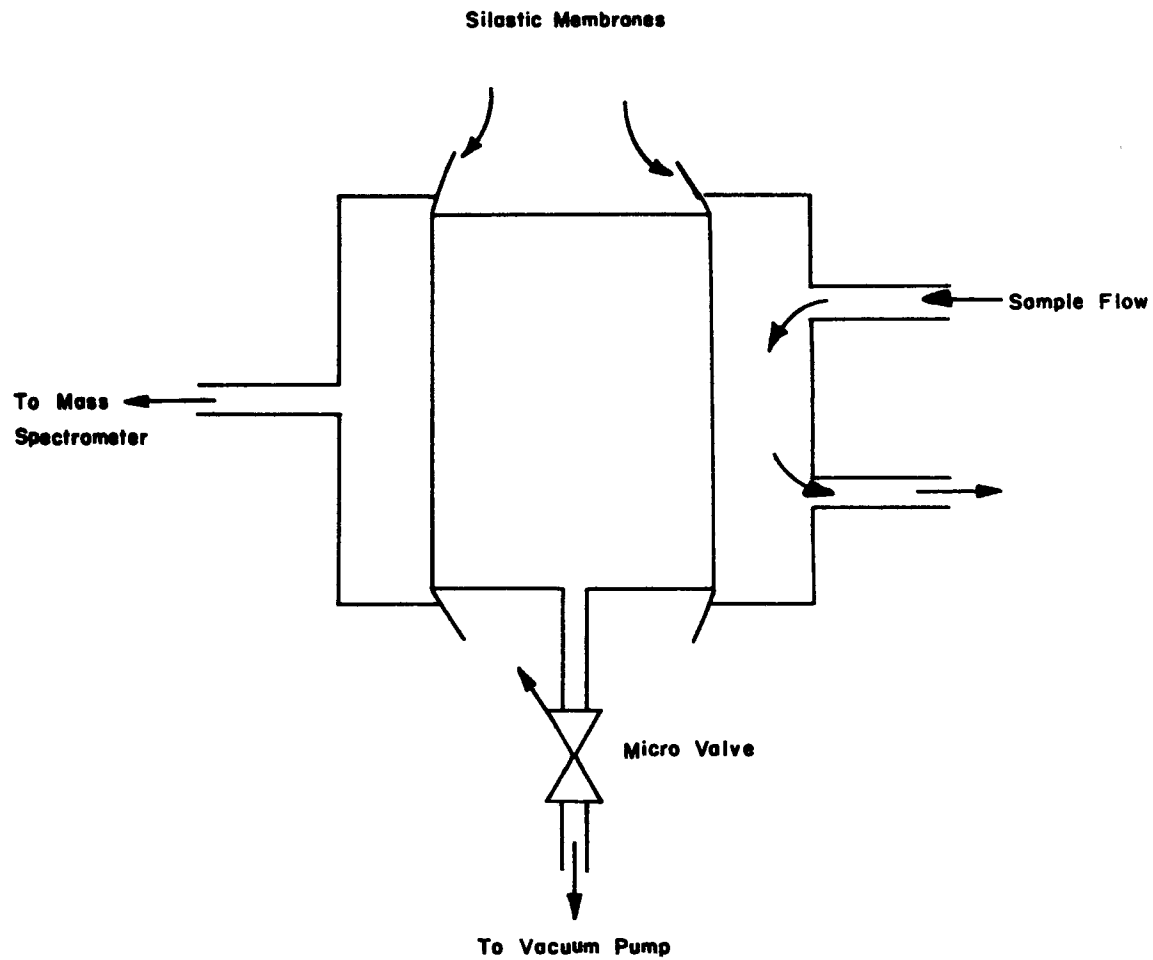


Figure A10. Membrane separator for mass spectrometer inlet system.

In the non-isothermal runs the mass spectrometer continuously scanned the mass range 1 to 84 resulting in a quasi-continuous record of the changes in the composition of the pyrolytic gases with time and temperature. Calibration factors for the sensitivity of the mass spectrometer to these gases were determined by measuring the spectrometer response to a known mixture of the component to be measured and helium. These known mixtures were prepared on the gas handling system. The calibration factor relative to helium is then given by

$$f = \left(\frac{P_x}{P_{He}} \right) \left(\frac{PH_{He}}{PH_x} \right)$$

where P_{He} is the partial pressure of helium in the mixture, P_x is the partial pressure of the component to be measured, PH_{He} is the spectrometer response to helium in millivolts of peak height, and PH_x is the spectrometer response to the component to be measured in millivolts of peak height. These calibration factors are listed in Table AII relative to helium and hydrogen. The concentration of a gas in the volatiles present at any given time in the pyrolysis was determined by multiplying the appropriate calibration factor for that gas by the ratio of the peak height of the mass indicated for that gas in Table AII to the mass 2 or mass 4 peak height.

PROCEDURE

Basically, the experimental procedure was to pyrolyze coal samples under different experimental conditions and collect and analyze the evolved gases, coke and tar for per cent sulfur by weight. The experimental parameters investigated included type of coal, mesh size, carrier gas, temperature, heating rate, etc. In addition, in the non-isothermal runs, the

TABLE AII. MASS SPECTROMETER CALIBRATIONS FOR
THE GASES MEASURED IN THIS WORK

MOLECULE	MASS NO.	CALIBRATION FACTOR	
		He (1)	H ₂ (2)
He	4	1	1.21
H ₂	2	0.83	1
CH ₄	16	0.11	0.13
CO	28	0.053	0.064
C ₂ H ₆	30	0.17	0.21
H ₂ S	34	0.055	0.067
C ₃ H ₈	43	0.14	0.17
CO ₂	44	0.033	0.040
CH ₃ SH	47	0.038	0.046
SO ₂	64	0.041	0.050
CS ₂	76	0.012	0.015
C ₆ H ₆	78	0.018	0.022

(1) Relative to He, calibration factor times ratio of peak height of indicated mass number to mass 4 peak height equals concentration.

(2) Relative to H₂, mass 2 peak.

gases evolved were continuously analyzed as a function of increasing temperature by the scanning mass spectrometer described previously.

Two different methods of inserting the coal sample into the reactor vessel were used. In isothermal fast heating rate experiments, the coal sample was placed in a section of flexible Tygon tubing at the inlet of the reactor tube, as shown in Figure A2. After the carrier gas flow rate was established and the desired temperature had been reached, the coal was gravity fed into the furnace by manually lifting the Tygon tubing so that the coal particles dropped into the furnace through the water cooled inlet. In the non-isothermal and slow heating rate experiments, the coal was placed in the furnace prior to the run. The carrier gas was turned on and sufficient time allowed for the system to be purged of air before commencing the heating.

In isothermal pyrolysis runs, experiments were timed from the coal insertion by gravity feed to the time at which the heat was turned off; in non-isothermal runs, experiments were timed from beginning to end of the heat application. In all cases, helium was used during the cooling off period, and gases were not collected during this time.

The gases evolved during the pyrolysis were swept through the furnace by the carrier gas and out to the collection traps. In coal Runs I13 and I15-I18 where the traps were arranged in parallel, the gases evolved during the first 15 minutes were collected in one trap and the gases evolved during the remainder of the pyrolysis were collected in another trap. In Runs N1-N9 the gases were collected in a series of 12 separate traps at 20 minute intervals by alternately changing traps. In all other runs, two traps were connected in series, and either the gases in one trap transferred to the other before analysis, or they were analyzed separately and the results combined.

After the pyrolysis was completed, the collection traps were vacuum-purged to remove completely the non-condensable gases, sealed off, and allowed to warm to room temperature. In Runs I1-I18 the gas was then expanded from the collection trap through a gas inlet on the GLC sampling system into the GLC sample loop shown in Figure A3. In all other runs, this method was replaced by one in which the gas traps were removed from the collection system and attached directly to the GLC sample line eliminating the need to expand the samples through a long segment of stainless steel tubing. Also, in all other runs, where large enough quantities of vapor had been collected in the traps for compounds to be present as a liquid, the material was transferred by freezing with liquid nitrogen into a larger volume, usually either a 1 liter or 5 liter bulb. This reduced the error due to H₂S and other vapors being dissolved in the liquids such as benzene, CS₂, etc., which were present in varying degree. After the gas was expanded into GLC loop, the sample was injected into the gas chromatograph and analyzed for sulfur.

An example of the calculation to determine the amount of sulfur in the H₂S gaseous product is shown below for Run N3.

Data: measured H₂S peak area - 8539 cm²

H₂S chromatograph calibration factor to convert peak area to psi in the loop (inverse slope of line in Figure A8) - $1.26 \times 10^{-3} \frac{\text{psia}}{\text{cm}^2}$

expansion volume used - 115.5 cc

Calculation:

Step 1 - using the H₂S calibration factor to convert the measured peak area to psia in the loop gives

$$8539 \text{ cm}^2 \times 1.26 \times 10^{-3} \frac{\text{psia}}{\text{cm}^2} = 10.76 \text{ psia}$$

Step 2 - using the calculated psia and the Perfect Gas Law to calculate the moles of H₂S in the loop (3.5 cc) gives

$$\frac{PV}{RT} = n$$

$$\frac{\left(\frac{10.76}{14.7}\right)(.0035)}{(.082)(300)} = 10.4 \times 10^{-7} \text{ moles H}_2\text{S}$$

Step 3 - using the calculated number of moles H₂S in the sample loop and knowing the ratio of the sampled gas to the total volume of gas gives

$$10.4 \times 10^{-7} \text{ moles} \times 32\text{g/mole} \times \frac{115.5 \text{ cc}}{3.5 \text{ cc}} = 109.8 \text{ mg S}$$

Quantities of sulfur in the other gaseous products were similarly calculated. Note that by using an assumed area of 1.0 cm² in the above calculation, the GLC sensitivity to H₂S is found to be 0.013 mg S as previously mentioned.

The coke was weighed and analyzed for per cent sulfur by standard ASTM methods. The reactor tube and the tar trap were rinsed out several times with acetone to collect the tar. The acetone was then evaporated and the tar was weighed and analyzed for per cent sulfur by the ATSM methods.

The sulfur balance and per cent sulfur recovery could then be easily determined from the total sulfur found in the gas, coke, and tar.

AP7.5-24

1969

Vestal, Marvin L. et al

AUTHOR Kinetic Studies on the Pyr-
olysis, Desulfurization, & Gasifi-
TITLE cation of Coals with Emphasis
on the Non-Isothermal Kinetic

Method LOANED	BORROWER'S NAME	DATE RETURNED
5/19/70	Frank Buegand	

AP7.5-24

1969

Vestal, Marvin L. et al

Kinetic Studies on the Pyrolysis,
Desulfurization, & Gasification of
Coals with Emphasis on the Non-Iso-
thermal Kinetic Method